TOPICS IN SUPERCONDUCTIVITY

TOPICS IN THE SUPERCONDUCTIVITY OF SIMPLE METALS AND ALLOYS

By

PETER NICHOLAS TROFIMENKOFF, B.E., M.Sc.

A Thesis
Submitted to the Faculty of Graduate Studies
in Partial Fulfilment of the Requirements
for the Degree
Doctor of Philosophy

McMaster University
November 1969

DOCTOR OF PHILOSOPHY (1969)
(Physics)

McMASTER UNIVERSITY
Hamilton, Ontario

TITLE: Topics in the Superconductivity of Simple Metals and Alloys

AUTHOR: Peter Nicholas Trofimenkoff,
B.E. (University of Saskatchewan)
M.Sc. (University of Saskatchewan)

SUPERVISOR: Professor J. P. Carbotte

NUMBER OF PAGES: vi, 166

SCOPE AND CONTENTS:

The effects of hydrostatic pressure on the superconducting transition temperatures of the simple metals aluminum, lead, mercury, tin and indium are investigated within the strong-coupling theory of superconductivity. The experimental variation of the transition temperature with volume change can be understood within a simple scaling model. Strong-coupling effects in the pressure dependence of superconductivity in lead and mercury are investigated.

A formalism which includes effects of force constant disorder on superconductivity in a binary alloy of simple metals is established within pseudopotential theory.

ACKNOWLEDGMENTS

I wish to thank Dr. J. P. Carbotte, my research supervisor, for his generous assistance, guidance and encouragement and for the many discussions which have furthered my understanding of Physics and research. I hope I have gained from his constant enthusiasm.

It has been a pleasure to be associated with the Theoretical Physics Groups at McGill and McMaster Universities over the past two years. In particular, I wish to thank Professor P. R. Wallace of McGill for encouraging my interest in Solid State Physics.

I wish to thank Dr. R. C. Dynes for his generous assistance during the early stages of this work. The assistance from Dr. D. W. Taylor and the discussions with Dr. P. Vashishta have been very helpful.

I wish to thank my fellow students for many valuable discussions.

The financial assistance of the National Research Council of Canada in the form of two studentships is gratefully acknowledged. I wish to thank the Theoretical Physics Group at McMaster for financial assistance during the final preparation of this thesis.

I wish to thank Miss Cathy Wivell for the excellent typing of the manuscript.

The encouragement of my wife, Diane, has been invaluable.

TABLE OF CONTENTS

Page

CHAPTER I: INTRODUCTION

1.1 Historical Introduction 1
1.2 Scope of Thesis 5

CHAPTER II: PHONONS, THE ELECTRON-PHONON INTERACTION AND STRONG-COUPLING SUPERCONDUCTIVITY

2.1 Phonons and the Born-von Kármán Theory 8
2.2 Pseudopotential Theory 16
2.3 The Structure-Dependent Crystalline Energy and Phonon Calculations with Pseudopotentials 26
2.4 The Electron-Phonon Interaction 32
2.5 Strong-Coupling Superconductivity 35

CHAPTER III: THE EFFECT OF PRESSURE ON SUPERCONDUCTIVITY

3.1 Previous Work 48
3.2 Calculation of $\alpha^2(\omega)\ F(\omega)$ 52
3.3 The Effect of Pressure on the Coulomb and Phonon Kernels 56
3.4 Calculations in Aluminum 59
3.5 Calculations in Lead 78
3.6 Calculations in Mercury 95
3.7 Calculations in Tin and Indium 100
3.8 Summary and Comparison with Other Work 105

CHAPTER IV: A CONTRIBUTION TO THE THEORY OF SUPERCONDUCTIVITY IN BINARY ALLOYS OF SIMPLE METALS

4.1 Introduction 119
4.2 The Structure-Dependent Energy of a Binary Alloy 121
4.3 Theory of Calculations of Phonon Widths 127
4.4 Theory of Strong-Coupling Superconductivity in Binary Alloys of Simple Metals 140

Page

CHAPTER V: CONCLUSIONS

5.1 Effect of Pressure on Superconductivity 144
5.2 Superconductivity in Binary Alloys 146

APPENDIX A: Configuration Averages 148

APPENDIX B: Equations of Motion 152

REFERENCES 160

CHAPTER I

INTRODUCTION

1.1 Historical Introduction

The liquefaction of helium in 1908 and the subsequent discovery in 1911 of the phenomenon of superconductivity in mercury by H. K. Onnes(1) added a great deal of fascination to the study of the low-temperature properties of metals. Early theoretical studies of superconductivity were mainly thermodynamic and were aided by the discovery by Meissner and Ochsenfeld(2) in 1933 that the magnetic flux in a solid cylinder of a superconducting metal is expelled below the critical temperature. Gorter and Casimir(3) extended the thermodynamic treatment and developed the two-fluid model. In 1935, F. London and H. London(4) developed the electromagnetic equations appropriate for a superconducting medium. Shoenberg(5) and Pippard(6) later observed penetration depth effects predicted by the London theory.

At the same time advances were being made in the understanding of metals, the role of conduction electrons in the screening of the ions and the theory of lattice vibrations. In 1950 Fröhlich(7) suggested that the electron-phonon interaction might be responsible for superconductivity.

The experimental discovery(8) of the isotope effect(9) was a confirmation of the belief that the lattice vibrations of the solid played a role in the phenomenon of superconductivity. In addition, experiments(10,11) that showed an exponential behaviour in the electronic specific heat at very low temperatures added to the belief of the existence of an energy gap. The 1957 theory of Bardeen, Cooper and Schrieffer(12,13) (B.C.S. theory) was based upon a phenomenological attractive phonon-mediated interaction between the conduction electrons. The theory was able to correlate a vast number of observed superconducting effects. Only in the cases in which the properties depended on the detailed nature of the interactions was elaboration of the theory necessary.

In 1960 Giaver(14) was able to determine the energy gap directly with electron tunneling in superconductor-insulator-metal films. The tunneling technique was subsequently developed(15,16) so that anomolies in the current-voltage characteristics could provide information about the phonon density of states in the superconductor as well as the electron density of states. In conjunction with the tunneling experiments, a theory of superconductivity that took into account the instantaneous Coulomb and retarded phonon interactions among the conduction electrons was developed by Eliashberg(17), Gorkov(18), Nambu (19), Morel and Anderson(20), Schrieffer, Scalapino and Wilkins and others(21-23) with a large assist from a theorem on normal metals due to Migdal(24) and information on the phonon density of states as calculated from measurements of the phonon modes by inelastic neutron scattering. Calculations of energy gaps, transition temperatures and other properties of the superconducting state have been made(22,25-31) based on information on the phonon modes and electron-ion scattering cross sections with some success in simple metals and alloys.

Several years after the discovery of superconductivity it was found that pressure could lower the superconducting transition temperature(32,33). With the growth of the technology of high pressures(34,35) and low temperatures, measurements of the effect of pressure on the superconducting transition temperature have been extended and even the question whether pressure can destroy superconductivity has been raised. Much of the early experimental data was fitted to phenomenological formulas that related the transition temperature and the pressure(34). This method of data reduction was due to the open state of the theory of superconductivity prior to the B.C.S. theory. In 1964 Olsen and co-workers(36) made a correlation between the volume dependence of the transition temperature and the B.C.S. attractive interaction. Chester and Jones(37) had first suggested the plotting of experimental results directly as a function of volume and this approach has been followed by others(38,39). The experimental results for the simple metals show a striking linear dependence on volume, at least for the results in the pressure ranges currently available(39).

The development of a theory of strong-coupling superconductivity has provided an impetus for the study of the effect of pressure on superconductivity from a more basic approach. Studies of the effect have been made by a number of superconducting tunneling experiments(40-42). Calculations of the superconducting transition temperature from nearly first principles with reasonable success in simple metals have added belief that at least rudimentary calculations of the effect of pressure will add to the understanding of the subject of superconductivity.

Calculations of the superconducting gap and transition temperature have been made(28,31) in disordered alloys of simple metals. In these calculations the properties of the alloy have been treated as those in a pure simple metal. An average ion approximation has been used and the phonon modes have been treated as in a pure metal. Phonon lifetime effects have been included in a phenomenological way(43) to account for phonon widths due to force constant disorder in alloys. Ng(44) has extended the work of Mattis(45) to obtain an expression for phonon widths in force constant disordered systems in first order time-dependent perturbation theory. First principle calculations of the phonon broadening due to force constant disorder have not as yet been made. The formulation of the structure-dependent energy and effective pairwise interatomic interactions in a binary alloy of simple metals in the pseudopotential theory as suggested by Harrison$^{(46)}$ and carried out by Hayes, Brooks and Bienenstock$^{(47)}$ provides a starting point for the development of expressions for phonon lifetime calculations within pseudopotential theory.

1.2 Scope of Thesis

The work of this thesis can be divided in two parts with results of work on the pressure dependence of superconductivity presented in Chapter III and those on the study of superconductivity in binary alloys in Chapter IV. Chapter II is common to both Chapter III and Chapter IV and presents some of the underlying theory necessary to understand the following chapters. The purpose of Chapter II is not to provide a rigorous review but to give some details of the ideas to be used later and to establish some notation.

In section 2.1 of Chapter II, the Born-von Kármán theory is described and the description of lattice vibrations is carried through to the second-quantized form. In section 2.2 pseudopotential theory is described and in section 2.3 the structure-dependent crystalline energy is introduced with a view to the calculation of phonon dispersion curves. The electron-phonon interaction is reviewed in section 2.4 and an outline of the theory of strong-coupling superconductivity is presented in section 2.5.

Chapter III deals with the effect of pressure on the superconducting transition temperature. In section 3.1 some of the previous work on this topic is discussed. Calculation of the phonon kernel entering the strong-coupling theory by the method of Carbotte and Dynes is reviewed in section 3.2. In section 3.3 the effect of pressure on the phonon and Coulomb kernels of the Eliashberg gap equations is discussed. Sections 3.4 to 3.7 describe the calculations carried out within the strong-coupling formalism in aluminum, lead, mercury, tin and indium. A comparison of this work with other work is given in section 3.8.

In section 4.1 of Chapter IV some of the previous work on alloys of simple metals is discussed. In section 4.2 the structure-dependent energy of a binary alloy is discussed. In section 4.3 the structure-dependent energy is used to describe the lattice dynamics of the alloy and a method of calculating phonon widths with pseudopotentials is outlined. In section 4.4 the theory of superconductivity appropriate for a binary alloy is discussed.

In section 5.1 of Chapter V conclusions are drawn on the work on the effect of pressure on superconductivity. In section 5.2 conclusions on the work on alloys are made.

In Appendix A the configuration averages necessary in the work of Chapter IV are discussed. In Appendix B the equations of motion for the one electron Green's function in a binary alloy are outlined and a perturbation series is developed.

CHAPTER II

PHONONS, THE ELECTRON-PHONON INTERACTION AND STRONG-COUPLING SUPERCONDUCTIVITY

2.1 Phonons and the Born-von Kármán Theory

It is believed that superconducting condensation is caused by an attractive phonon-mediated interaction between the conduction electrons of a metal. Thus a knowledge of the lattice dynamics of the metal is a prerequisite for calculations in superconductivity. One source of information on the phonon modes in metals and alloys is from the inelastic scattering of slow neutrons(48). A Born-von Kármán(49) force constant model is fitted to measurements of the phonon modes along the symmetry directions by the method of linear least squares. The force constants are used to calculate phonon modes in off-symmetry directions and give a complete, if not always completely accurate(50), description of the lattice dynamics of the crystal. In this section, the Born-von Kármán theory is described in some detail. The transformation to normal coördinates is outlined and the description of the lattice dynamics is carried through to the second-quantized form.

The classical Born-von Kármán theory is based on the assumption that the lattice vibrations in a solid can be described in terms of effective interatomic interactions. For a Bravais lattice with N atoms and one atom per unit cell the classical Hamiltonian is

$$H = \sum_{\ell} \frac{\underset{\sim}{p}^2(\ell,t)}{2M} + V(\underset{\sim}{R}(1,t),\ \underset{\sim}{R}(2,t)\ldots\underset{\sim}{R}(N,t)) \qquad (2.1)$$

where $\underset{\sim}{p}(\ell,t)$ and $\underset{\sim}{R}(\ell,t)$ are the momentum and position of the atom of mass M in the ℓ'th cell at time t. $V(\underset{\sim}{R}(1,t)\ldots\underset{\sim}{R}(N,t))$ is the potential energy of the configuration of atoms. The harmonic approximation is achieved by an expansion of the potential energy in a Taylor series including the second-order term, with the derivatives evaluated with all atoms at their equilibrium positions $\underset{\sim}{R}_{\ell}^{0}$ with

$$\underset{\sim}{R}(\ell,t) = \underset{\sim}{R}_{\ell}^{0} + \underset{\sim}{u}(\ell,t) \qquad .(2.2)$$

The $u_{\alpha}(\ell,t)$ with α one of x,y,z are the excursions of the atoms from their equilibrium positions in the designated direction. The Taylor-expanded Hamiltonian in the harmonic approximation is

$$H = \sum_{\ell} \frac{\underset{\sim}{p}^2(\ell,t)}{2M} + V(\underset{\sim}{R}_{1}^{0}\ldots\underset{\sim}{R}_{N}^{0})$$

$$+ \frac{1}{2} \sum_{\substack{\alpha,\beta \\ \ell,\ell'}} \left[\frac{\partial^2 V}{\partial R_{\alpha}(\ell,t)\ \partial R_{\beta}(\ell,t)}\right]_0 u_{\alpha}(\ell,t)\ u_{\beta}(\ell',t) \qquad ,(2.3)$$

where the subscript 0 denotes evaluation at the equilibrium positions. The potential energy of the equilibrium atomic configuration is a constant and can be dropped; the first-order derivative does not appear because it vanishes upon evaluation with all atoms in their equilibrium positions. The atomic force constants $\Phi_{\alpha\beta}(\ell,\ell')$ are defined by

$$\Phi_{\alpha\beta}(\ell,\ell') \equiv \left[\frac{\partial^2 V}{\partial R_\alpha(\ell,t)\ \partial R_\beta(\ell',t)}\right]_0 \qquad .(2.4)$$

The force constant $\Phi_{\alpha\beta}(\ell,\ell')$ gives the force on the atom ℓ in the direction α due to a unit displacement of the atom ℓ' in the direction β. The commutation of the derivatives in equation (2.4) leads to

$$\Phi_{\alpha\beta}(\ell,\ell') = \Phi_{\beta\alpha}(\ell',\ell) \qquad ,(2.5)$$

and for a system with translational symmetry

$$\Phi_{\alpha\beta}(\ell,\ell') = \Phi_{\alpha\beta}(\ell-\ell',0) \qquad .(2.6)$$

Equation (2.6) expresses the fact that in a pure crystal the force constants do not depend upon the absolute position of atoms ℓ and ℓ' but only on their relative separation $\underset{\sim}{R}^0_\ell - \underset{\sim}{R}^0_{\ell'}$.

With the aid of Hamilton's equations of motion and the Hamiltonian

$$H = \sum_{\ell} \frac{\underset{\sim}{p}^2(\ell,t)}{2M} + \frac{1}{2} \sum_{\substack{\alpha,\beta \\ \ell,\ell'}} \Phi_{\alpha\beta}(\ell,\ell')\ u_\alpha(\ell,t)\ u_\beta(\ell',t) \qquad (2.7)$$

equations relating the $u_\alpha(\ell,t)$ are obtained. They are

$$\frac{\partial^2 u_\alpha(\ell,t)}{\partial t^2} = -\frac{1}{M} \sum_{\beta,\ell'} \Phi_{\alpha\beta}(\ell,\ell')\, u_\beta(\ell',t) \qquad .(2.8)$$

These are a set of coupled equations for the excursions from equilibrium. The excursion of one atom is expressed in terms of the excursions of all the other atoms.

For a pure crystal the Hamiltonian of equation (2.7) can be diagonalized by a unitary transformation to normal coördinates,

$$u_\alpha(\ell,t) = \frac{1}{\sqrt{MN}} \sum_{\underset{\sim}{k},\lambda} Q(\underset{\sim}{k};\lambda)\, \xi_\alpha(\underset{\sim}{k};\lambda)\, e^{i\underset{\sim}{k}\cdot\underset{\sim}{R}_\ell^0} \qquad ,(2.9)$$

$$p_\alpha(\ell,t) = \sqrt{\frac{M}{N}} \sum_{\underset{\sim}{k},\lambda} P(\underset{\sim}{k};\lambda)\, \xi_\alpha(\underset{\sim}{k};\lambda)\, e^{i\underset{\sim}{k}\cdot\underset{\sim}{R}_\ell^0} \qquad .(2.10)$$

The time dependence on the right-hand-sides of equations (2.9) and (2.10) is implicit in the $Q(\underset{\sim}{k};\lambda)$ and the $P(\underset{\sim}{k};\lambda)$ and has the harmonic form $e^{-i\omega(\underset{\sim}{k};\lambda)t}$. The wave vector $\underset{\sim}{k}$ takes N equally spaced values in the first Brillouin zone. The index λ, the branch index, takes three values that correspond to the two transverse and one longitudinal branches given by

$$\omega = \omega(\underset{\sim}{k};\lambda) \qquad (2.11)$$

with $\omega(\underset{\sim}{k};\lambda)$ the frequency of the mode with wave vector $\underset{\sim}{k}$ and branch index λ. The vectors $\underset{\sim}{\xi}(\underset{\sim}{k};\lambda)$ satisfy the orthogonality and completeness relations

$$\sum_{\alpha} \xi_{\alpha}^{*}(\underset{\sim}{k};\lambda)\ \xi_{\alpha}(\underset{\sim}{k};\lambda') = \delta_{\lambda\lambda'} \quad ,(2.12)$$

$$\sum_{\lambda} \xi_{\alpha}(\underset{\sim}{k};\lambda)\ \xi_{\beta}^{*}(\underset{\sim}{k};\lambda) = \delta_{\alpha\beta} \quad (2.13)$$

and satisfy

$$\xi_{\alpha}^{*}(\underset{\sim}{k};\lambda) = \xi_{\alpha}(-\underset{\sim}{k};\lambda) \quad .(2.14)$$

Consider the contribution of the component $(\underset{\sim}{k};\lambda)$ of equation (2.9) to $u_{\beta}(\ell',t)$,

$$u_{\beta}(\ell',t) = \frac{1}{\sqrt{MN}}\, Q(\underset{\sim}{k};\lambda)\ \xi_{\alpha}(\underset{\sim}{k};\lambda)\ e^{i\underset{\sim}{k}\cdot\underset{\sim}{R}_{\ell'}^{0}} \quad .(2.15)$$

Equation (2.15) is substituted into equation (2.8) to obtain the set of linear algebraic equations

$$\omega^{2}(\underset{\sim}{k};\lambda)\ \xi_{\alpha}(\underset{\sim}{k};\lambda) = \sum_{\beta} D_{\alpha\beta}(\underset{\sim}{k})\ \xi_{\beta}(\underset{\sim}{k};\lambda) \quad (2.16)$$

where $D_{\alpha\beta}(\underset{\sim}{k})$ is the dynamical matrix of Born and Huang$^{(51)}$,

$$D_{\alpha\beta}(\underset{\sim}{k}) = \frac{1}{M}\sum_{\ell'} \Phi_{\alpha\beta}(\ell,\ell')\ e^{-i\underset{\sim}{k}\cdot(\underset{\sim}{R}_{\ell}^{0}-\underset{\sim}{R}_{\ell'}^{0})} \quad .(2.17)$$

For a pure crystal, that is, for a crystal with translational symmetry, the force constants depend only on the relative distance between the atoms ℓ and ℓ'. With this in mind and the relationship

$$\sum_{\ell'} \Phi_{\alpha\beta}(\ell,\ell') = 0 \tag{2.18}$$

derived from the invariance of the Hamiltonian under a displacement of the entire crystal, the dynamical matrix can be written in the familiar form

$$D_{\alpha\beta}(\underset{\sim}{k}) = \frac{1}{M} \sum_{\substack{m \\ m\neq 0}} \Phi_{\alpha\beta}(m,0) \left(e^{-i\underset{\sim}{k}.\underset{\sim}{R}_m} - 1\right) \quad . \tag{2.19}$$

where $m=\ell-\ell'$.

Equation (2.13) may be written in the form

$$\sum_{\beta}(D_{\alpha\beta}(\underset{\sim}{k}) - \omega^2(\underset{\sim}{k};\lambda)\ \delta_{\alpha\beta})\ \xi_\beta(\underset{\sim}{k};\lambda) = 0 \quad . \tag{2.20}$$

A knowledge of the dynamical matrix $D_{\alpha\beta}(\underset{\sim}{k})$ reduces the problem of generating the frequencies and eigenvectors of the modes $(\underset{\sim}{k};\lambda)$ to that of diagonalizing a three-by-three matrix. The eigenvalues give the frequencies and the eigenvectors are the polarization vectors. Thus the knowledge of the dynamical matrix at every point $\underset{\sim}{k}$ in the first Brillouin zone completely specifies the crystal dynamics of the metal.

For certain symmetry directions in the Brillouin zone the polarization vectors $\underset{\sim}{\xi}(\underset{\sim}{k};\lambda)$ are fixed by symmetry$^{(48)}$. In such directions the frequency can be written as a linear combination of the force constants. In practice the frequencies along the symmetry directions are determined by neutron spectroscopy and the linear relationship between the frequencies and the force constants is used to obtain the force constants by a linear least squares fit(48). Since the amount of orthogonal data available from the experimental measurements is finite, the force constants are fitted in shells of nearest neighbours beginning with the nearest neighbours. Thus the force constants that cannot be fitted due to a lack of orthogonal data refer to the forces between distant neighbours and are set equal to zero; this is reasonable because it is expected that the forces between the atoms are reduced with increasing distance. This finite and hence tractable number of force constants determines the dynamical matrix and hence provides a complete description of the lattice dynamics of the metal. It will be seen later that the dynamical matrix provides all the necessary information on the lattice dynamics for calculations in the theory of superconductivity.

A transformation of the Hamiltonian of equation (2.7) to normal coördinates diagonalizes the Hamiltonian with

$$H = \frac{1}{2} \sum_{\underset{\sim}{k},\lambda} [P^*(\underset{\sim}{k};\lambda)\ P(\underset{\sim}{k};\lambda) + \omega^2(\underset{\sim}{k};\lambda)\ Q^*(\underset{\sim}{k};\lambda)\ Q(\underset{\sim}{k};\lambda)] \tag{2.21}$$

where

$$Q^*(\underset{\sim}{k};\lambda) = Q(-\underset{\sim}{k};\lambda) \quad ,$$

$$P^*(\underset{\sim}{k};\lambda) = P(-\underset{\sim}{k};\lambda) \quad . \tag{2.22}$$

Equation (2.21) is recognized as a harmonic oscillator equation. The quantized Hamiltonian follows from the commutation rules

$$[u_\alpha(\ell,t),\ u_\beta(\ell',t)] = [p_\alpha(\ell,t),\ p_\beta(\ell',t)] = 0 \quad ,$$

$$[u_\alpha(\ell,t),\ p_\beta(\ell',t)] = i\hbar\ \delta_{\ell\ell'}\ \delta_{\alpha\beta} \qquad (2.23)$$

which lead to the equal time commutation rules for the normal coördinates

$$[Q^*(\underset{\sim}{k};\lambda),\ Q(\underset{\sim}{k}';\lambda')] = [P^*(\underset{\sim}{k};\lambda),\ P(\underset{\sim}{k}';\lambda')] = 0 \quad ,$$

$$[Q^*(\underset{\sim}{k};\lambda),\ P(\underset{\sim}{k}';\lambda')] = i\hbar\ \delta_{\underset{\sim}{k}\underset{\sim}{k}'}\ \delta_{\lambda\lambda'} \qquad ,(2.24)$$

where $\hbar$ is Planck's constant divided by 2π. In the standard fashion the harmonic oscillator equation (2.21) can be written in terms of creation and annihilation operators(52) with

$$Q(\underset{\sim}{k};\lambda) = \sqrt{\frac{\hbar}{2\omega(\underset{\sim}{k};\lambda)}}\ (a^\dagger_{-\underset{\sim}{k}\lambda} + a_{\underset{\sim}{k}\lambda}) \qquad ,(2.25)$$

$$P(\underset{\sim}{k};\lambda) = i\ \sqrt{\frac{\hbar\omega(\underset{\sim}{k};\lambda)}{2}}\ (a^\dagger_{\underset{\sim}{k}\lambda} - a_{-\underset{\sim}{k}\lambda}) \qquad .(2.26)$$

The Hamiltonian of equation (2.21) is then

$$H = \sum_{\underset{\sim}{k},\gamma} \hbar\omega(\underset{\sim}{k};\lambda)\ [a^\dagger_{\underset{\sim}{k}\lambda}\ a_{\underset{\sim}{k}\lambda} + \tfrac{1}{2}] \qquad (2.27)$$

where the operators $a^\dagger_{\underset{\sim}{k}\lambda}$, $a_{\underset{\sim}{k}\lambda}$ respectively create and destroy a phonon of wave vector $\underset{\sim}{k}$ and polarization $\underset{\sim}{\xi}(\underset{\sim}{k};\lambda)$. It will be seen later that the Hamiltonian of equation (2.27) enters in the formulation of the strong-coupling theory of superconductivity. In addition, the coupling of the electrons to the phonon field provides the interaction between conduction electrons that leads to a bound state.

2.2 Pseudopotential Theory

In this thesis information on the electron-ion scattering cross section is used in two ways. It will be seen that this information is needed to describe the electron-phonon interaction, that is, it enters in the calculation of the electron-phonon coupling constant. The same information is also required to calculate the structure-dependent conduction electron energy which, along with the Coulomb interaction energy of the bare ions, determines the total structure-dependent energy from which the crystal dynamics of the metal can be determined.

Information on the electron-ion cross section used in this work is based on pseudopotential theory(53-58). In the neighbourhood of the ion site, a valence electron is subject to a large negative Coulomb potential. Also, the Pauli exclusion principle restricts the valence electron state to be orthogonal to the ion core electron states so the valence electron wavefunction has rapid oscillations in the region of the core. These oscillations are manifested in a large kinetic energy of the valence electron in the region of the core. In pseudopotential theory, these two contributions to the valence electron energy are largely cancelled and the net effect is that a reasonably weak potential, the pseudopotential, acts on the valence electron in the region of the core. This allows one to start with a basis of plane waves and use perturbation theory to account for the effects of the relatively weak pseudopotential to calculate properties that depend on the electron-ion interaction.

For the simple metals it is generally sufficient to treat the core electrons in the tight-binding approximation(59) and to neglect any overlap between core electron states on adjacent ion sites. In the tight-binding approximation the set of core wavefunctions that satisfy the Bloch condition are denoted by $\psi_{[nlm;\underset{\sim}{k}]}(r)$ and are defined by

$$\psi_{[nlm;\underset{\sim}{k}]}(r) \equiv \frac{1}{\sqrt{N}} \sum_{\ell} e^{i\underset{\sim}{k}\cdot\underset{\sim}{R}_{\ell}^{0}} \phi_{nlm}(\underset{\sim}{r}-\underset{\sim}{R}_{\ell}^{0}) \qquad (2.28)$$

where $\phi_{nlm}(\underset{\sim}{r}-\underset{\sim}{R}_{\ell}^{0})$ is the core state localized at the site $\underset{\sim}{R}_{\ell}^{0}$ and specified by the principal, orbital and magnetic quantum numbers n,l,m respectively.

A conduction electron state, ψ_v, must be orthogonal to the core states as dictated by the Pauli exclusion principle. The orthogonality can be achieved explicitly by an appropriate subtraction of a linear combination of core states to produce a more accurate conduction state χ_v from an approximate valence wavefunction ψ_v^0:

$$\chi_v = \psi_v^0 - \sum_{\substack{n,l,m\\ \underset{\sim}{k}}} \psi_{[nlm;\underset{\sim}{k}]} \left(\psi_{[nlm;\underset{\sim}{k}]}, \psi_v^0\right) \qquad .(2.29)$$

χ_v is orthogonal to all core states. If ψ_v^0 is a plane wave, ψ_k, then χ_v is an orthogonalized plane wave (O.P.W.)$^{(60)}$. The conduction electron states can be written as a linear combination of orthogonalized plane waves,

$$\psi_v = \sum_{\underset{\sim}{k}} a_{\underset{\sim}{k}} \chi_{\underset{\sim}{k}} \qquad ,(2.30)$$

and it is expected that a relatively small number of orthogonalized plane waves in the expansion will sufficiently describe the conduction state.

With the subscript c as a short-hand notation for $[nlm,\underset{\sim}{k}]$, equations (2.29) and (2.30) can be combined to write the valence wavefunction χ_v as

$$\psi_v = \sum_{\underset{\sim}{k}} a_{\underset{\sim}{k}} \psi_k - \sum_c \psi_c \left(\psi_c, \sum_{\underset{\sim}{k}} a_{\underset{\sim}{k}} \psi_{\underset{\sim}{k}}\right) \qquad .(2.31)$$

A valence pseudowavefunction ϕ_v is defined by

$$\phi_v \equiv \sum_{\underset{\sim}{k}} a_{\underset{\sim}{k}} \psi_{\underset{\sim}{k}} \qquad (2.32)$$

and in terms of this function ψ_v is written as

$$\psi_v = \phi_v - \sum_c \psi_c (\psi_c, \phi_v) \qquad .(2.33)$$

If ψ_v can be expressed in terms of a few orthogonalized plane waves in equation (2.30), then equation (2.32) states that ϕ_v can be expressed in terms of the same number of plane waves.

The pseudopotential can be introduced with the assumption that all the electron states in the solid can be obtained by the solution of the Schrödinger equation

$$H\psi = [-\frac{\hbar^2}{2m} \nabla^2_{\underset{\sim}{r}} + V(\underset{\sim}{r})]\psi = \varepsilon\psi \tag{2.34}$$

where $V(\underset{\sim}{r})$ is a self-consistent potential and m is the electron mass. For a valence state ψ_v equation (2.33) can be used to write

$$H[\phi_v + \sum_c \psi_c(\psi_c, \phi_v)] = H\phi_v - \sum_c \varepsilon_c \psi_c(\psi_c, \phi_v) \tag{2.35}$$

and the equation for the pseudowavefunction is

$$H\phi_v + \sum_c(\varepsilon-\varepsilon_c) \psi_c(\psi_c, \phi_v) = \varepsilon\phi_v \quad . \tag{2.36}$$

With the definition

$$V_R \equiv \sum_c(\varepsilon-\varepsilon_c) \psi_c(\psi_c, \phi_v) \tag{2.37}$$

the equation for the pseudowavefunction is

$$(H+V_R) \phi_v = \varepsilon\phi_v \quad . \tag{2.38}$$

V_R is not a local potential but contains a projection operator. In addition, the energy eigenvalue is explicitly contained in the definition of V_R. The net effect of

$$W(r) \equiv V(r) + V_R \tag{2.39}$$

is a weak potential. W(r) as defined in equation (2.39) is the pseudopotential of Phillips and Kleinman(53).

Austin, Heine and Sham(58) have investigated pseudopotentials and have shown that the most general form of the repulsive potential is

$$V_R \phi = \sum_c (f_c, \phi)\psi_c \tag{2.40}$$

with the f_c completely arbitrary functions. That the f_c can be completely arbitrary seems less unusual if it is noted that any linear combination of core states can be added to the pseudowavefunction of equation (2.32) and it will still satisfy equation (2.38) with the same eigenvalue.

Equation (2.33) can be rewritten as

$$\phi_v = \psi_v + \sum_c \psi_c(f_c, \phi_v) \tag{2.41}$$

within the general formalism. This form, as well as that of equation (2.33), shows that at a long distance from an ion where the core wavefunction can be neglected the pseudowavefunction is equivalent to the true wavefunction. In effect, the potential V(r) has been replaced by a weaker potential with the restriction that at a long distance from the core the pseudowavefunction and the true wavefunction must coincide.

In the foregoing discussion the pseudopotential was thought to be derived in a self-consistent manner so that the effect of the screening by the conduction electrons was included in W(r). In practice an unscreened pseudopotential is derived or chosen within some model. In the conduction electron medium of the metal the bare pseudopotential is screened by the conduction electrons so that in the single particle approximation a valence electron experiences a weaker potential than the bare pseudopotential. In the diffraction model which will be discussed in more detail in section 2.3 a bare pseudopotential w^o is attributed to each ion. The matrix element for the scattering of an electron from a state with wave vector $\underset{\sim}{k}$ to a state with wave vector $\underset{\sim}{k}+\underset{\sim}{q}$ is

$$w^o(\underset{\sim}{q}) = \langle \underset{\sim}{k}+\underset{\sim}{q} | w^o | \underset{\sim}{k} \rangle \tag{2.42}$$

in the local approximation with the matrix element evaluated in a basis of plane wave states $|\underset{\sim}{k}\rangle$. In analogy to the screening of a bare charge in a free electron gas, the screening of the bare pseudopotential is described by a dielectric function $\varepsilon(\underset{\sim}{q})$ with

$$w(\underset{\sim}{q}) = \frac{w^o(\underset{\sim}{q})}{\varepsilon(\underset{\sim}{q})} \quad . \tag{2.43}$$

In this work the Hubbard(61) form of the dielectric function is used. This form includes correlation effects in a phenomenological way. The appropriate dielectric function is

$$\varepsilon(\underset{\sim}{q}) = 1 + \frac{k_s{}^2}{q^2} f(t)\ A(t) \qquad (2.44)$$

with

$$t = \frac{q}{2k_F} \qquad (2.45)$$

where k_F is the Fermi wave vector and

$$f(t) = \frac{1}{2} + \frac{1-t^2}{4t} \ln\left|\frac{1+t}{1-t}\right| \qquad ,(2.46)$$

$$A(t) = 1 - \frac{2t^2}{1 + 4t^2 + \frac{1}{2}(\frac{k_s}{k_F})^2} \qquad .(2.47)$$

The parameter k_s is the Fermi-Thomas(62) screening wave number defined by

$$k_s{}^2 = \frac{4k_F}{\pi\ a_0} \qquad ,(2.48)$$

where a_0 is the Bohr radius,

$$a_0 = \frac{\hbar^2}{me^2} \qquad .(2.49)$$

In equation (2.49) $\hbar$ is Planck's constant divided by 2π, m is the electron mass and e is the unit charge.

If A(t) is set equal to unity in equation (2.44) the resulting dielectric function is the one obtained in the Hartree approximation,

$$\varepsilon(\underset{\sim}{q}) = 1 + 2v(\underset{\sim}{q})\ Q(\underset{\sim}{q}) \qquad ,(2.50)$$

with

$$v(\underset{\sim}{q}) = \frac{4\pi e^2}{q^2} \qquad .(2.51)$$

Q(q) is the polarization function and is related to the function f of equation (2.46) by

$$Q(t) = \frac{{k_s}^2}{8\pi e^2} f(t) \qquad .(2.52)$$

The Fermi-Thomas (F.T.) screening limit results if the long-wavelength limit of the dielectric function is used for all momentum transfers, that is, if the static limit is used. Then

$$Q_{F.T.}(q) = \frac{{k_s}^2}{8\pi e^2} \qquad (2.53)$$

and the screened Coulomb potential V_c seen by a conduction electron due to an impurity of valence number Z is

$$V_c = - \frac{Ze^2}{r} e^{-k_s r} \qquad ,(2.54)$$

so ${k_s}^{-1}$ is a characteristic screening length. A useful property of the Fourier transform of the screened Coulomb potential in a conduction electron medium is

$$\underset{q\to 0}{\text{limit}}\ [-\frac{1}{\Omega_0}\frac{4\pi\ Ze^2}{q^2+k_s{}^2}] = -\frac{2}{3}E_F \qquad ,(2.55)$$

where E_F is the Fermi energy and Ω_0 is the volume per ion.

A pseudopotential based on some model is screened with a dielectric function according to equation (2.43). A particularly simple local pseudopotential is the point-ion pseudopotential$^{(46)}$. The bare potential is

$$w^o(\underset{\sim}{r}) = -\frac{Ze^2}{r} + \beta\ \delta(\underset{\sim}{r}) \qquad .(2.56)$$

The delta-function term simulates the core repulsion due to the Pauli principle. The Fourier transform of this potential, screened with a dielectric function $\varepsilon(\underset{\sim}{q})$ is

$$w(\underset{\sim}{q}) = [-\frac{4\pi\ Ze^2}{q^2} + \beta]/\Omega_0\varepsilon(\underset{\sim}{q}) \qquad .(2.57)$$

The one parameter point-ion pseudopotential has the unattractive feature that it does not vanish for large values of q. This feature can be removed by the introduction of a second parameter r_c so that

$$w(\underset{\sim}{q}) = [-\frac{4\pi\ Ze^2}{q^2} + \frac{\beta}{[1+(qr_c)^2]^2}]/\Omega_0\varepsilon(\underset{\sim}{q}) \qquad .(2.58)$$

For small values of q the pseudopotential of equation (2.58) is nearly identical to that of equation (2.57) and for large values of q it vanishes.

Another pseudopotential that has been widely used is the Ashcroft pseudopotential$^{(63)}$. In real space the potential is zero to a core radius R_c; for separations greater than R_c the potential is the Coulomb potential. The potential is screened and the parameter R_c can be determined by a fit to the experimentally determined band gaps.

The pseudopotentials used in this work are those of Animalu and Heine$^{(64)}$ as tabulated in Harrison$^{(46)}$ and calculated by the method of Heine and Abarenkov$^{(65)}$. In the method of Heine and Abarenkov the atomic energy levels from spectroscopic data are used to give the description of the ion core potential and the core electron wavefunctions. This procedure has the advantage of including exchange and correlation effects that are difficult to calculate from first principles. A sphere of radius R_M is constructed about the ion and the potential for a valence electron in the state with energy E and orbital and magnetic quantum numbers l and m is chosen to be

$$V(r) = -\frac{Ze^2}{r} \quad , \quad r>R_M$$

$$V(r) = -A_l(E) \quad , \quad r<R_M \qquad .(2.59)$$

The wavefunction is joined continuously across the potential discontinuity at R_M. For an eigenstate, $A_l(E)$ is taken from experiment; for intermediate values of E interpolation between the term values is used. This allows the evaluation of the potential and Hubbard(61) screening is used to obtain the screened potential appropriate for a metal.

2.3 Structure-Dependent Crystalline Energy and Pseudopotential Phonon Calculations

In this section the contribution to the total crystalline energy of the structure-dependent conduction-electron energy to second order in the pseudopotential is reviewed. The notation of Harrison(46) is closely followed. The contribution of this energy to the effective ion-ion interaction energy is given. The bare ion-ion interaction energy can be added to the conduction electron contribution and the total structure-dependent energy will be used to calculate phonons in a metal.

The model consists of N atoms of mass M in a volume Ω located at positions $\underset{\sim}{R}_{\ell}$ in a Bravais lattice. To each ion a bare pseudopotential $w^{o}(\underset{\sim}{r}-\underset{\sim}{R}_{\ell})$ is attributed and the bare pseudopotential is screened with an electron gas of appropriate density. The lattice potential for a conduction electron is $W(\underset{\sim}{r})$ where

$$W(\underset{\sim}{r}) = \sum_{\ell} w(\underset{\sim}{r}-\underset{\sim}{R}_{\ell}) \qquad .(2.60)$$

A factorization that is known as the diffraction model can be made if the matrix element $\langle \underset{\sim}{k}+\underset{\sim}{q}|W|\underset{\sim}{k}\rangle$ evaluated in a basis of plane waves is written

$$<\underset{\sim}{k}+\underset{\sim}{q}|W|\underset{\sim}{k}> = \frac{1}{\Omega} \int_{\text{crystal}} e^{-i(\underset{\sim}{k}+\underset{\sim}{q}).r} \sum_{\ell} w(\underset{\sim}{r}-\underset{\sim}{R}_{\ell})\ e^{i\underset{\sim}{k}.\underset{\sim}{r}}\ d^3r \qquad .(2.61)$$

A substitution $\underset{\sim}{x} = \underset{\sim}{r}-\underset{\sim}{R}_{\ell}$ leads to

$$<\underset{\sim}{k}+\underset{\sim}{q}|W|\underset{\sim}{k}> = [\frac{1}{N} \sum_{\ell} e^{-i\underset{\sim}{q}.\underset{\sim}{R}_{\ell}}]\ \frac{N}{\Omega} \int e^{-i(\underset{\sim}{k}+\underset{\sim}{q}).x}\ w(\underset{\sim}{x})$$

$$\times\ e^{i\underset{\sim}{k}.\underset{\sim}{x}}\ d^3x \qquad .(2.62)$$

The structure factor $S(\underset{\sim}{q})$ is defined by

$$S(\underset{\sim}{q}) \equiv \frac{1}{N} \sum_{\ell} e^{-i\underset{\sim}{q}.\underset{\sim}{R}_{\ell}} \qquad (2.63)$$

and with the definition of $<\underset{\sim}{k}+\underset{\sim}{q}|w|\underset{\sim}{k}>$ by

$$<\underset{\sim}{k}+\underset{\sim}{q}|w|\underset{\sim}{k}> = \frac{N}{\Omega} \int e^{i(\underset{\sim}{k}+\underset{\sim}{q}).\underset{\sim}{x}}\ w(\underset{\sim}{x})\ e^{i\underset{\sim}{k}.\underset{\sim}{x}}\ d^3x \qquad ,(2.64)$$

the lattice potential evaluated in a basis of plane waves is

$$<\underset{\sim}{k}+\underset{\sim}{q}|W|\underset{\sim}{k}> = S(\underset{\sim}{q})\ <\underset{\sim}{k}+\underset{\sim}{q}|w|\underset{\sim}{k}> \qquad .(2.65)$$

For all atoms in their equilibrium positions, $\underset{\sim}{R}_{\ell} = \underset{\sim}{R}_{\ell}^{0}$, the structure factor $S(\underset{\sim}{q})$ has the property

$$\begin{aligned} S(\underset{\sim}{q}) &= 1, \quad \text{if } \underset{\sim}{q} \text{ is some reciprocal lattice vector } \underset{\sim}{K}_n, \\ &= 0, \quad \text{otherwise,} \end{aligned} \qquad (2.66)$$

and the potential of equation (2.65) reduces to the usual crystal potential. The potential as written in equation (2.65) depends on a factor $S(\mathbf{q})$ that depends on the ion positions and a factor $\langle\mathbf{k}+\mathbf{q}|w|\mathbf{k}\rangle$ that is independent of the ion arrangement.

The structure-dependent conduction electron energy is calculated in second order perturbation theory with the zero order wavefunctions taken to be plane waves. In second order perturbation theory the valence electron energy is

$$E_{\mathbf{k}} = \frac{\hbar^2 k^2}{2m} + \langle\mathbf{k}|W|\mathbf{k}\rangle$$

$$+ \sum_{\mathbf{q}}{}' \frac{\langle\mathbf{k}|W|\mathbf{k}+\mathbf{q}\rangle \; \langle\mathbf{k}+\mathbf{q}|W|\mathbf{k}\rangle}{\frac{\hbar^2}{2m}\,[\,|\mathbf{k}|^2 - |\mathbf{k}+\mathbf{q}|^2]} \quad .(2.67)$$

The total contribution to the energy per ion from the conduction electron states is a sum of $E_{\mathbf{k}}$ over all states in the Fermi sphere divided by the number of ions N. The three terms that correspond to the three terms of equation (2.67) are

$$E_e = \frac{3}{5}\, Z\, \frac{\hbar^2 k_F^{\,2}}{2m} + Z\, \overline{\langle\mathbf{k}|W|\mathbf{k}\rangle}$$

$$+ \sum_{\mathbf{q}}{}' S^*(\mathbf{q})\; S(\mathbf{q})\; \frac{2\Omega_0}{(2\pi)^3} \int_{\substack{\text{sphere}\\ k_F}} d^3k \; \frac{\langle\mathbf{k}|w|\mathbf{k}+\mathbf{q}\rangle \; \langle\mathbf{k}+\mathbf{q}|w|\mathbf{k}\rangle}{\frac{\hbar^2}{2m}\,[\mathbf{k}^2 - |\mathbf{k}+\mathbf{q}|^2]} \quad ,(2.68)$$

where Z is the ion valence number, Ω_0 is the volume per ion and the bar in the second term denotes the average. The prime in the summation over $\underset{\sim}{q}$ in the third term denotes exclusion of the $\underset{\sim}{q}=0$ term. The structure-dependent conduction electron energy is the last term on the right hand side of equation (2.68). If w in this term is interpreted as a screened pseudopotential, the electron-electron interactions are counted twice and the subtraction of

$$E_{ee} = \frac{1}{2N} \int \rho(\underset{\sim}{r}) \; W_s(\underset{\sim}{r}) \; d^3r \tag{2.69}$$

must be made. $W_s(\underset{\sim}{r})$ is the potential of the screening electrons and $\rho(\underset{\sim}{r})$ is the electron charge density. With the aid of Poisson's equation and the definition of $Q(\underset{\sim}{q})$ in equation (2.52) the structure-dependent conduction electron energy can be written$^{(46)}$

$$E_{sd} = \Omega_0 \sum_{q}{}' \; S^*(\underset{\sim}{q}) \; S(\underset{\sim}{q}) \; \{- Q(\underset{\sim}{q}) \; w(\underset{\sim}{q}) \; w^*(\underset{\sim}{q})$$

$$- \frac{1}{2} \frac{1}{v(\underset{\sim}{q})} \; w_s(\underset{\sim}{q}) \; w_s^*(\underset{\sim}{q})\} \tag{2.70}$$

where the pseudopotential has been localized and

$$w(\underset{\sim}{q}) = w^o(\underset{\sim}{q}) + w_s(\underset{\sim}{q}) \qquad .(2.71)$$

A combination of equations (2.70) and (2.71) leads to

$$E_{sd} = \sum_{\underset{\sim}{q}}{}' \; S^*(\underset{\sim}{q}) \; S(\underset{\sim}{q}) \; E(\underset{\sim}{q}) \tag{2.72}$$

with

$$E(\mathbf{q}) = -\frac{\Omega_0\, q^2}{8\pi\, e^2}\, |w^o(\mathbf{q})|^2 \left(\frac{\varepsilon(\mathbf{q})-1}{\varepsilon(\mathbf{q})}\right) \qquad .(2.73)$$

The indirect ion-ion interaction due to the contribution of the structure-dependent conduction electron density can be found by explicitly writing the structure factors in equation (2.72),

$$E_{sd} = \sum_{\mathbf{q}}{}' \sum_{\ell,\ell'} \frac{1}{N^2}\, E(\mathbf{q})\, e^{-i\mathbf{q}\cdot(\mathbf{R}_\ell-\mathbf{R}_{\ell'})} \qquad .(2.74)$$

The right hand side of equation (2.75) can be separated into two parts

$$E_{sd} = \sum_{\mathbf{q}}{}' \sum_{\substack{\ell,\ell' \\ \ell\neq\ell'}} \frac{1}{N^2}\, E(\mathbf{q})\, e^{-i\mathbf{q}\cdot(\mathbf{R}_\ell-\mathbf{R}_{\ell'})} + \sum_{\mathbf{q}}{}' \frac{1}{N}\, E(\mathbf{q}) \qquad .(2.75)$$

The first term on the right hand side of equation (2.75) can be used to define an effective indirect interatomic potential $V_{IND}(\mathbf{R}_\ell-\mathbf{R}_{\ell'})$ by

$$\sum_{\mathbf{q}}{}' \sum_{\substack{\ell,\ell' \\ \ell\neq\ell'}} \frac{1}{N^2}\, E(\mathbf{q})\, e^{-i\mathbf{q}\cdot(\mathbf{R}_\ell-\mathbf{R}_{\ell'})} = \frac{1}{2N} \sum_{\substack{\ell,\ell' \\ \ell\neq\ell'}} V_{IND}(\mathbf{R}_\ell-\mathbf{R}_{\ell'}) \qquad ,(2.76)$$

so that

$$V_{IND}(\mathbf{R}_\ell-\mathbf{R}_{\ell'}) = \frac{2}{N} \sum_{\mathbf{q}}{}' E(\mathbf{q})\, e^{-i\mathbf{q}\cdot(\mathbf{R}_\ell-\mathbf{R}_{\ell'})} \qquad .(2.77)$$

The second term on the right hand side of equation (2.75) is independent of the ion arrangement. The sum over $\mathbf{q}$ in equation (2.77) can be changed to an integral and the angular integrations performed to obtain(46)

$$V_{IND}(\underset{\sim}{R}) = \frac{\Omega_0}{\pi^2}\int_0^\infty E(q)\,\frac{\sin\,(qR)}{qR}\,q^2 dq \qquad .(2.78)$$

This is a two-body central potential that describes the effective interaction between ions due the conduction electrons.

The total effective two-body interionic potential is the sum of $V_{IND}(R)$ of equation (2.78) and the Coulomb interaction potential $V_c(R)$,

$$V_c(\underset{\sim}{R}) = \frac{Z^2e^2}{R} \qquad ,(2.79)$$

and will be denoted by $V(\underset{\sim}{R})$. The dynamical matrix of equation (2.19) for a system of atoms interacting via a two-body central potential $V(\underset{\sim}{R})$ with

$$V(\underset{\sim}{R}) = \frac{1}{\Omega}\sum_{\underset{\sim}{q}} e^{i\underset{\sim}{q}\cdot\underset{\sim}{R}}\, V(\underset{\sim}{q}) \qquad (2.80)$$

is

$$D_{\alpha\beta}(\underset{\sim}{k}) = \frac{1}{M\Omega_0}\sum_{\kappa_n}\left[V(\underset{\sim}{k}+\underset{\sim}{\kappa}_n)(\underset{\sim}{k}+\underset{\sim}{\kappa}_n)_\alpha(\underset{\sim}{k}+\underset{\sim}{\kappa}_n)_\beta - V(\underset{\sim}{\kappa}_n)(\underset{\sim}{\kappa}_n)_\alpha(\underset{\sim}{\kappa}_n)_\beta\right] \qquad (2.81)$$

where the sum is over all reciprocal lattice vectors. In the case of the potential of equation (2.80), $V(\underset{\sim}{q})$ is

$$V(\underset{\sim}{q}) = \frac{4\pi\ Z^2e^2}{q^2} - \frac{\Omega_0{}^2q^2}{4\pi\ e^2}\left|w^o(\underset{\sim}{q})\right|^2\left(\frac{\varepsilon(\underset{\sim}{q}) - 1}{\varepsilon(\underset{\sim}{q})}\right) \qquad .(2.82)$$

Equations (2.81) and (2.82) can be combined; with

$$F(\underset{\sim}{q}) = \frac{1}{q^2} - \frac{\Omega_0{}^2 q^2}{16\pi^2 \; Z^2 e^4} \left| w^o(\underset{\sim}{q}) \right|^2 \left(\frac{\varepsilon(\underset{\sim}{q}) - 1}{\varepsilon(\underset{\sim}{q})} \right) \qquad ,(2.83)$$

and the square of the ion plasma frequency $\omega_p{}^2$,

$$\omega_p{}^2 = \frac{4\pi \; Z^2 e^2}{M\Omega_0} \qquad ,(2.84)$$

so the dynamical matrix is

$$D_{\alpha\beta}(\underset{\sim}{k}) = \omega_p{}^2 \sum_{\kappa_n} \left[F(\underset{\sim}{k}+\underset{\sim}{\kappa}_n)(\underset{\sim}{k}+\underset{\sim}{\kappa}_n)_\alpha (\underset{\sim}{k}+\underset{\sim}{\kappa}_n)_\beta - F(\underset{\sim}{\kappa}_n)(\underset{\sim}{\kappa}_n)_\alpha (\underset{\sim}{\kappa}_n)_\beta \right] \qquad .(2.85)$$

This is the form of the dynamical matrix used to calculate phonons from pseudopotentials. From equation (2.83) it is seen that the requirements, apart from constants, are the bare pseudopotential $w^o(\underset{\sim}{q})$ and the dielectric function. For any $\underset{\sim}{k}$ in the first Brillouin zone the elements of the dynamical matrix are obtained by a sum over reciprocal lattice vectors. Special care must be taken with the Coulomb sum due to convergence difficulties, but the term can be handled by the usual Ewald(66) technique.

2.4 The Electron-Phonon Interaction

The electron-phonon interaction arises from the interaction potential energy between a conduction electron and an ion(52) of the form $w(\underset{\sim}{r}_i - \underset{\sim}{R}_\ell)$ where $\underset{\sim}{r}_i$ is the position of the i'th electron. The contribution to the total energy of all the electrons interacting with all the ions of the lattice is

$\sum_i W(\underset{\sim}{r}_i)$ where

$$W(\underset{\sim}{r}) = \sum_{\ell} w(\underset{\sim}{r}-\underset{\sim}{R}_{\ell}) \qquad .(2.86)$$

With the electron variables expressed in second quantized form this potential takes the form

$$H = \sum_{\underset{\sim}{k},\underset{\sim}{q},\sigma} \langle\underset{\sim}{k}+\underset{\sim}{q}|W|\underset{\sim}{k}\rangle \; c^{\dagger}_{\underset{\sim}{k}+\underset{\sim}{q},\sigma} \; c_{\underset{\sim}{k},\sigma} \qquad .(2.87)$$

The operators $c^{\dagger}_{\underset{\sim}{k},\sigma}$ and $c_{\underset{\sim}{k},\sigma}$ create and destroy an electron with momentum $\underset{\sim}{k}$ and spin σ. The variable σ has two degrees of freedom corresponding to the two independent degrees of freedom for the electron spin. The matrix element $\langle\underset{\sim}{k}+\underset{\sim}{q}|W|\underset{\sim}{k}\rangle$ can be factored according to the diffraction model (equation (2.65)),

$$\langle\underset{\sim}{k}+\underset{\sim}{q}|W|\underset{\sim}{k}\rangle = S(\underset{\sim}{q}) \; \langle\underset{\sim}{k}+\underset{\sim}{q}|w|\underset{\sim}{k}\rangle \qquad ,(2.88)$$

so that H is

$$H = \sum_{\underset{\sim}{k},\underset{\sim}{q},\sigma} S(\underset{\sim}{q}) \; \langle\underset{\sim}{k}+\underset{\sim}{q}|w|\underset{\sim}{k}\rangle \; c^{\dagger}_{\underset{\sim}{k}+\underset{\sim}{q},\sigma} \; c_{\underset{\sim}{k},\sigma} \qquad .(2.89)$$

The $\underset{\sim}{R}_{\ell}$ in the exponent of $S(\underset{\sim}{q})$ can be written as in equation (2.2),

$$\underset{\sim}{R}_{\ell} = \underset{\sim}{R}_{\ell}{}^{0} + \underset{\sim}{u}(\ell) \qquad ,(2.90)$$

and for small displacements the exponent can be expanded,

$$e^{-i\underset{\sim}{q}\cdot\underset{\sim}{R}_\ell} = e^{-i\underset{\sim}{q}\cdot\underset{\sim}{R}_\ell^0}\,[1 - i\underset{\sim}{q}\cdot\underset{\sim}{u}(\ell)] \quad .(2.91)$$

The leading term on the right hand side of equation (2.91) contributes to the equilibrium energy. The second term leads to the electron-phonon interaction

$$H_{e-p} = \sum_{\underset{\sim}{k},\underset{\sim}{q},\sigma} \frac{1}{N}\sum_\ell -i\underset{\sim}{q}\cdot\underset{\sim}{u}(\ell)\ \langle \underset{\sim}{k}+\underset{\sim}{q}|w|\underset{\sim}{k}\rangle\ e^{-i\underset{\sim}{q}\cdot\underset{\sim}{R}_\ell^0}\ c^\dagger_{\underset{\sim}{k}+\underset{\sim}{q},\sigma}\ c_{\underset{\sim}{k},\sigma} \quad .(2.92)$$

The $\underset{\sim}{u}(\ell)$ can be expanded in terms of normal coördinates (equation (2.9))

$$\underset{\sim}{u}(\ell) = \frac{1}{\sqrt{MN}}\sum_{\underset{\sim}{k}'\lambda} Q(\underset{\sim}{k}';\lambda)\ \underset{\sim}{\xi}(\underset{\sim}{k}';\lambda)\ e^{i\underset{\sim}{k}'\cdot\underset{\sim}{R}_\ell^0} \quad (2.93)$$

so the electron-phonon interaction is

$$H_{e-p} = \frac{1}{\sqrt{MN}}\sum_{\underset{\sim}{k},\underset{\sim}{q},\underset{\sim}{k}'}\ \sum_{\sigma\lambda} Q(\underset{\sim}{k}';\lambda)\ [-i\underset{\sim}{q}\cdot\underset{\sim}{\xi}(\underset{\sim}{k}';\lambda)]$$

$$\times\ \langle \underset{\sim}{k}+\underset{\sim}{q}|w|\underset{\sim}{k}\rangle\ \delta_{\underset{\sim}{k}'-\underset{\sim}{q},\underset{\sim}{\kappa}_n}\ c^\dagger_{\underset{\sim}{k}+\underset{\sim}{q},\sigma}\ c_{\underset{\sim}{k},\sigma} \quad (2.94)$$

with κ_n a reciprocal lattice vector. The relationship

$$\frac{1}{N}\sum_\ell e^{-i(\underset{\sim}{q}-\underset{\sim}{k}')\cdot\underset{\sim}{R}_\ell^0} = \delta_{\underset{\sim}{k}'-\underset{\sim}{q},\underset{\sim}{\kappa}_n} \quad (2.95)$$

has been used to obtain equation (2.94). The $\underset{\sim}{k}'$ sum can be performed; as $\underset{\sim}{k}'$ sweeps the first Brillouin zone, the Kronecker delta will be non-zero for only one value of $\underset{\sim}{k}'$, that with $\underset{\sim}{\kappa}_n+\underset{\sim}{q}=\underset{\sim}{k}'$ in the first Brillouin zone for one and only one reciprocal lattice vector. Since the phonons are completely described in the first Brillouin zone, $\underset{\sim}{k}'$ can be formally replaced by $\underset{\sim}{q}$ where $\underset{\sim}{q}$ in the phonon variables is to be read as reduced to the first Brillouin zone. This is equivalent to treating the phonons in a repeated zone scheme.

With the $\underset{\sim}{k}'$ sum accomplished, equation (2.25) can be used to express $Q(\underset{\sim}{q};\lambda)$ in terms of phonon creation and annihilation operators so that

$$H_{e-p} = \sum_{\underset{\sim}{k},\underset{\sim}{q},\sigma,\lambda} g_{\underset{\sim}{k}+\underset{\sim}{q},\underset{\sim}{k};\lambda}\, c^{\dagger}_{\underset{\sim}{k}+\underset{\sim}{q},\sigma}\, c_{\underset{\sim}{k},\sigma} (a^{\dagger}_{-\underset{\sim}{q}\lambda} + a_{\underset{\sim}{q}\lambda}) \qquad ,(2.96)$$

where $g_{\underset{\sim}{k}+\underset{\sim}{q},\underset{\sim}{k};\lambda}$ is the electron-phonon coupling constant,

$$g_{\underset{\sim}{k}+\underset{\sim}{q},\underset{\sim}{k};\lambda} \equiv -\, i\, \frac{\sqrt{\hbar}}{\sqrt{2\omega(\underset{\sim}{q};\lambda)MN}}\, \underset{\sim}{q}\cdot\underset{\sim}{\xi}(\underset{\sim}{q};\lambda)\ \langle \underset{\sim}{k}+\underset{\sim}{q}|w|\underset{\sim}{k}\rangle \qquad .(2.97)$$

The phonon frequencies and polarization vectors, $\omega(\underset{\sim}{q};\lambda)$ and $\underset{\sim}{\xi}(\underset{\sim}{q};\lambda)$, and the pseudopotential matrix elements $\langle \underset{\sim}{k}+\underset{\sim}{q}|w|\underset{\sim}{k}\rangle$ are necessary to calculate the coupling constant. It will be seen that the electron-phonon interaction Hamiltonian of equation (2.96) is exactly the one that enters the microscopic theory of superconductivity.

2.5 Strong-Coupling Superconductivity

Superconducting condensation is believed to occur when the net force between two conduction electrons of opposite spins and momenta at the Fermi surface is attractive(13,52). Then the electrons form Cooper pairs and become part of a many-electron bound state, the condensate. A negative electron propagating through the metal attracts positive ions, that is, it polarizes the lattice; a second electron may be attracted to the first because of the positive polarization cloud. This attractive force must overcome the screened Coulomb force between the two electrons to produce a net attractive force.

The B.C.S. theory of superconductivity was based on an attractive force between electrons at the Fermi surface described by a constant average interaction V. The B.C.S. theory gave a relationship between the superconducting transition temperature and the interaction which is$^{(13)}$

$$k_B T_c = 1.41 \hbar\omega \, e^{-\frac{1}{N(0)V}} \quad ,(2.98)$$

where ω is an average phonon frequency and N(0) is the single spin electron density of states at the Fermi surface. The details of the interactions are contained in V in an average way and are thus lost. The details of the interaction are contained in the electron-phonon interaction which describes the motion of the ions and hence the lattice polarization, and the screened Coulomb interaction. The Coulomb interaction is a long range instantaneous interaction but the electron-electron interaction mediated by the phonons is local in space but retarded in time so one can appreciate the difficulty in attempting to describe the total interaction in an average way.

The strong-coupling theory of superconductivity takes into account(23,42,67) the retarded nature of the phonon-mediated electron-electron interaction. It is based on the electron-phonon interaction Hamiltonian of equation (2.96) and on instantaneous Coulomb interaction between the conduction electrons. The electronic properties are described in the language of Green's functions by the propagators(42)

$$G_{\uparrow\uparrow}(\underset{\sim}{p},\tau) = -\langle N|T\ c_{\underset{\sim}{p}\uparrow}(\tau)\ c^{\dagger}_{\underset{\sim}{p}\uparrow}(0)|N\rangle \qquad ,$$

$$G_{\downarrow\downarrow}(\underset{\sim}{p},\tau) = -\langle N|T\ c_{\underset{\sim}{p}\downarrow}(\tau)\ c^{\dagger}_{\underset{\sim}{p}\downarrow}(0)|N\rangle \qquad (2.99)$$

where T is Wick's time ordering operator and the thermal averages are in the grand cononical ensemble with

$$\langle 0\rangle \equiv \mathrm{Tr}(e^{-\beta H}\ 0)/\mathrm{Tr}\ e^{-\beta H} \qquad (2.100)$$

where

$$\beta = \frac{1}{k_B T} \qquad (2.101)$$

where k_B is Boltzmann's constant and T is the temperature. In this and the following sections Planck's constant divided by 2π, $\hbar$, will generally be unity in the units that are chosen. In some equations $\hbar$ will be written explicitly, but no confusion should occur. The electron creation and annihilation operators evolve according to

$$c_{\underset{\sim}{p}}(\tau) = e^{H\tau}\ c_{\underset{\sim}{p}}(0)\ e^{-H\tau} \qquad (2.102)$$

in the thermal Green's function formulation(23,68). The two Green's functions of equation (2.99) describe the propagation of spin up and down electrons and holes. These are insufficient to describe a superconductor. For a superconductor it is necessary to introduce the anomolous F and F^+ Green's functions of Gorkov(18) defined by

$$F_{\uparrow\downarrow}(\underset{\sim}{p},\tau) = - \langle N+2|T\, c^{\dagger}_{-\underset{\sim}{p}\downarrow}(\tau)\; c^{\dagger}_{\underset{\sim}{p}\uparrow}(0)\,|N\rangle$$

$$F^{+}_{\downarrow\uparrow}(\underset{\sim}{p},\tau) = - \langle N|T\, c_{-\underset{\sim}{p}\uparrow}(\tau)\; c_{\underset{\sim}{p}\downarrow}(0)\,|N+2\rangle \qquad .(2.103)$$

These describe the pairing of two electrons which disappear into the condensate and the excitation of two electrons out of the condensate.

Nambu(19) formally simplified the problem of treating all four electron Green's functions with the introduction of a two-component spinor field $\psi_{\underset{\sim}{p}}(\tau)$,

$$\psi_{\underset{\sim}{p}}(\tau) = \begin{pmatrix} c_{\underset{\sim}{p}\uparrow}(\tau) \\ \\ c^{\dagger}_{-\underset{\sim}{p}\downarrow}(\tau) \end{pmatrix} \qquad ,(2.104)$$

and in a similar way introduced a one particle Green's function

$$G(\underset{\sim}{p},\tau) = - \langle T\, \psi_{\underset{\sim}{p}}(\tau)\; \psi^{\dagger}_{\underset{\sim}{p}}(0)\rangle \qquad .(2.105)$$

The Green's function of equation (2.105) is a two-by-two matrix with the diagonal components just the usual Green's functions of equations (2.99) and the off-diagonal components the Gorkov F and F^+ functions of equations (2.103).

The next step is to set up a perturbation expansion of $G(\underset{\sim}{p},\tau)$ in terms of the non-interacting electron Green's function $G_0(\underset{\sim}{p},\tau)$ with the Hamiltonian$^{(23)}$

$$H = \sum_{\underset{\sim}{p}} \varepsilon_{\underset{\sim}{p}} \psi^\dagger_{\underset{\sim}{p}} \tau_3 \psi_{\underset{\sim}{p}} + \sum_{\underset{\sim}{q},\lambda} \omega^0(\underset{\sim}{q};\lambda)\, a^\dagger_{\underset{\sim}{q}\lambda} a_{\underset{\sim}{q}\lambda}$$

$$+ \sum_{\underset{\sim}{p},\underset{\sim}{p}',\lambda} g^0_{\underset{\sim}{p},\underset{\sim}{p}';\lambda} \phi_{\underset{\sim}{p}-\underset{\sim}{p}';\lambda} \psi^\dagger_{\underset{\sim}{p}'} \tau_3 \psi_{\underset{\sim}{p}}$$

$$+ \frac{1}{2} \sum_{\substack{\underset{\sim}{p}_1,\underset{\sim}{p}_2 \\ \underset{\sim}{p}_3,\underset{\sim}{p}_4}} \langle \underset{\sim}{p}_3\underset{\sim}{p}_4 | V_c{}^0 | \underset{\sim}{p}_1\underset{\sim}{p}_2 \rangle (\psi^\dagger_{\underset{\sim}{p}_3} \tau_3 \psi_{\underset{\sim}{p}_1}) (\psi^\dagger_{\underset{\sim}{p}_4} \tau_3 \psi_{\underset{\sim}{p}_2})$$

$$+ \text{constant} \qquad ,(2.106)$$

which is just the Hamiltonian of the electron and phonon system with the electron-phonon interaction and the Coulomb interaction between the electrons included in the Nambu notation; τ_1, τ_2, τ_3 are the Pauli spin matrices. $\varepsilon_{\underset{\sim}{p}}$ is the energy, measured relative to the Fermi energy E_F of the electrons in a Bloch state of crystal momentum $\underset{\sim}{p}$. The quantities $\omega^0(\underset{\sim}{q};\lambda)$, $g^0_{\underset{\sim}{p},\underset{\sim}{p}';\lambda}$ and $V_c{}^0$ are the bare phonon frequencies, electron-phonon coupling constant and Coulomb interaction potential. $\phi_{\underset{\sim}{q}\lambda}$ is defined as

$$\phi_{\underset{\sim}{q}\lambda} \equiv a^\dagger_{-\underset{\sim}{q}\lambda} + a_{\underset{\sim}{q}\lambda} \qquad .(2.107)$$

The second term in equation (2.106) is the phonon energy of equation (2.27) exclusive of the zero point energy and the third term is the electron-phonon interaction of equation (2.96).

For the non-interacting system the electron Green's function is

$$G_0(\underset{\sim}{p}, i\omega_n) = [i\omega_n - \varepsilon_{\underset{\sim}{p}} \tau_3]^{-1} \qquad ,(2.108)$$

where

$$G(\underset{\sim}{p}, \tau) = \frac{1}{\beta} \sum_{n=-\infty}^{\infty} e^{-i\omega_n \tau} G(\underset{\sim}{p}, i\omega_n) \qquad (2.109)$$

in the finite temperature formalism with ω_n taking the value $(2n+1)\pi/\beta$. For the fully interacting system the perturbation series for G is written in terms of G_0, the screened Coulomb interaction, the screened electron-phonon interaction and the phonon Green's function

$$D_\lambda(\underset{\sim}{q}, \tau) = - \langle T\{\phi_{\underset{\sim}{q}\lambda}(\tau)\ \phi^\dagger_{\underset{\sim}{q}\lambda}(0)\}\rangle \qquad (2.110)$$

with

$$D_\lambda(\underset{\sim}{q}, \tau) = \frac{1}{\beta} \sum_{n=-\infty}^{\infty} e^{i\nu_n \tau} D_\lambda(\underset{\sim}{q}, i\nu_n) \qquad (2.111)$$

with ν_n taking the value $2n\pi/\beta$.

For the fully interacting system the Dyson equation is

$$[G(\underset{\sim}{p}, i\omega_n)]^{-1} = [G_0(\underset{\sim}{p}, i\omega_n)]^{-1} - \Sigma(\underset{\sim}{p}, i\omega_n) \qquad .(2.112)$$

Several representative terms of G expanded in terms of G_0 are shown in figure (2.1a). Now it must be remembered that the superconducting state is a bound state. A bound state cannot be achieved in finite order perturbation theory. Thus an infinite number of terms must be summed to correctly specify Σ for the superconducting state. In the Nambu self-consistent scheme(19) this is achieved by replacing G_0 in the expansion of Σ by the renormalized electron propagator G. A further simplification arises from a theorem by Migdal(24) which shows that phonon corrections to the electron-phonon vertex are smaller by a factor $(\frac{m}{M})^{\frac{1}{2}}$ where m and M are the electron and ion masses. Thus these corrections can be neglected. The Coulomb corrections to the electron-phonon vertex are also neglected(23). In the Nambu self-consistent scheme the self-energy Σ becomes

$$\Sigma(\underset{\sim}{p},i\omega_n) = -\frac{1}{\beta}\sum_{\underset{\sim}{p}'n'} \tau_3\, G(\underset{\sim}{p}',i\omega_{n'})\tau_3$$

$$\times \{\sum_{\lambda}|g_{p,p';\lambda}|^2\, D_\lambda(\underset{\sim}{p}-\underset{\sim}{p}',i\omega_n-i\omega_{n'}) + V_c(\underset{\sim}{p}-\underset{\sim}{p}')\}. \quad (2.113)$$

The diagrams representing the Nambu approximation are shown in figure (2.1b). The double line represents the renormalized electron propagator G. In this approximation only the nested diagrams as shown in figure (2.1c) are included.

Figure 2.1 (a) Several representative terms in the perturbation expansion of the Green's function G in terms of G_0 (solid line), the bare electron propagator. The dashed line is the screened Coulomb interaction and the wavy line is the renormalized phonon propagator. (b) The self-energy Σ in the Nambu self-consistent scheme. The double line is the renormalized electron propagator. (c) An expansion of Σ of (b) in the Nambu scheme in terms of G_0. Only the nested diagrams are included.

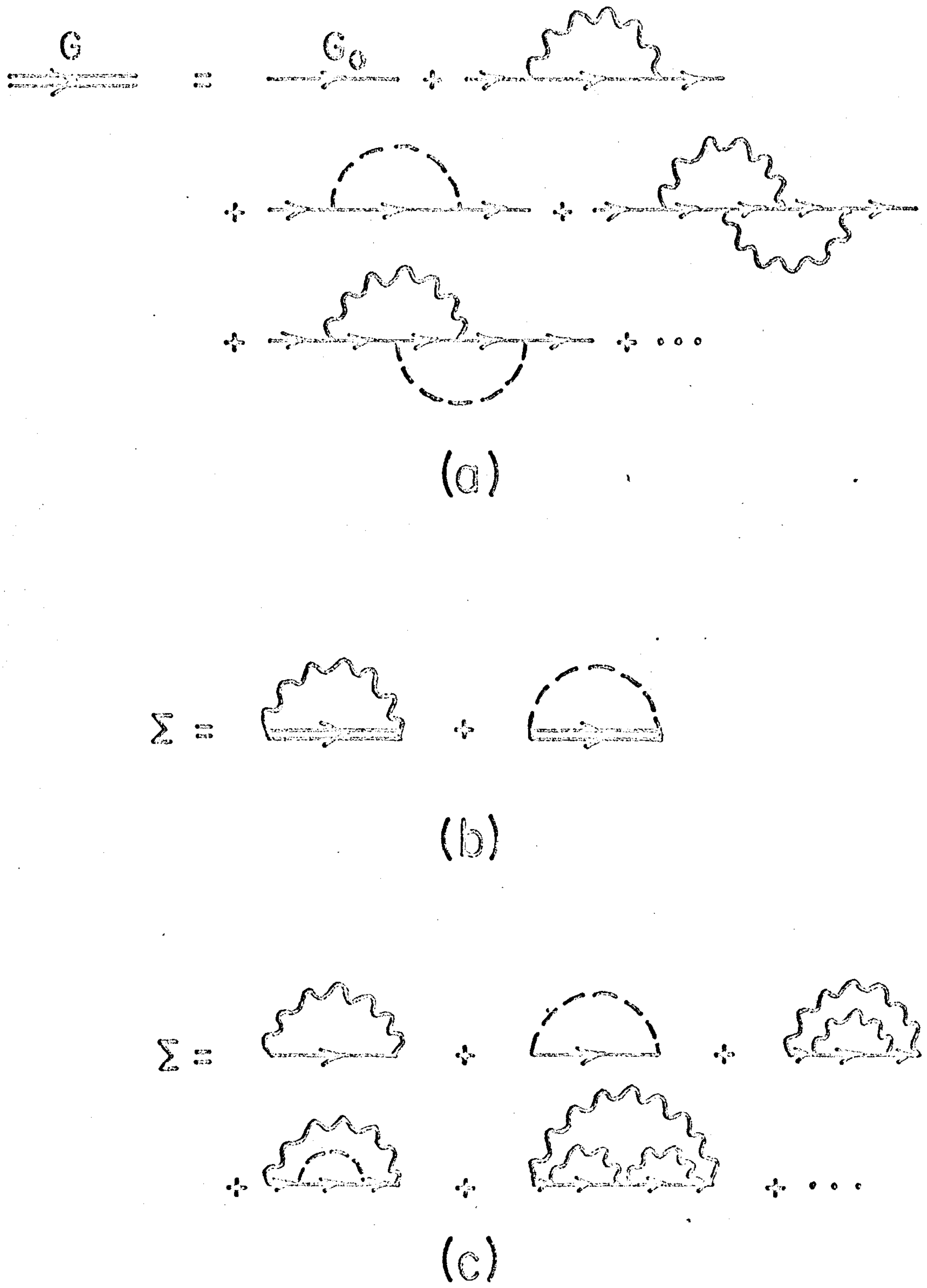

Figure 2.1

The Dyson equation, equation (2.112), and the equation for the self-energy, equation (2.113), serve to determine the electron Green's function G,(23)

$$G(\underset{\sim}{p},\omega) = \left[\frac{\omega Z(\underset{\sim}{p},\omega)1 + \bar{\varepsilon}(\underset{\sim}{p},\omega)\tau_3 + \phi(\underset{\sim}{p},\omega)\tau_1}{\omega^2 Z^2(\underset{\sim}{p},\omega) - \bar{\varepsilon}(\underset{\sim}{p},\omega) - \phi^2(\underset{\sim}{p},\omega)} \right]_{\mathrm{Im}\ \omega = 0^+} \qquad (2.114)$$

where

$$\bar{\varepsilon}(\underset{\sim}{p},\omega) = \varepsilon_{\underset{\sim}{p}} + \chi(\underset{\sim}{p},\omega) \qquad .(2.115)$$

The function $\phi(\underset{\sim}{p},\omega)/Z(\underset{\sim}{p},\omega)$ is the energy gap function $\Delta(\underset{\sim}{p},\omega)$,(23)

$$\Delta(\underset{\sim}{p},\omega) = \phi(\underset{\sim}{p},\omega)/Z(\underset{\sim}{p},\omega) \qquad .(2.116)$$

The major contributions to G come from contributions with $\underset{\sim}{p}$ near the Fermi surface $\underset{\sim}{p}_F$.(23) By straightforward but labourious manipulation, the functions determining G are reduced to one-dimensional form with the momentum evaluated at the Fermi surface. The one-dimensional form consists of two coupled equations for $\Delta(\omega)$ and $Z(\omega)$. These are(25,67,69)

$$\Delta(\omega) = [Z(\omega)]^{-1} \int_0^{\omega_c} d\omega' \ \mathrm{Re}\left[\frac{\Delta(\omega')}{[\omega'^2 - \Delta^2(\omega')]^{\frac{1}{2}}}\right]$$

$$\times \{D_+(\omega,\omega') - D_+(\omega,-\omega') - N(0)\ U_c \tanh(\tfrac{\beta\omega'}{2})\} \qquad (2.117)$$

and

$$[1-Z(\omega)]\omega = \int_0^{\infty} d\omega' \ \mathrm{Re}\left[\frac{\omega'}{[\omega'^2-\Delta^2(\omega')]^{\frac{1}{2}}}\right] \{D_-(\omega,\omega') + D_-(\omega,-\omega')\} \qquad (2.118)$$

where

$$D_{\pm}(\omega,\omega') = \int_{0}^{\infty} d\nu\ \alpha^2(\nu)\ F(\nu)$$

$$\times\ [\{N(\nu) + f(\omega')\}\ \{\frac{1}{\omega'+\omega+\nu+io^+} \pm \frac{1}{\omega'-\omega+\nu-io^+}\}], \quad (2.119)$$

and

$$N(\nu) = [e^{\beta\nu} - 1]^{-1} \quad ,(2.120)$$

$$f(\omega') = [e^{\beta\omega'} + 1]^{-1} \quad ,(2.121)$$

are the Bose and Fermi functions. The two coupled non-linear integral equations can be numerically solved to determine $\Delta(\omega)$ and $Z(\omega)$ by iteration on a computer. The function $\alpha^2(\nu)\ F(\nu)$ and Coulomb pseudopotential U_c completely specify the solutions. These equations are fundamental to the work in this thesis and later their solutions will be discussed with respect to the determination of the gap and the transition temperature of a superconductor.

The function $\alpha^2(\nu)\ F(\nu)$ is given by

$$\alpha^2(\nu)\ F(\nu) = \sum_{\lambda} \int_{S_F} d^2\underset{\sim}{p} \int_{S_{F'}} \Omega d^2\underset{\sim}{p}'\ \frac{|g_{\underset{\sim}{p},\underset{\sim}{p}';\lambda}|^2}{(2\pi)^3\ v_F}\ \delta(\nu-\omega(\underset{\sim}{p}-\underset{\sim}{p}';\lambda) \Big/ \int_{S_F} d^2\underset{\sim}{p} \quad (2.122)$$

where the integrals are over the Fermi surface and v_F is the Fermi velocity. The ingredients necessary to completely specify $\alpha^2(\nu)\ F(\nu)$ are the phonon frequencies and the electron-phonon coupling constant for scattering from one point on the Fermi surface to another. The electron-phonon coupling constant is that of equation (2.97) and is completely determined by the phonon frequencies and polarization vectors and the pseudopotential form factor. The evaluation of $\alpha^2(\nu)\,F(\nu)$ will be discussed in more detail in Chapter III.

U_c is the Coulomb pseudopotential introduced in conjunction with the integration cut-off ω_c in equation (2.117) for $\Delta(\omega)$. A relation between U_c and the screened Coulomb potential V_c is$^{(23)}$

$$U_c = \frac{V_c}{1+N(0)\;V_c\;\ell n(\frac{E_F}{\omega_c})} \qquad .(2.123)$$

N(0) is the single spin electron density of states at the Fermi surface and E_F is the Fermi energy. With a knowledge of ω_c amd screening in the Fermi-Thomas approximation, U_c is completely determined by the electron density.

At zero temperature the equations for $\Delta(\omega)$ and $Z(\omega)$ reduce to

$$\Delta(\omega) = [Z(\omega)]^{-1}\int_0^{\omega_c} d\omega'\;\mathrm{Re}[\frac{\Delta(\omega')}{[\omega'^2-\Delta^2(\omega')]^{\frac{1}{2}}}]$$

$$\times\;\{K_+(\omega,\omega') - N(0)\;U_c\} \qquad ,(2.124)$$

$$[1-Z(\omega)]\omega = \int_0^{\infty} d\omega'\;\mathrm{Re}[\frac{\omega'}{[\omega'^2-\Delta^2(\omega')]^{\frac{1}{2}}}]\;\{K_-(\omega,\omega')\} \qquad (2.125)$$

where

$$K_{\pm}(\omega,\omega') = \int_0^\infty d\nu\ \alpha^2(\nu)\ F(\nu)$$

$$\times\left\{\frac{1}{\omega'+\omega+\nu+io^+} \pm \frac{1}{\omega'-\omega+\nu-io^+}\right\} \quad .(2.126)$$

The zero-temperature version of the gap equations is also specified completely by the function $\alpha^2(\nu)\ F(\nu)$ and the Coulomb pseudopotential. This version is also solved in this thesis to obtain the zero-temperature gap.

The function $\mathrm{Re}\left[\frac{\omega}{[\omega^2-\Delta^2(\omega)]^{\frac{1}{2}}}\right]$ relates the effective electron tunneling density of states $N_T(\omega)$ in the superconductor to that of the normal metal by$^{(23)}$

$$N_T(\omega) = N(0)\ \mathrm{Re}\left[\frac{\omega}{[\omega^2-\Delta^2(\omega)]^{\frac{1}{2}}}\right] \quad .(2.127)$$

Information on $\alpha^2(\nu)\ F(\nu)$ and U_c can be obtained from the structure in the current-voltage characteristics of superconductor-insulator-normal metal or superconductor-insulator-superconductor tunnel junctions. McMillan and Rowell$^{(70,71)}$ have developed a method of inverting the gap equations, equations (2.124) and (2.125), to obtain an $\alpha^2(\nu)\ F(\nu)$ and a U_c that accurately reproduces the tunneling electron density of states of equation (2.127) as obtained from the tunneling experiments. The method provides information on the coupling parameter $\alpha^2(\omega)$, the phonon density of states $F(\omega)$ and the Coulomb pseudopotential U_c. The procedure has been extended by McMillan and Rowell to several metals in which the electron-phonon interaction is sufficiently large for the method to be reasonably accurate. More recently Franck, Keeler and Wu(42) have used the inversion method to obtain information on $\alpha^2(\omega)\ F(\omega)$ in lead under pressure. In Chapter III of this thesis some of the McMillan-Rowell data will be used and more will be said about the work of Franck, Keeler and Wu.

CHAPTER III

THE EFFECT OF PRESSURE ON SUPERCONDUCTIVITY

3.1 Previous Work

Much of the early experimental data on the effect of pressure on superconductivity in simple metals was fitted with phenomenological formulas relating the pressure and the transition temperature. One such formula is the Ginzburg form(72),

$$T_c = A\, e^{-\left[\frac{a}{P_c - P}\right]} \qquad ,(3.1)$$

where T_c is the critical temperature, P is the pressure, A and a are fitted constants and P_c is the extrapolated pressure at which the transition temperature is thought to vanish. With this form Brandt and Ginzburg(34) were able to fit the data for cadmium and zinc.

For the case of weak coupling superconductors the B.C.S. theory proposed a relationship between the critical temperature T_c and an attractive phonon-mediated electron-electron interaction V. It is (equation (2.98))

$$k_B T_c = 1.14\, \hbar\omega\, e^{-\frac{1}{N(0)V}} \qquad (3.2)$$

where $\hbar\omega$ is an average phonon energy and N(0) is the single spin electron density of states at the Fermi surface. The interaction V is an ill-defined quantity and can be thought of as a phenomenological constant for a given material. Olsen and co-workers(36) used equation (3.2) in the form

$$k_B T_c = \hbar\ \Theta_D\ e^{-\frac{1}{N(0)V}} \qquad (3.3)$$

with $\hbar\ \Theta_D$ the Debye energy and postulated that

$$\ell n\left(\frac{k_B T_c}{\hbar\ \Theta_D}\right) \alpha\ \Omega^{-\phi} \qquad (3.4)$$

where Ω is the volume. Equations (3.3) and (3.4) are combined to give for ϕ

$$\phi = \frac{\partial\ \ell n(N(0)V)}{\partial\ \ell n\ \Omega} \qquad .(3.5)$$

They attempted to fit the experimental data with a constant ϕ and in this way obtain information on the variation of the strength of the B.C.S. interaction with pressure. Levy and Olsen(35) fitted their data for aluminum with ϕ=3.7. However, Brandt and Ginzburg were not able to fit the data for cadmium and zinc with a constant ϕ.(34)

Smith and Chu(39) have analyzed the effect of pressure on superconductivity in several metals in the context of a straight-line variation of the transition temperature with volume change and have extended the treatment of equation (3.5) to finite volume changes. They have found that the present experimental results are inconsistent with a constant value of ϕ in aluminum, cadmium and tin, although ϕ is approximately constant for small volume changes.

McMillan$^{(73)}$ has studied the variation of the critical temperature for a niobium-like spectrum $\alpha^2(\omega)\ F(\omega)$ rescaled for various coupling strengths $\alpha^2(\omega)$ and frequency cut-offs of the phonon density of states $F(\omega)$. He used the density of states of niobium as derived from inelastic neutron scattering and a constant α^2 to fit the results to an analytical formula. The formula is written in terms of ω_u, the upper cut-off of the phonon density of states spectrum, and the parameters

$$\lambda = 2 \int \frac{\alpha^2(\omega)\ F(\omega)}{\omega} d\omega \qquad (3.6)$$

and

$$\mu^* = N(0)U_c \qquad .(3.7)$$

The parameter λ is related to the phonon-renormalized electronic effective mass m^* by

$$\frac{m^*}{m} = 1+\lambda \qquad .(3.8)$$

McMillan's formula is

$$k_B T_c = \frac{\hbar\omega_u}{1.45}\ e^{-\left[\frac{1.04(1+\lambda)}{\lambda-\mu^*(1+0.62\lambda)}\right]} \qquad .(3.9)$$

Seiden(74) and Hodder(75) have recently used McMillan's formula to investigate the effect of pressure on the superconducting transition temperature. Seiden has used the point-ion pseudopotential and a jellium model for the phonon frequencies, corrected to give the measured zero pressure transition temperature, to calculate λ. For the phonon shifts Seiden used a Grüneisen parameter which he fitted to reproduce the measured critical temperature change with volume. The work of Hodder is also closely related to this work. He investigated the effect of pressure on the critical temperature of lead. He used the two-Lorenztian model(23) for the density of phonon states and calculated the coupling constant with the point-ion pseudopotential. With the experimental phonon shifts from the tunneling work of Franck and Keeler(41), he obtained good agreement with the experimental pressure dependence of the transition temperature in lead.

In the previous chapter it was seen that the interatomic force constants $\Phi_{\alpha\beta}(\ell-\ell',0)$ can be derived from inelastic neutron scattering measurements of the phonon dispersion curves in high symmetry directions. It was also seen that the interatomic force constants completely determine the lattice dynamics. The dynamical matrix for any wave vector $\underset{\sim}{k}$ is easily constructed from the force constants and the phonon eigenvectors and frequencies follow directly from the diagonalization of the dynamical matrix. In addition to a complete knowledge of the lattice dynamics, a knowledge of the pseudopotential for scattering at the Fermi surface allows the calculation of the electron-phonon coupling constant and $\alpha^2(\omega)\ F(\omega)$. The function $\alpha^2(\omega)\ F(\omega)$ and $N(0)U_c$ permit the evaluation of the Eliashberg gap equations and hence the gap at the gap edge and the critical temperature. In the following sections calculations of $\alpha^2(\omega)\ F(\omega)$ at zero and finite pressure will be described and the Eliashberg gap equations will be solved for the kernels appropriate for zero and finite pressure.

3.2 Calculation of $\alpha^2(\omega)\ F(\omega)$

From the complete knowledge of the lattice dynamics as specified by the Born-von Kármán atomic force constants and the Heine-Abarenkov pseudopotential Carbotte and Dynes$^{(29,30)}$ have evaluated $\alpha^2(\omega)\ F(\omega)$ for some simple metals and Dynes, Carbotte, Taylor and Campbell$^{(31)}$ have evaluated $\alpha^2(\omega)\ F(\omega)$ for an alloy series. In this section the method of evaluating $\alpha^2(\omega)\ F(\omega)$ is discussed.

In the approximation of a spherical Fermi surface and a local pseudopotential the relationship

$$\frac{\Omega \int_{S_F} d^2\underset{\sim}{p} \int_{S_F'} d^2\underset{\sim}{p}' \ \dfrac{f(\underset{\sim}{p}-\underset{\sim}{p}')}{(2\pi)^3\ v_F}}{\int_{S_F} d^2\underset{\sim}{p}} = \frac{N(0)}{8\pi\ k_F{}^2} \int_{<2k_F} \frac{1}{q}\ d^3q\ f(\underset{\sim}{q}) \qquad (3.10)$$

can be used to rewrite $\alpha^2(\omega)\ F(\omega)$ (equation (2.122)) as

$$\alpha^2(\omega)\ F(\omega) = \frac{N(0)}{8\pi\ k_F{}^2} \sum_{\lambda} \int_{<2k_F} \frac{1}{q}\, d^3q\ \frac{|w(\underset{\sim}{q})|^2\ |\underset{\sim}{q}\cdot\underset{\sim}{\xi}(\underset{\sim}{q};\lambda)|^2}{2MN_0\omega}$$

$$\times\ \delta(\omega-\omega(\underset{\sim}{q};\lambda)) \qquad ,(3.11)$$

where N(0) is the free electron value of the single spin electron density of states at the Fermi surface

$$N(0) = \frac{m\ k_F}{2\pi^2} \qquad ,(3.12)$$

and N_0 is the ion number density.

The quantity $\alpha^2(\omega)\ F(\omega)$ is related to the density of phonon states $F(\omega)$

$$F(\omega) = \frac{1}{N_0} \sum_{\lambda} \int_{F.B.Z.} \frac{d^3q}{(2\pi)^3}\ \delta(\omega-\omega(\underset{\sim}{q};\lambda)) \qquad (3.13)$$

with the integral restricted to the first Brillouin zone (F.B.Z.). Gilat and Raubenheimer$^{(76)}$ have constructed a computer programme to diagonalize the dynamical matrix for $\underset{\sim}{q}$ values at the center of small cubes in the irreducible $\frac{1}{48}$ sector of the first Brillouin zone. The irreducible $\frac{1}{48}$ sector of the face-centered cubic lattice is depicted in figure (3.1a). In each cube the gradients of the dynamical matrix with respect to variations in the wave vector $\underset{\sim}{q}$ are also determined and are used to extrapolate to other points in the cube. The extrapolation method reduces the number of cubes to be sampled and reduces the

Figure 3.1 (a) Irreducible $\frac{1}{48}$ sector of the first Brillouin zone for the face-centered cubic structure.

(b) A (001) section of the cone subtended by the irreducible $\frac{1}{48}$ sector. The arc corresponds to a radius $2k_F$ in lead.

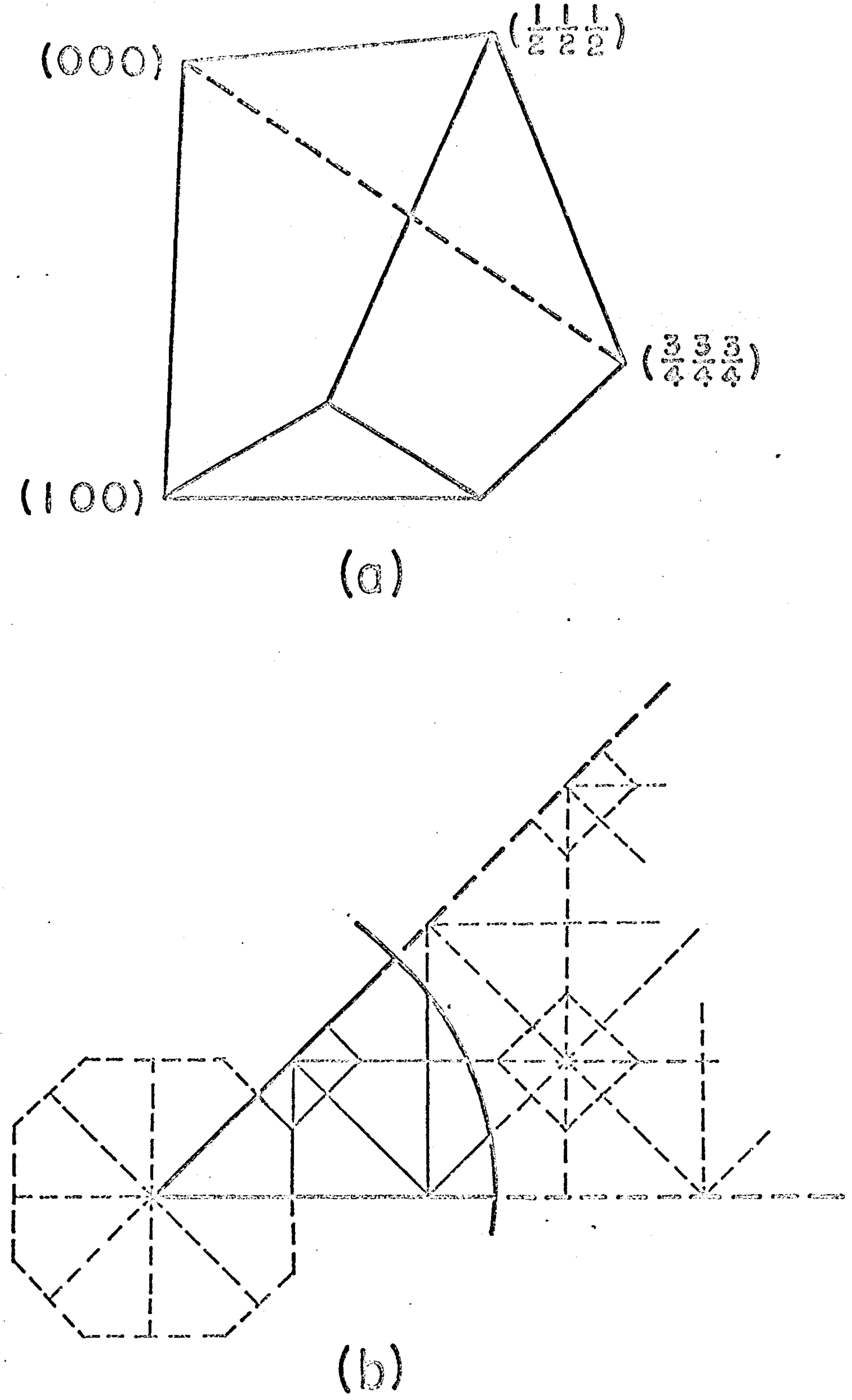

Figure 3.1

computation time for calculating F(ω). The sampling method is good enough to clearly resolve the van Hove(77) singularities.

In the calculation of $\alpha^2(\omega)$ F(ω) the contribution of each cube in the F(ω) calculation is weighted by a $\underset{\sim}{q}$-dependent factor $L_\lambda(\underset{\sim}{q})$,

$$L_\lambda(\underset{\sim}{q}) = \frac{1}{4}\,\frac{m}{M}\,\frac{|\underset{\sim}{q}\cdot\underset{\sim}{\xi}(\underset{\sim}{q};\lambda)|^2}{k_F\; q\; \omega(\underset{\sim}{q};\lambda)}\,|w(\underset{\sim}{q})|^2 \qquad ,(3.14)$$

where now

$$\alpha^2(\omega)\;F(\omega) = \frac{1}{N_0}\sum_\lambda \int_{<2k_F} \frac{d^3q}{(2\pi)^3}\,L_\lambda(\underset{\sim}{q})\;\delta(\omega-\omega(\underset{\sim}{q};\lambda)) \qquad ,(3.15)$$

and the integration must be extended beyond the first Brillouin zone to a sphere of radius $2k_F$ as shown in figure (3.1b). The knowledge that the phonon modes are completely described in the first Brillouin zone and that the first Brillouin zone can be constructed by the 48 cubic symmetry operations on the $\frac{1}{48}$ irreducible sector can be used to extend the integration beyond the Brillouin zone boundary. The phonon modes at any point in the cone subtended by the irreducible $\frac{1}{48}$ sector are equivalent to those in one of the 48 sectors of the first Brillouin zone. A symmetry operation on the eigenvectors at the appropriate point in the irreducible $\frac{1}{48}$ sector constructs the eigenvectors of any phonon mode in the cone. The required transformations are listed by Dynes(78) for face-centered and body-centered cubic lattices.

The $\alpha^2(\omega)\ F(\omega)$ programme developed by Carbotte and Dynes from the Gilat-Raubenheimer programme requires the specification of the phonon modes by a force constant model and a knowledge of the pseudopotential form factor for scattering at the Fermi surface. With this information the evaluation of $\alpha^2(\omega)\ F(\omega)$ is direct and, as previously stated, has been used to calculate the spectrum in some simple metals and alloys.

3.3 The Effect of Pressure on the Coulomb and Phonon Kernels

The calculation of $\alpha^2(\omega)\ F(\omega)$ and the solutions of the Eliashberg gap equations are to be repeated with the metal under conditions of hydrostatic pressure. The zero and finite temperature kernels of the Eliashberg gap equations are completely specified with a knowledge of $\alpha^2(\omega)\ F(\omega)$ and the Coulomb pseudopotential $N(0)U_c$. In this section these two quantities are discussed with a view to their evaluation with the metal under pressure.

The Coulomb pseudopotential $N(0)U_c$ is related to the angular average of the screened repulsive Coulomb interaction between the conduction electrons at the Fermi surface V_c by equation (2.123),

$$N(0)U_c = \frac{N(0)V_c}{1+N(0)V_c\ \ell n(\frac{E_F}{\omega_c})} \qquad .(3.16)$$

In the Fermi-Thomas screening approximation $N(0)V_c$ is$^{(20)}$

$$N(0)V_c = \frac{k_s^2}{8k_F^2} \ln\left[\frac{k_s^2 + 4k_F^2}{k_s^2}\right] \qquad (3.17)$$

where k_s is the Fermi-Thomas screening parameter. Equations (3.16) and (3.17) can be used to show that $N(0)U_c$ varies more slowly than $1/k_F$ with volume change. This variation is very small and $N(0)U_c$ can be considered to be a constant for the purposes of this work.

The calculation of $\alpha^2(\omega)\ F(\omega)$ under pressure presents much more difficulty. There are as yet no extensive measurements of the phonon dispersion curves by inelastic neutron scattering in materials under pressure. Some information on the long-wavelength shifts is available from sound velocity measurements. These results are given in the form of mode Grüneisen parameters$^{(79)}$ $\gamma(\underset{\sim}{q};\lambda)$

$$\gamma(\underset{\sim}{q};\lambda) = \frac{\partial \ \ln\ \omega(\underset{\sim}{q};\lambda)}{\partial\ \ln\ \Omega} \qquad ,(3.18)$$

where Ω is the volume. A small amount of information for lead is available from superconducting tunneling experiments under conditions of hydrostatic pressure$^{(40-42)}$.

The simplest approximation that can be made is to assume that all phonon modes shift according to an average Grüneisen parameter γ. This is a simplification that may not be altogether warranted in a final analysis but insofar as more detailed information is only scantily available this appears to be a reasonable starting point. Some information on the phonon frequency shifts can also be obtained from pseudopotential calculations at zero and finite volume changes. Calculations of mode Grüneisen parameters have been made in several alkali metals by Wallace(80) with the use of pseudopotentials.

In addition to the phonon frequencies and eigenvectors, the pseudopotential for scattering at the Fermi surface is necessary to evaluate $\alpha^2(\omega)\ F(\omega)$ in equation (3.15) at finite pressure. With the phonon frequencies and eigenvectors specified, the pseudopotential to be determined at finite pressure enters in the calculation of $\alpha^2(\omega)\ F(\omega)$ through the $|w(\underset{\sim}{q})|^2$ factor in the coupling constant. The screened pseudopotential $w(\underset{\sim}{q})$ is

$$w(\underset{\sim}{q}) = \frac{1}{\Omega_0}\frac{v^0(\underset{\sim}{q})}{\varepsilon(\underset{\sim}{q})} \tag{3.19}$$

where $v^0(\underset{\sim}{q})$ is related to the bare pseudopotential $w^o(\underset{\sim}{q})$ by the volume per ion Ω_0. The procedure used in this work to obtain the pseudopotential for finite volume changes was to assume that $v^0(\underset{\sim}{q})$ does not change for the volume changes considered. The volume dependence of $w(\underset{\sim}{q})$ in equation (3.19) is then contained in the dielectric function $\varepsilon(\underset{\sim}{q})$ and the volume factor Ω_0. This procedure neglects any energy dependence contained in $v^0(\underset{\sim}{q})$ by virtue of its dependence on the Heine-Abarenkov parameters $A_l(E)$, that is A_0, A_1, A_2 (the A_l for l greater than 2 are taken to be equal to A_2).

This uncertainty only affects the coupling constant since the phonon frequencies and eigenvectors are determined separately.

Within the assumed model the calculations can now be performed. The Born-von Kármán force constants determine the lattice dynamics of the metal at standard volume. The spectrum $\alpha^2(\omega)\ F(\omega)$ can be determined from the force constants and the pseudopotential by the method of Carbotte and Dynes. At finite pressure the phonon frequencies are to be shifted with a constant Grüneisen parameter γ and the pseudopotential rescreened with the dielectric function for the electron density of the compressed metal. The change in the Coulomb pseudopotential $N(0)U_c$ is known to be small. The calculations of Carbotte and Dynes can be repeated with the metal under pressure.

3.4 Calculations in Aluminum

The spectrum $\alpha^2(\omega)\ F(\omega)$ for aluminum at standard volume was calculated from equation (3.15),

$$\alpha^2(\omega)\ F(\omega) = \frac{1}{N_0} \sum_\lambda \int \frac{d^3q}{(2\pi)^3} L_\lambda(\underset{\sim}{q})\ \delta(\omega-\omega(\underset{\sim}{q};\lambda)) \qquad (3.20)$$

with

$$L_\lambda(\underset{\sim}{q}) = \frac{1}{4}\frac{m}{M}\frac{|\underset{\sim}{q}.\underset{\sim}{\xi}(\underset{\sim}{q};\lambda)|^2}{k_F\ q\ \omega(\underset{\sim}{q};\lambda)}\ |w(\underset{\sim}{q})|^2 \qquad .(3.21)$$

Information on the phonons was taken from the Born-von Kármán force constant fit to the phonon dispersion curves measured by inelastic neutron scattering by Gilat and Nicklow(81). The pseudopotential form factor of Animalu and Heine(64) as tabulated by Harrison(46) was used for the electron-ion scattering cross section. The calculated spectrum is shown in figure (3.2). This calculation has been previously performed by Carbotte and Dynes(29) and is not new.

At finite pressure the calculations were carried out at 2½% and 5% volume changes. The Heine-Abarenkov pseudopotential was rescreened according to equation (3.19),

$$w(\underset{\sim}{q}) = \frac{1}{\Omega_0}\frac{v^0(\underset{\sim}{q})}{\varepsilon(\underset{\sim}{q})} \qquad ,(3.22)$$

for the two volume changes. The screened pseudopotential form factors for 0% and 5% volume changes are compared in figure (3.3). The phonon energies were shifted by a constant Grüneisen parameter $\gamma = 2.6$ according to

$$\omega_{\frac{\Delta\Omega}{\Omega_s}} = \beta\omega_0 \qquad (3.23)$$

where

$$\beta = (1 - \gamma\frac{\Delta\Omega}{\Omega_s}) \qquad .(3.24)$$

Here Ω is the volume and Ω_s is the standard or zero pressure volume. The value $\gamma = 2.6$ for the Grüneisen parameter is an approximate average of the microscopic Grüneisen parameters of several branches of the acoustic spectrum in

Figure 3.2 $\alpha^2(\omega)\,F(\omega)$ spectra in aluminum for volume decreases of 0% (solid line), 2½% (long-dashed line) and 5% (short-dashed line) versus the phonon energy ω. The Grüneisen parameter is 2.6.

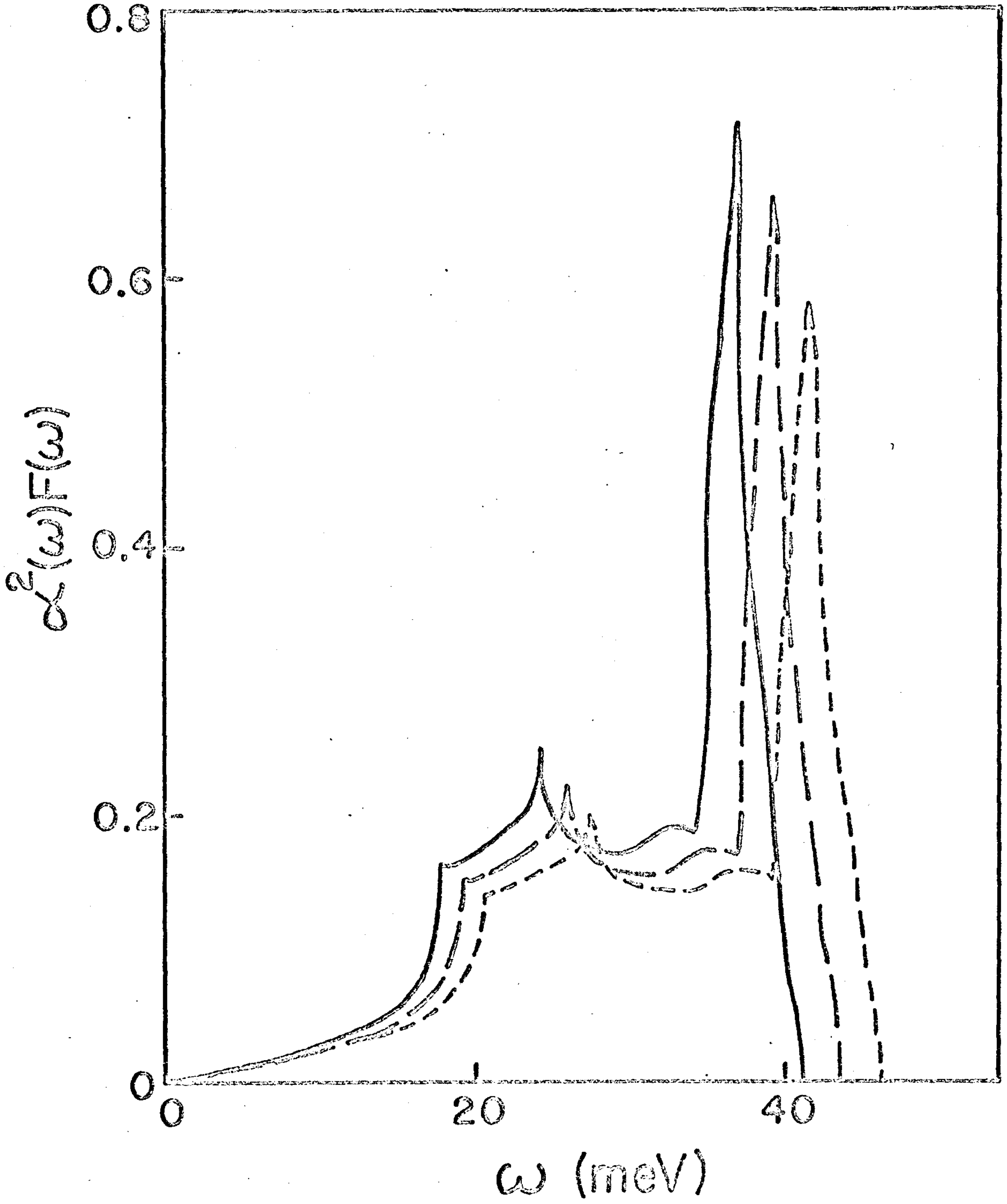

Figure 3.2

Figure 3.3 The Heine-Abarenkov pseudopotential form factor in aluminum at standard volume (solid line) and the form factor rescreened for a 5% volume decrease (dashed line) versus the momentum transfer $q/2k_F$.

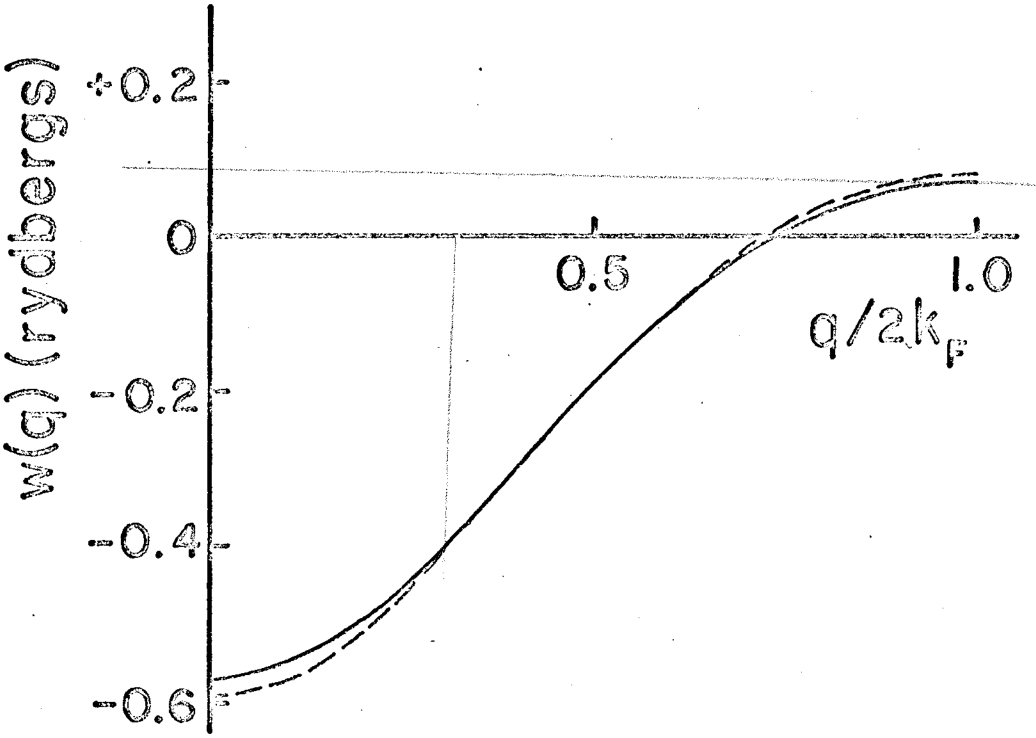

Figure 3.3

aluminum(79). The spectra calculated for 2½% and 5% volume changes are compared to the zero pressure spectrum in figure (3.2). The shift to higher energies is clearly evident and a general lowering of the spectra at higher pressures is evident, although the general shape of the spectra is not altered.

The zero temperature Eliashberg gap equations, equations (2.124) and (2.125),

$$\Delta(\omega) = [Z(\omega)]^{-1} \int_0^{\omega_c} d\omega' \ \mathrm{Re}\left[\frac{\Delta(\omega')}{[\omega'^2-\Delta^2(\omega')]^{\frac{1}{2}}}\right] \{K_+(\omega,\omega') - N(0)U_c\} \qquad ,(3.25)$$

$$[1-Z(\omega)]\omega = \int_0^{\infty} d\omega' \ \mathrm{Re}\left[\frac{\omega'}{[\omega'^2-\Delta^2(\omega')]^{\frac{1}{2}}}\right] \{K_-(\omega,\omega')\} \qquad ,(3.26)$$

with

$$K_\pm(\omega,\omega') = \int_0^{\infty} d\nu \ \alpha^2(\nu) \ F(\nu) \times \left\{\frac{1}{\omega'+\omega+\nu+io^+} \pm \frac{1}{\omega'-\omega+\nu-io^+}\right\} \qquad (3.27)$$

were solved the $\alpha^2(\omega)\ F(\omega)$ spectra of figure (3.2). For the zero pressure (P=0) spectrum $N(0)U_c$ was fixed to reproduce the measured gap at the gap edge Δ_0,

$$\mathrm{Re}\{\Delta(\Delta_0)\} = \Delta_0 \qquad .(3.28)$$

With $\Delta_0(P=0) = 0.18$ meV, $N(0)U_c$ was found to be 0.16.

$N(0)U_c$ was kept fixed at the same value for the solutions at 2½% and 5% volume change.

An example of the gap functions $\Delta_1(\omega)$ and $\Delta_2(\omega)$ with

$$\Delta(\omega) = \Delta_1(\omega) + i\,\Delta_2(\omega) \tag{3.29}$$

for standard volume are shown in figure (3.4). In figures (3.5a) and (3.5b) solutions for 2½% and 5% volume changes are given. These solutions were calculated with a Grüneisen parameter $\gamma=2.22$; this will be explained later. However, the main features correspond to the solutions for the spectra of figure (3.2). The shifts to higher energies of the peaks in the $\alpha^2(\omega)\,F(\omega)$ spectra with decreasing volume are reproduced. There is a general decrease in the gap functions with decreasing volume and it is evident that this effect is more pronounced than the shifts in the $\alpha^2(\omega)\,F(\omega)$ spectra of figure (3.2).

For the spectra of figure (3.2) the calculated gaps were 0.18 meV, 0.079 meV, 0.032 meV for volume changes of 0%, 2½% and 5%. In order to obtain the transition temperatures corresponding to the calculated gap values the B.C.S. ratio which relates the gap Δ_0 and the transition temperature T_c by

$$\frac{2\Delta_0}{k_B T_c} = 3.52 \tag{3.30}$$

was used. The transition temperatures for 2½% and 5%

Figure 3.4 The gap functions $\Delta_1(\omega)$ (solid line) and $\Delta_2(\omega)$ (dashed line) in aluminum at standard volume versus the energy ω.

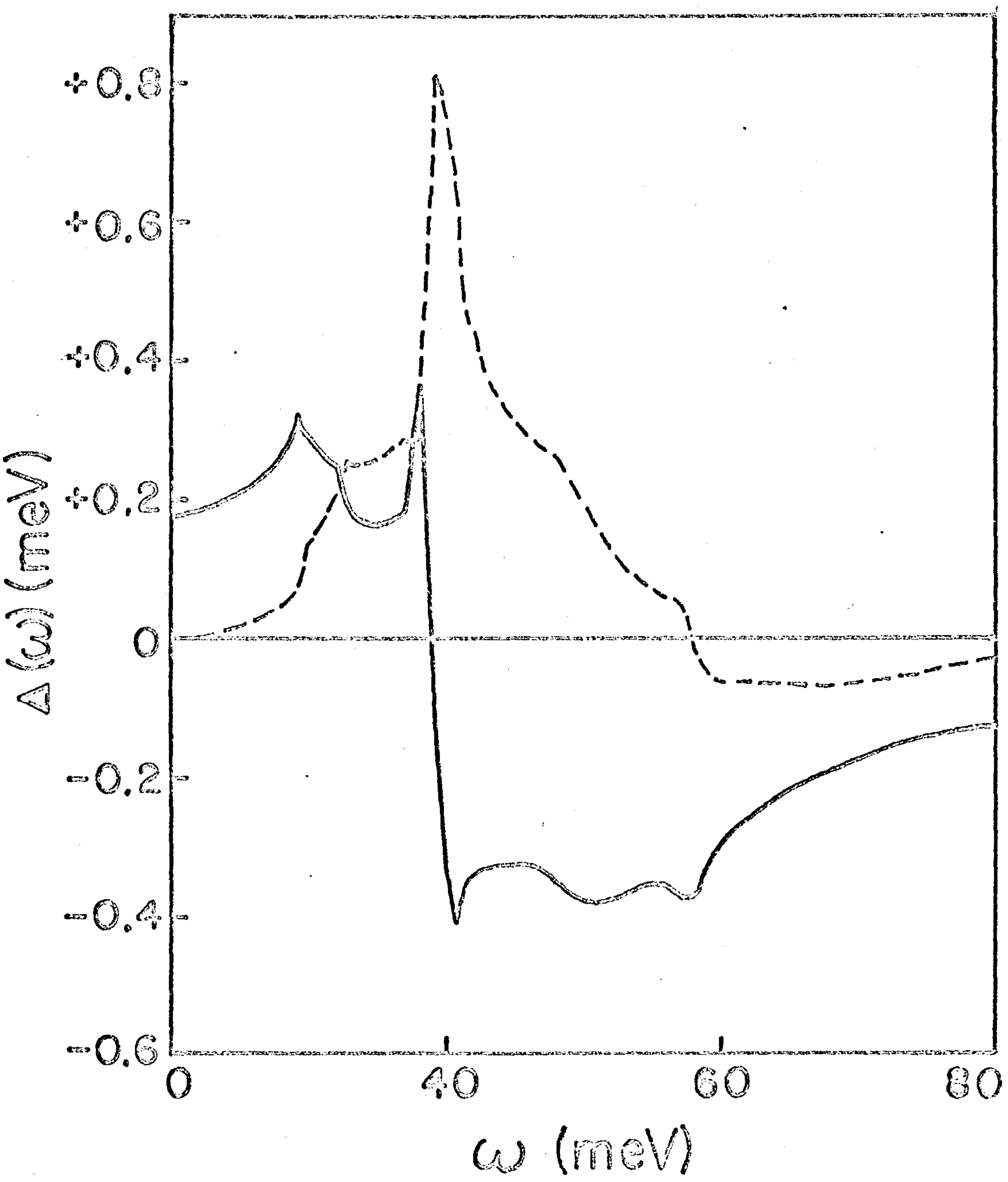

Figure 3.4

Figure 3.5 (a) The gap function $\Delta_1(\omega)$ (solid line) and $\Delta_2(\omega)$ (dashed line) in aluminum for a 2½% volume decrease versus the energy ω.

(b) The gap functions $\Delta_1(\omega)$ (solid line) and $\Delta_2(\omega)$ (dashed line) in aluminum for a 5% volume decrease versus the energy ω.

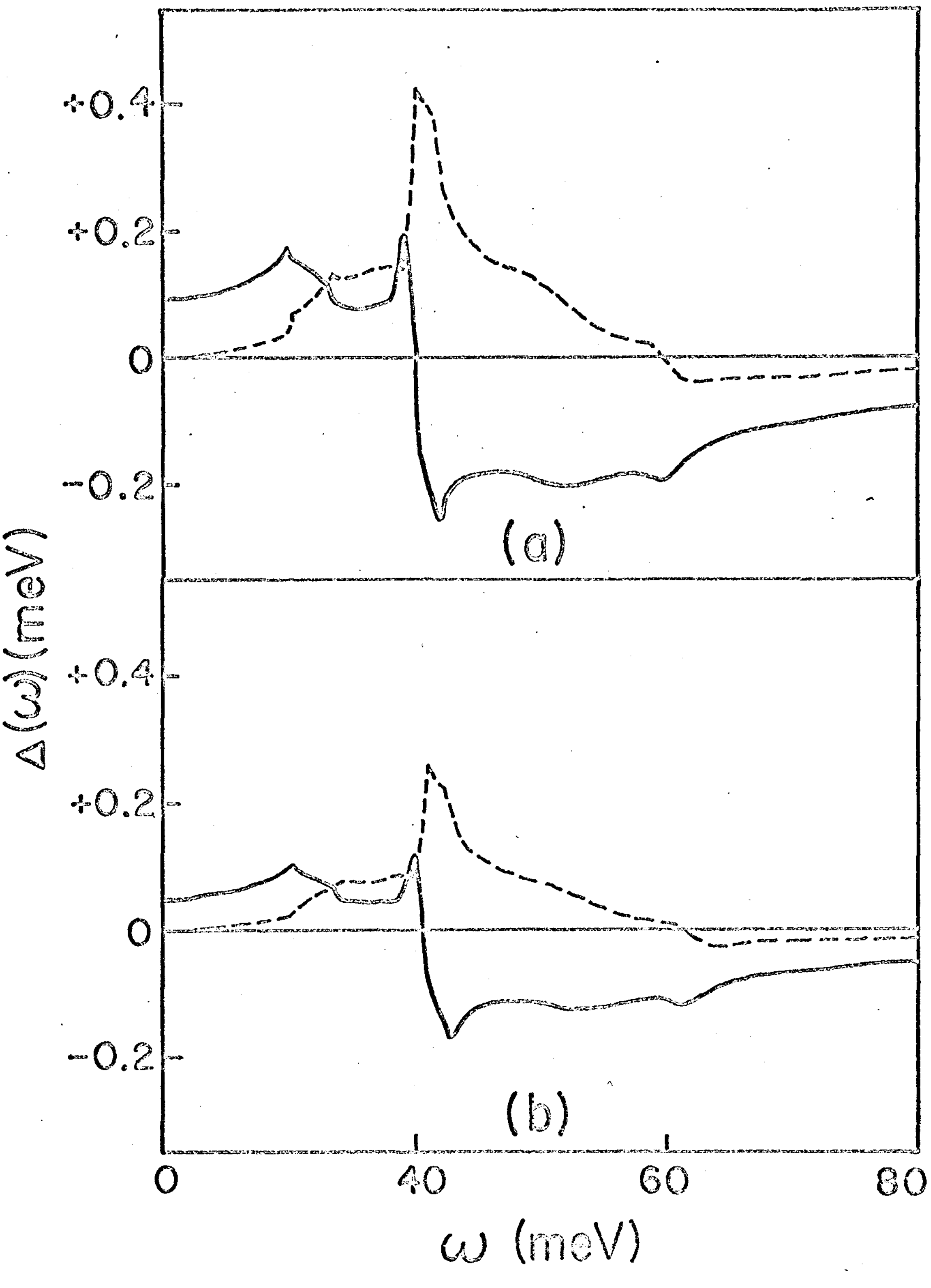

Figure 3.5

volume changes are plotted as ratios of the zero pressure transition temperature in figure (3.6). The calculated values are compared with an extrapolation of the straight line variation quoted by Smith and Chu(39). The ratio for the 2½% volume change is low whereas the ratio for the 5% volume change agrees fairly well with a straight line extrapolation of the existing data.

As has already been noted, the spectra of figure (3.2) indicate that the general shape of $\alpha^2(\omega)\ F(\omega)$ is not altered at finite pressure except for the general shift to higher energies and a general lowering on the vertical scale. To investigate the dependence of $\alpha^2(\omega)\ F(\omega)$ on the rescreened pseudopotential at 2½% volume change a calculation was performed without rescreening the pseudopotential. In figure (3.7), this spectrum is compared with the spectrum at 2½% volume change of figure (3.2). From figure (3.7) it is evident that the effect of the rescreened pseudopotential is essentially a constant scaling factor that shifts $\alpha^2(\omega)\ F(\omega)$ upwards by a small amount.

The small scaling factor that shifts the spectrum upward due to rescreening can be determined in the following way. If $\alpha^2(\omega)\ F(\omega)$ of equation (3.20) is multiplied by ω and an integration over all energies performed the equation is(73)

$$\int_0^\infty d\omega\ \omega\ \alpha^2(\omega)\ F(\omega) = \int_0^\infty d\omega\ \omega\ \frac{1}{N_0} \sum_\lambda \int_{<2k_F} \frac{d^3q}{(2\pi)^3}$$

Figure 3.6 A comparison of the calculated variation of the transition temperature T_c with volume change $-\frac{\Delta\Omega}{\Omega_s}$ in aluminum for a Grüneisen parameter $\gamma=2.60$ (circled points) and $\gamma=2.22$ (boxed points) with the experimental straight line variation. The dashed extension of the solid line is an extrapolation of the existing experimental data.

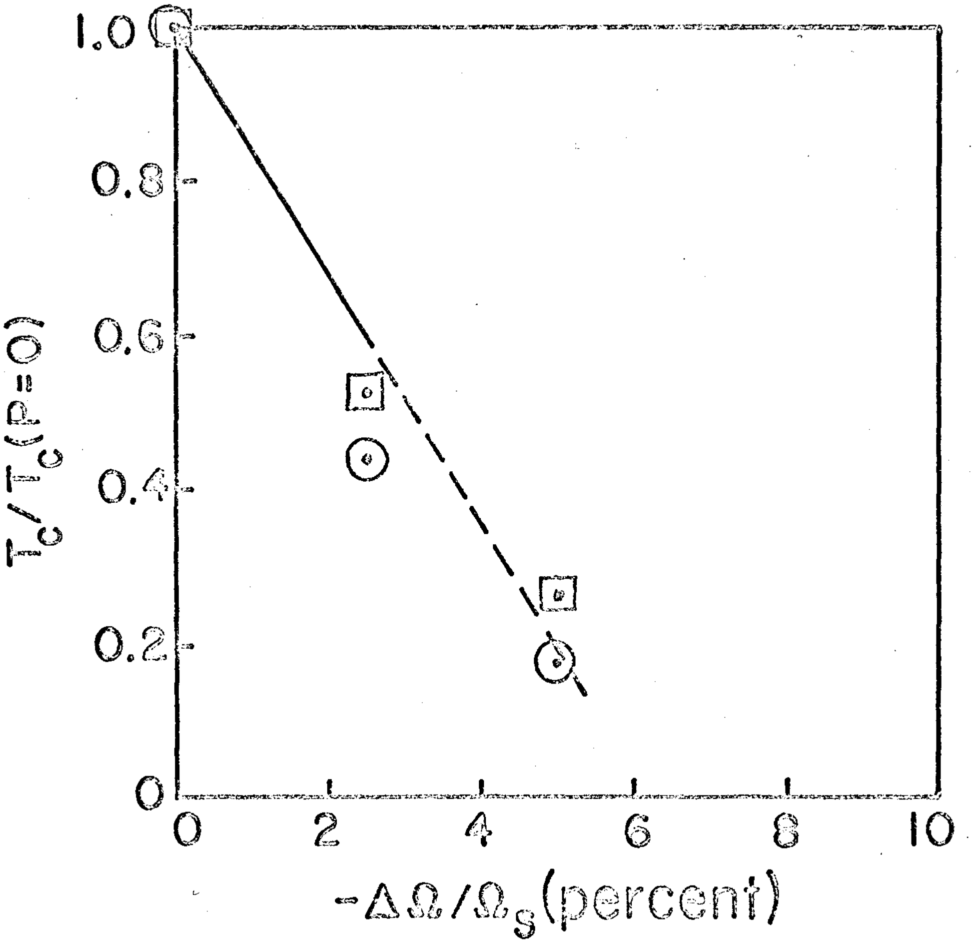

Figure 3.6

Figure 3.7 $\alpha^2(\omega)\ F(\omega)$ spectrum in aluminum for a $2\frac{1}{2}\%$ volume decrease calculated without rescreening the pseudopotential (solid line) and the $\alpha^2(\omega)\ F(\omega)$ spectrum for a $2\frac{1}{2}\%$ volume decrease of figure 3.2 (dashed line) versus the phonon energy ω.

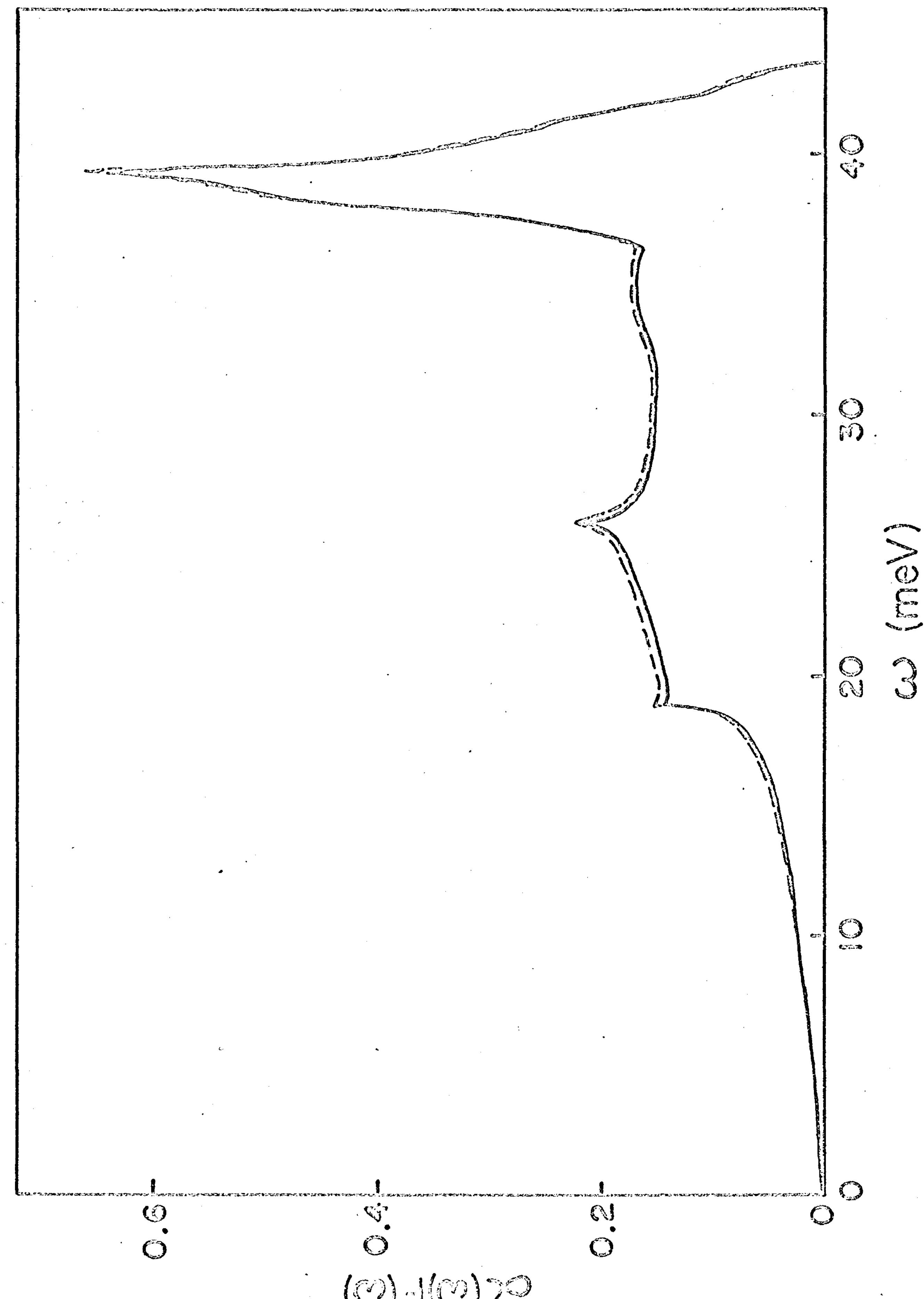

Figure 3.7

$$\times \left[\frac{1}{4}\,\frac{m}{M}\,\frac{|\underset{\sim}{q}.\underset{\sim}{\xi}(\underset{\sim}{q};\lambda)|^2}{k_F\; q\; \underset{\sim}{\omega}(\underset{\sim}{q};\lambda)}\;|w(\underset{\sim}{q})|^2\right]\;\delta(\omega-\omega(\underset{\sim}{q};\lambda)) \qquad .(3.31)$$

The ω integration on the right hand side can be performed due to the delta-function. The resulting equation is

$$\int_0^\infty d\omega\;\omega\;\alpha^2(\omega)\;F(\omega) = \frac{1}{N_0}\sum_\lambda \int_{<2k_F} \frac{d^3q}{(2\pi)^3}\;\frac{1}{4}\;\frac{m}{M}\;\frac{|\underset{\sim}{q}.\underset{\sim}{\xi}(\underset{\sim}{q};\lambda)|^2}{k_F q}\;|w(\underset{\sim}{q})|^2 \qquad .(3.32)$$

The closure relationship for the polarization vectors (equation (2.13)),

$$\sum_\lambda \xi_\alpha(\underset{\sim}{q};\lambda)\;\xi^*_\beta(\underset{\sim}{q};\lambda) = \delta_{\alpha\beta} \qquad ,(3.33)$$

can be used on the right hand side of equation (3.32) to obtain

$$\int_0^\infty d\omega\;\omega\;\alpha^2(\omega)\;F(\omega) = \frac{1}{N_0}\int_{<2k_F} \frac{d^3q}{(2\pi)^3}\;\frac{1}{4}\;\frac{m}{M}\;\frac{q}{k_F}\;|w(\underset{\sim}{q})|^2 \qquad ,(3.34)$$

and the angular integration can be performed to obtain

$$\int_0^\infty d\omega\;\omega\;\alpha^2(\omega)\;F(\omega) = \frac{m}{8\pi^2\;Mk_F\;N_0}\int_0^{2k_F} q^3dq\;|w(\underset{\sim}{q})|^2 \qquad .(3.35)$$

With q in units of $2k_F$, equation (3.35) is

$$\int_0^\infty d\omega\;\omega\;\alpha^2(\omega)\;F(\omega) = \text{constant} \times \int_0^1 t^3dt\;|w(t)|^2 \qquad ,(3.36)$$

where

$$t = \frac{q}{2k_F} \qquad .(3.37)$$

Equation (3.36) can be used to rescale $\alpha^2(\omega)\ F(\omega)$ by a factor B,

$$B_{\frac{\Delta\Omega}{\Omega_s}} = \frac{\left[\int_0^1 dt\ t^3\ |w(t)|^2\right]_{\frac{\Delta\Omega}{\Omega_s}}}{\left[\int_0^1 dt\ t^3\ |w(t)|^2\right]_0} \qquad .(3.38)$$

The parameter B can be determined from the standard volume pseudopotential and a pseudopotential rescreened for the appropriate volume change.

In aluminum for 2½% and 5% volume decreases the parameter B was found to be 1.0263 and 1.0563 by direct evaluation of equation (3.38). With the phonon energies shifted by a constant Grüneisen parameter the relationship between the spectrum under pressure and the standard volume spectrum $\alpha_0^2(\omega)\ F_0(\omega)$ is

$$\alpha^2(\beta\omega)\ F(\beta\omega) = \frac{B}{\beta^2}\ \alpha_0^2(\omega) F_0(\omega) \qquad (3.39)$$

where

$$\beta = (1 - \gamma\frac{\Delta\Omega}{\Omega_s}) \qquad (3.40)$$

is the phonon energy shift of equation (3.23).

A comparison of the $\alpha^2(\omega)\ F(\omega)$ spectrum for a 2½% volume decrease of figure (3.2) and a spectrum corresponding to a 2½% volume decrease calculated directly from the scaling procedure of equation (3.39) is shown in figure (3.8). The agreement is very good. The gaps calculated with the spectra scaled according to equation (3.39) were in good agreement with those calculated from the spectra of figure (3.2). The rescaling procedure of equation (3.39) is very important for it allows one to calculate a spectrum at finite volume change from a standard volume spectrum in a very simple manner and with little intermediate calculation.

It has been seen that a constant Grüneisen parameter $\gamma=2.6$ provides phonon energy shifts that are too large for agreement with the measured transition temperature decrease at 2½% volume decrease. In order to investigate the phonon shifts under pressure in more detail, phonon dispersion curves along the symmetry directions were calculated by the pseudopotential method. The dynamical matrix of equation (2.85),

$$D_{\alpha\beta}(\underset{\sim}{k}) = \omega_p^2 \sum_{\kappa_n} [F(\underset{\sim}{k}+\underset{\sim}{\kappa}_n) \quad (\underset{\sim}{k}+\underset{\sim}{\kappa}_n)_\alpha \quad (\underset{\sim}{k}+\underset{\sim}{\kappa}_n)_\beta$$

$$- F(\underset{\sim}{\kappa}_n) \quad (\underset{\sim}{\kappa}_n)_\alpha \quad (\underset{\sim}{\kappa}_n)_\beta] \qquad ,(3.41)$$

with

$$F(\underset{\sim}{q}) = \frac{1}{q^2} - \frac{\Omega_0^2 \; q^2}{16\pi^2 \; Z^2 e^4} \left|w^o(\underset{\sim}{q})\right|^2 \left(\frac{\varepsilon(q)-1}{\varepsilon(\underset{\sim}{q})}\right) \qquad ,(3.42)$$

provides the frequencies upon diagonalization. The phonon dispersion curves along the symmetry directions as measured

Figure 3.8 A comparison of the rescaled $\alpha^2(\omega)\ F(\omega)$ spectrum for a 2½% volume decrease (solid line) in aluminum with the $\alpha^2(\omega)\ F(\omega)$ spectrum for a 2½% volume decrease of figure 3.2 (dashed line).

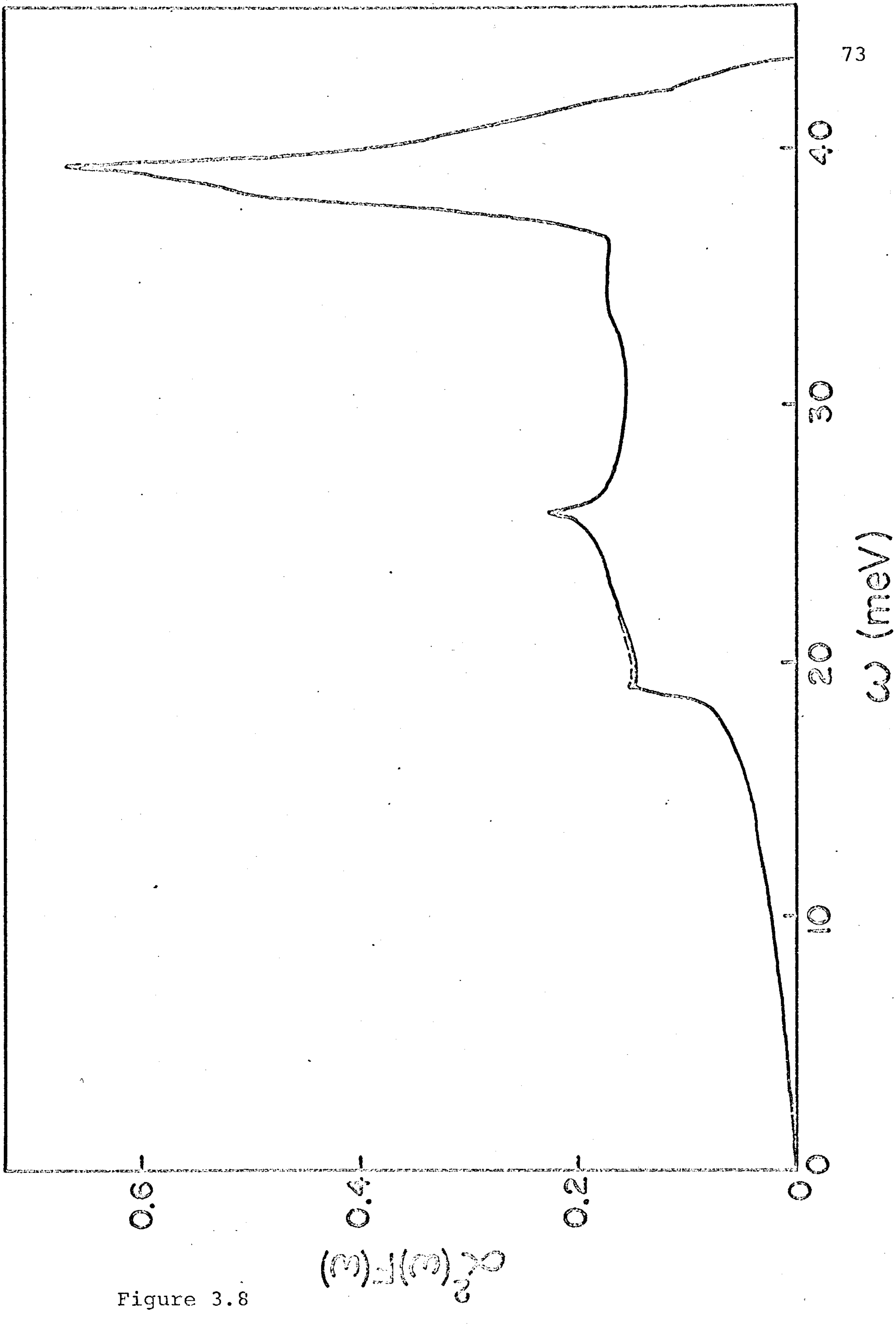

Figure 3.8

by inelastic neutron scattering(81) were fitted by a variation(82) of the parameters in the Heine-Abarenkov model pseudopotential. This procedure has been previously used by Dynes, Carbotte, Taylor and Campbell(31) to obtain an average pseudopotential in an alloy series. The fit for aluminum is shown in figure (3.9) and compared with a representative sample of measured(83) modes denoted by crosses. The parameters for the Heine-Abarenkov form factor used to obtain the curves were $A_0=1.38$ $A_1=1.66$ $A_2=1.85$. The calculation was repeated for 2½% and 5% volume changes with the parameters of the Heine-Abarenkov pseudopotential held constant. This procedure neglected the energy dependence of the parameters which is more serious in the phonon frequency calculations than in the calculation of the pseudopotential that enters the coupling constant in the calculation of $\alpha^2(\omega)\ F(\omega)$ at finite pressure. However, for aluminum it is believed that the energy dependence will not considerably alter the results(82).

In figure (3.10) the phonon frequencies calculated with a 5% volume decrease are compared to the standard volume phonon frequencies of figure (3.9). The frequency shifts at 2½% volume change were found to be almost exactly one half the shifts at 5% volume decrease. A detailed analysis of the shifts showed that the transverse modes were somewhat more affected than the longitudinal modes but the difference was not large. The longitudinal shifts

Figure 3.9 The phonon dispersion curves (solid line) in aluminum calculated with a pseudopotential form factor fitted to the experimental data (crosses). The frequencies are given in terms of the ion plasma frequency ω_p.

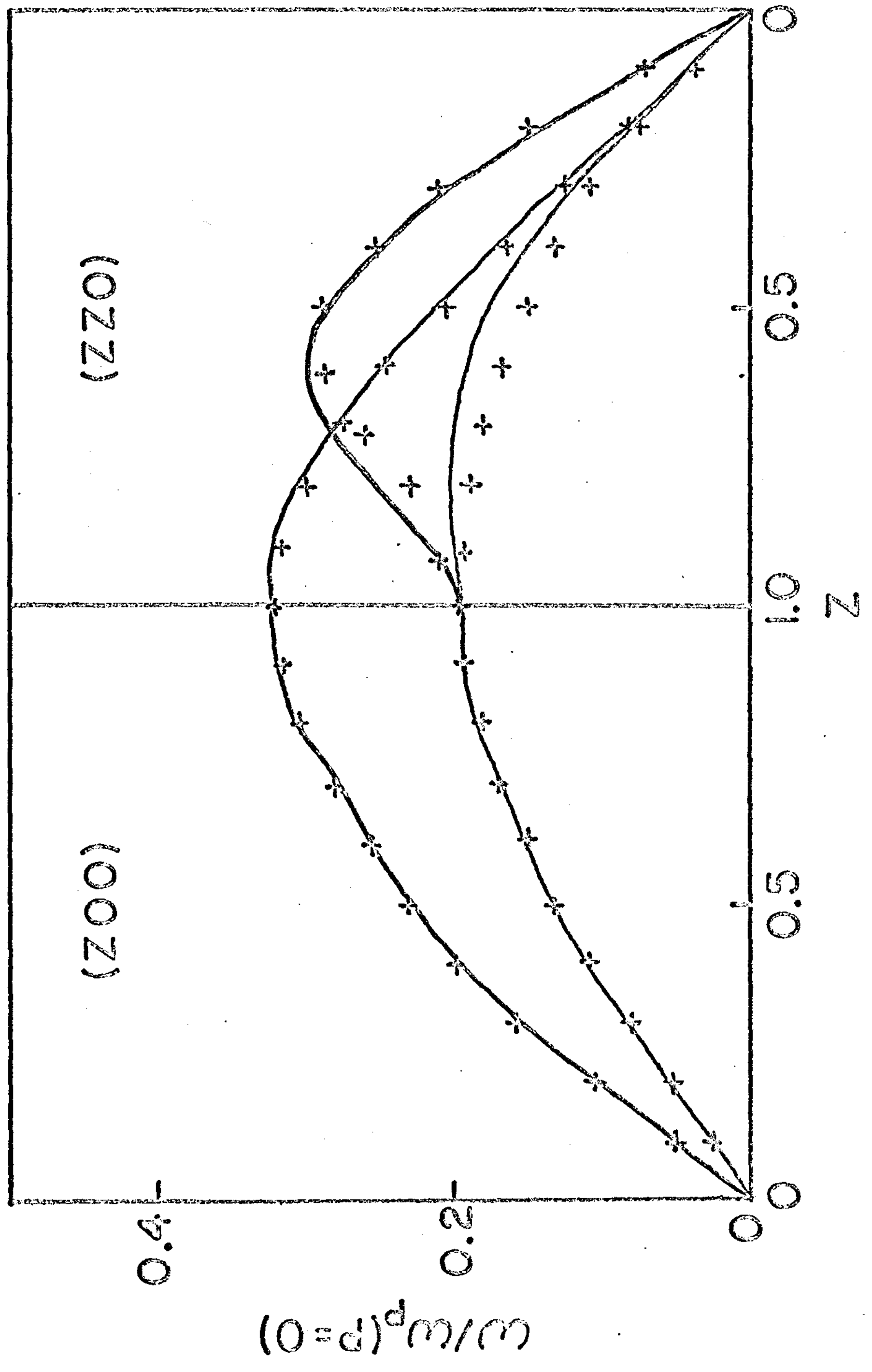

Figure 3.9

Figure 3.10 The phonon dispersion curves in aluminum calculated for a 5% volume decrease (solid lines) and the standard volume dispersion curves as in figure 3.9 (dashed lines).

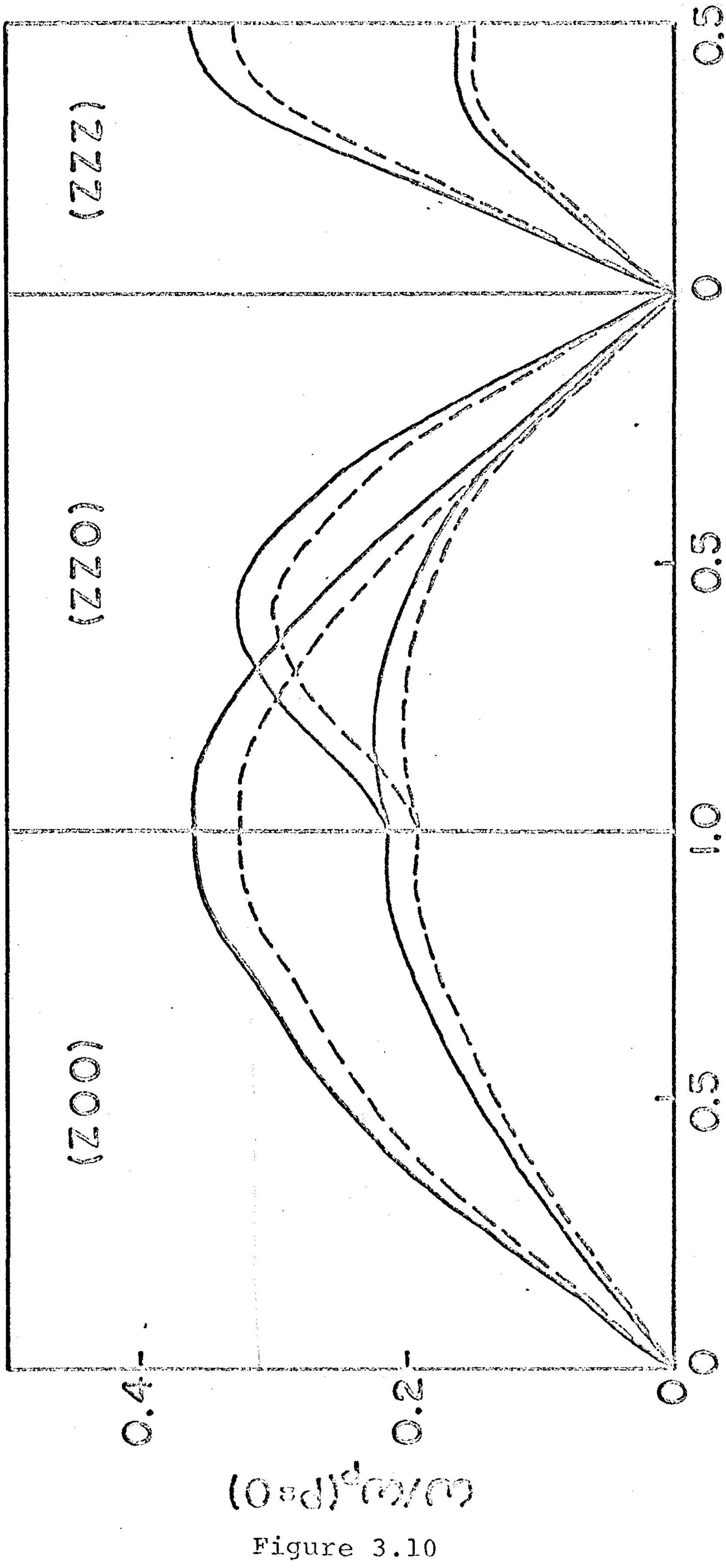

Figure 3.10

Figure 3.11 A comparison of the standard volume phonon dispersion curves in aluminum shifted with a Grüneisen parameter $\gamma=2.22$ (solid line) with the calculated frequencies (crosses) of figure 3.10 for a 5% volume decrease.

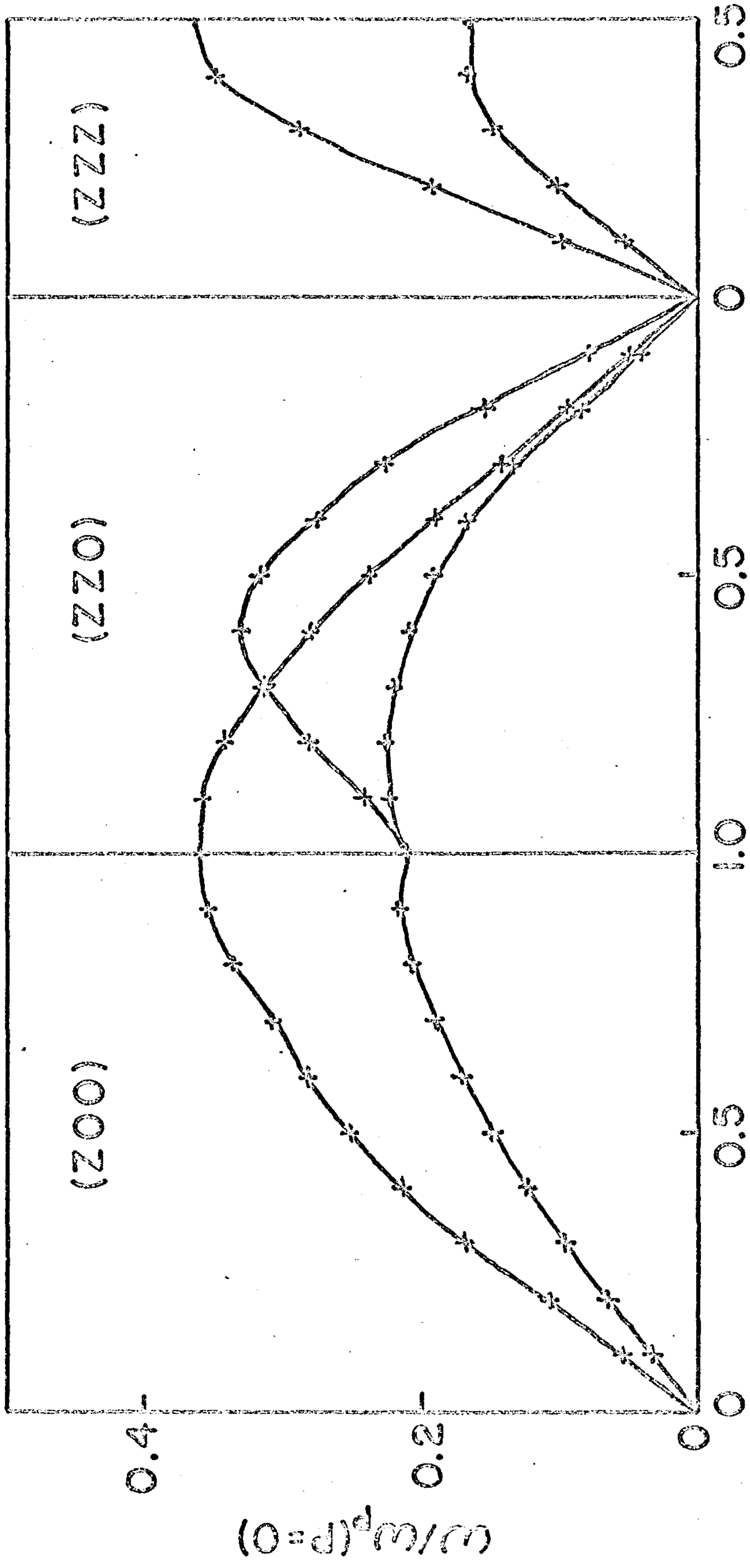

Figure 3.11

were reasonably reproduced by a constant shift with $\gamma=2.22$ as shown in figure (3.11). In figure (3.11) the solid lines are the zero pressure modes shifted by a constant and the crosses are representative of the frequencies calculated with a 5% volume reduction.

With $\gamma=2.22$ the zero pressure $\alpha^2(\omega)\,F(\omega)$ spectrum was scaled according to equation (3.39) for 2½% and 5% volume changes. The gap functions $\Delta_1(\omega)$ and $\Delta_2(\omega)$ calculated with the zero temperature Eliashberg gap equations are those of figures (3.4), (3.5a) and (3.5b). The gaps at the gap edges for 2½% and 5% volume decreases were found to be 0.095 meV and 0.048 meV. With the B.C.S. ratio these gaps were converted to transition temperatures and are compared to the straight line variation in figure (3.6). The agreement at 2½% is better but there is some loss of agreement at 5% volume change as compared to the result with $\gamma=2.6$.

3.5 Calculations in Lead

In lead the electron-phonon interaction is particularly strong and its superconducting properties show many deviations from the B.C.S. behaviour. In particular the B.C.S. ratio in lead is experimentally found to be

$$\frac{2\Delta_0}{k_B T_c} = 4.3 \qquad (3.43)$$

compared to the weak coupling value of 3.52. The strong electron-phonon interaction is manifested in large anomolies in the current-voltage characteristics of superconductor-insulator-metal tunnel junctions. Thus lead is a prime candidate for tunneling inversions as discussed in Chapter II. In addition, tunneling studies of lead under pressure have been made(40-42) and Franck, Keeler and Wu(42) have used the inversion method to obtain $\alpha^2(\omega)\ F(\omega)$ in lead under pressure. Franck and Keeler(41) have found that the gap and the transition temperature in lead do not scale identically under pressure with

$$\frac{d\ \ell n\ \Delta_0}{d\ \ell n\ T_c} = 2.06 \qquad .(3.44)$$

In this section results of the study of the effect of pressure on superconductivity in lead will be presented.

Initial calculations that are very similar to the calculations already described for aluminum were performed at standard volume and a 5% volume decrease. The Heine-Abarenkov pseudopotential as tabulated in Harrison was rescreened for a 5% volume change and is compared to the standard volume pseudopotential in figure (3.12). The Born-von Kármán atomic force constants fitted to the phonon dispersion curves as measured by inelastic neutron scattering(44) were used to generate $\alpha_0^2(\omega)\ F_0(\omega)$ as shown in figure (3.13). This calculation is not new(78). For the 5% volume change,

Figure 3.12 The Heine-Abarenkov pseudopotential form factor in lead at standard volume (solid line) and the form factor rescreened for a 5% volume decrease (dashed line) versus the momentum transfer $q/2k_F$.

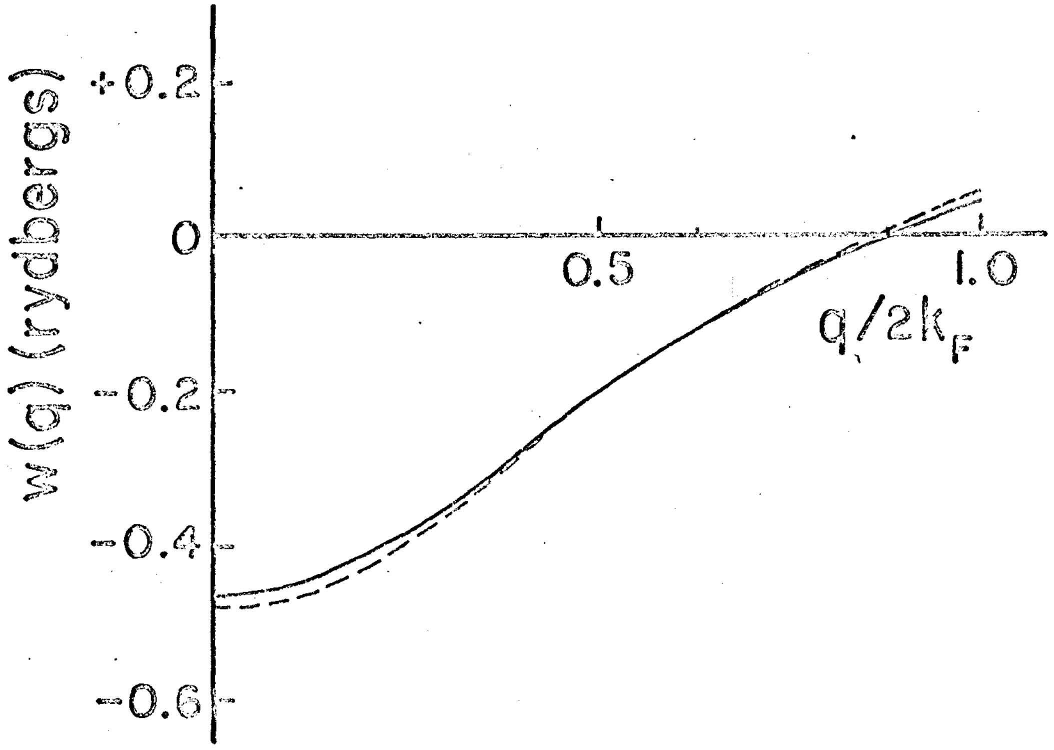

Figure 3.12

Figure 3.13 Calculated $\alpha^2(\omega)\ F(\omega)$ spectra in lead for standard volume (solid) and a 5% volume decrease (dashed) with a Grüneisen parameter $\gamma=2.85$ versus the phonon energy ω.

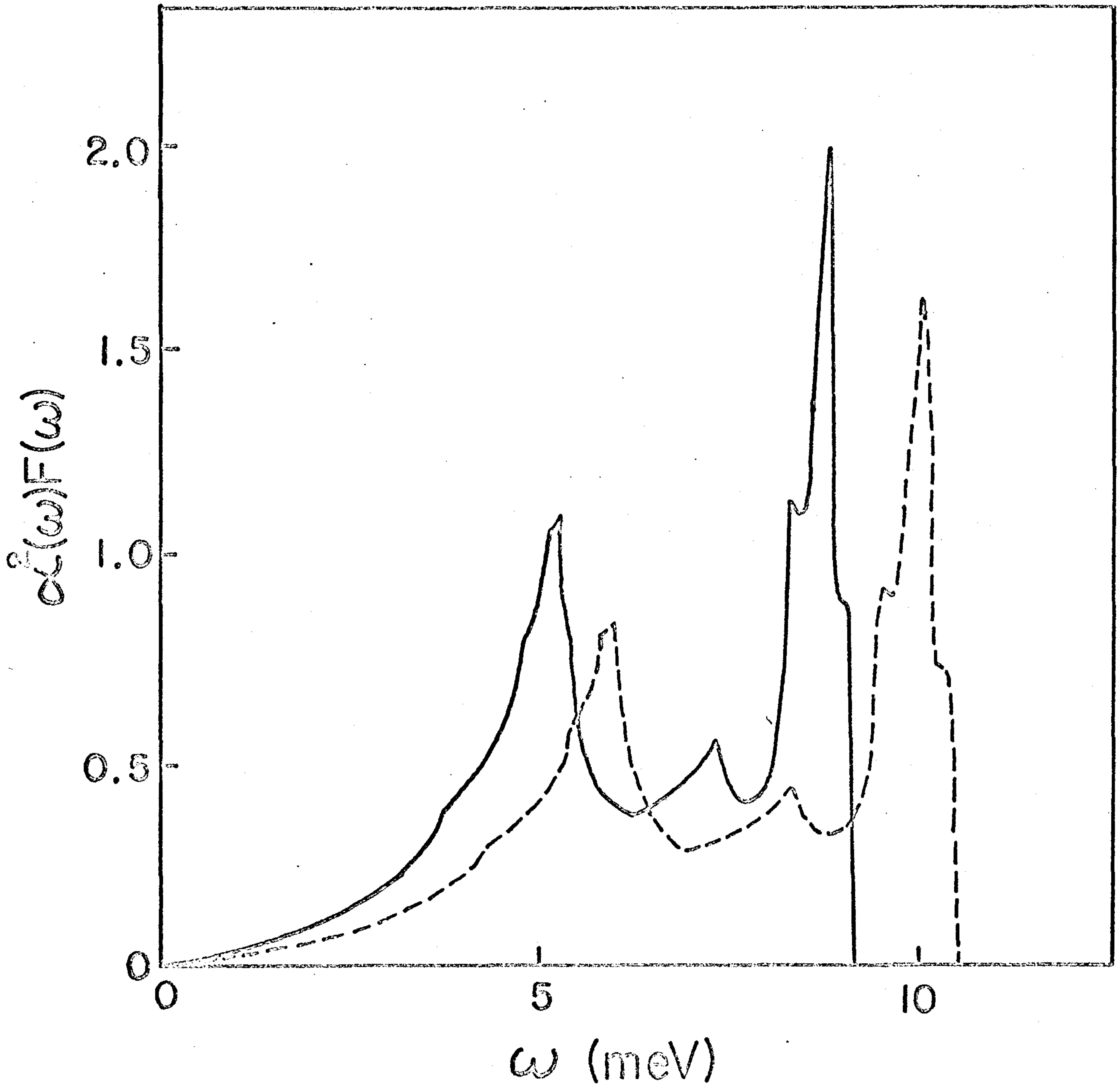

Figure 3.13

the phonon frequencies were shifted with a constant Grüneisen parameter $\gamma=2.85$ (84) and the rescreened pseudopotential was used to calculate $\alpha^2(\omega)\ F(\omega)$. The two functions are compared in figure (3.13).

The zero temperature gap equations were solved with the gap fixed at the value 1.35 meV to determine $N(0)U_c$ with the standard volume $\alpha_0^2(\omega)\ F_0(\omega)$. For the $\alpha^2(\omega)\ F(\omega)$ spectrum at 5% volume decrease the gap was calculated to be 1.01 meV. In figure (3.14) a comparison of $\alpha^2(\omega)\ F(\omega)$ calculated at 5% and $\alpha^2(\omega)\ F(\omega)$ obtained for 5% from the scaling law of equation (3.39) with B=1.0348 calculated from equation (3.38). The two $\alpha^2(\omega)\ F(\omega)$ functions give essentially the same gap.

Since the scaling law appears to be reasonable for lead as well as for aluminum and since the $\alpha^2(\omega)\ F(\omega)$ function obtained by inversion of the tunneling results is expected to be more accurate at this time than that calculated from force constants the McMillan-Rowell spectrum(71) was used for further work with lead. The first principle calculations have served to verify the approximate scaling law, equation (3.39), first established for aluminum.

The McMillan-Rowell spectrum rescaled for a 5% volume change with a constant phonon shift $\gamma=2.85$ and the factor B calculated from the Heine-Abarenkov pseudopotentials is compared to the standard volume spectrum in figure (3.15). The $\alpha^2(\omega)\ F(\omega)$ spectra of figure (3.15) can be compared to

Figure 3.14 A comparison of the rescaled $\alpha^2(\omega)\ F(\omega)$ spectrum in lead (solid line) with the calculated $\alpha^2(\omega)\ F(\omega)$ spectrum of figure 3.13 (dashed line) for a 5% volume decrease. The dashed curve is displaced upward on the vertical scale by 0.5 to prevent near total overlap.

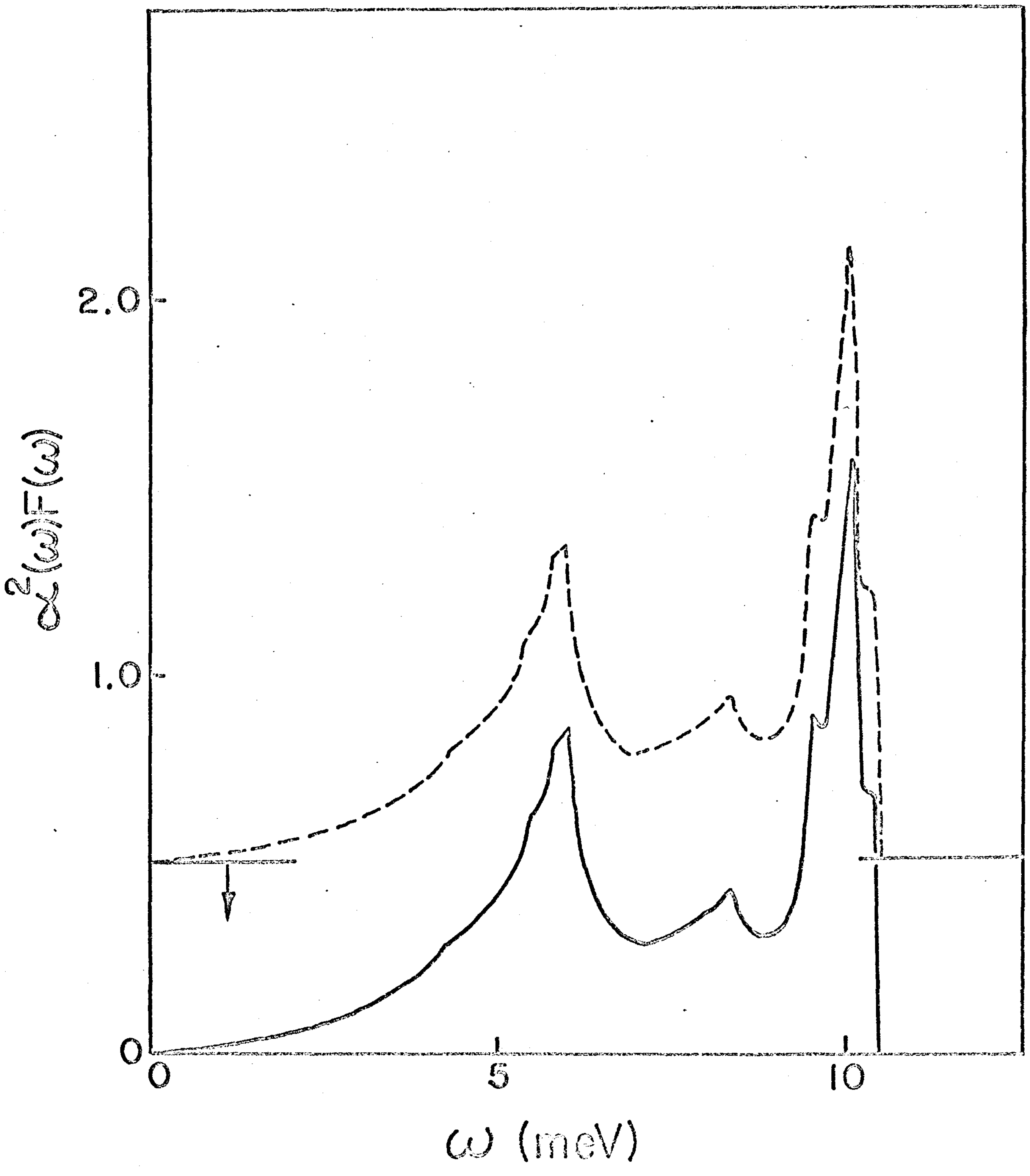

Figure 3.14

Figure 3.15 The McMillan-Rowell $\alpha^2(\omega)\ F(\omega)$ spectrum for lead (solid line) as obtained from inversion of tunneling results and the rescaled spectrum for a 5% volume decrease (dashed line) versus the phonon energy ω.

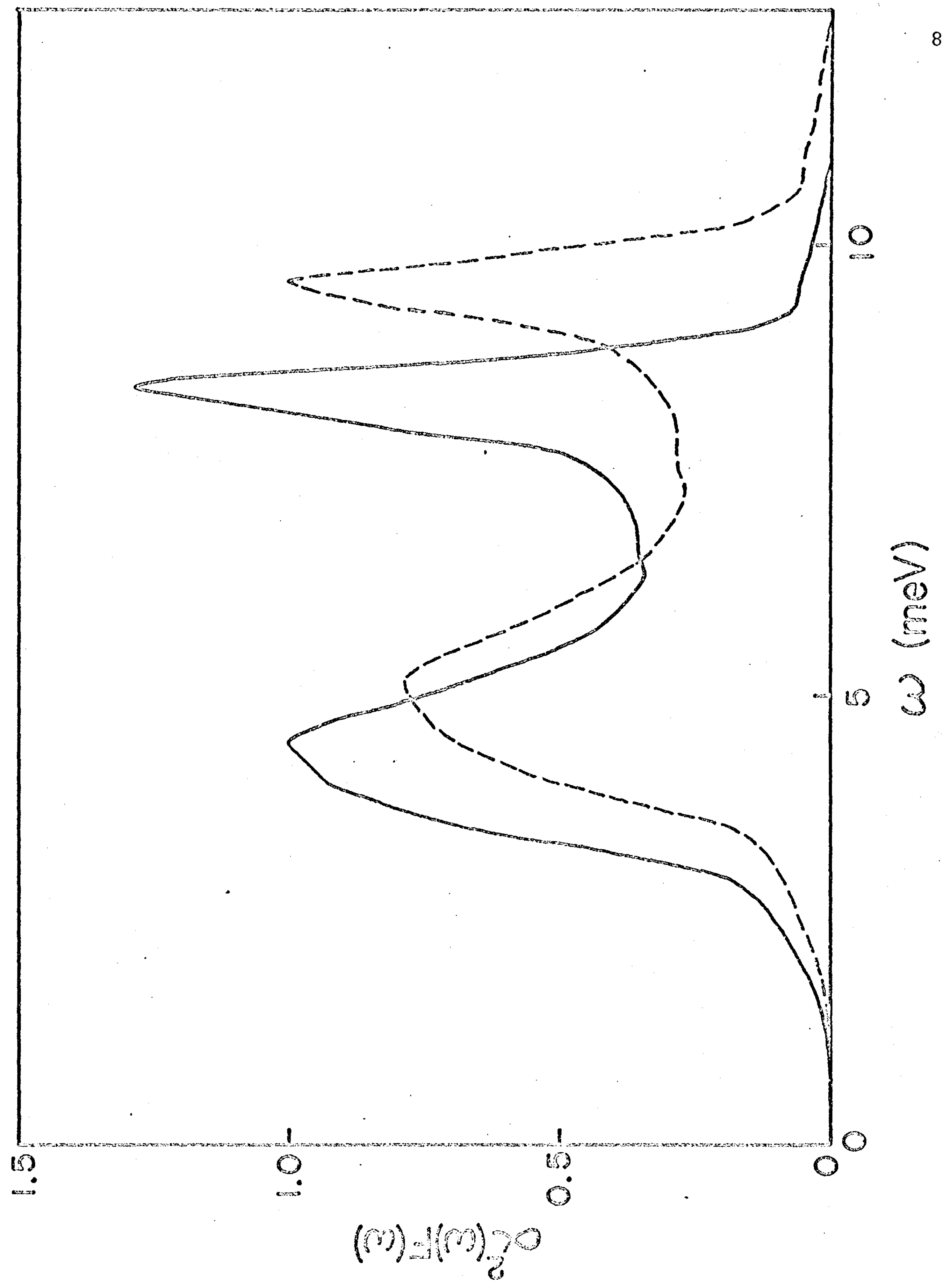

Figure 3.15

the tunneling inversions of Franck, Keeler and Wu(42). They have inverted the Eliashberg gap equations and have obtained the functions $\alpha^2(\omega)$ $F(\omega)$ for pressures of 0 and 3,445 bar. Their zero pressure $\alpha^2(\omega)$ $F(\omega)$ is in good agreement with the McMillan-Rowell spectrum of figure (3.15). The finite pressure shifts of Franck, Keeler and Wu are much smaller than the scaled shifts for a 5% volume change of figure (3.15); however, the general shifts to higher energies are clearly evident although their longitudinal peak is shifted more than the transverse peak with Grüneisen parameters γ_T=2.6 and γ_L=3.4. The Grüneisen parameter γ=2.85 used in the scaling shift of figure (3.15) falls between Franck and Keeler's γ_T and γ_L. The changes on the vertical scale in the inverted $\alpha^2(\omega)$ $F(\omega)$ of Franck, Keeler and Wu do not as clearly correspond to this work. The peak in the $\alpha^2(\omega)$ $F(\omega)$ at 3,445 bar do not appear to show a decrease whereas the minimum between the peaks suggests a decrease that corresponds to figure (3.15). Since the van Hove singularities are rather sharp, a comparison at the peaks may not be very meaningful so the evidence is not conclusive.

The different shifts in the longitudinal and transverse modes observed in the tunneling work of Franck and Keeler can be included in a calculation. A calculation was performed with the transverse and longitudinal peaks shifted by γ_T=2.6 and γ_L=3.4 for the spectrum derived from the force constant model. The gap value obtained at a 5%

volume change was not significantly different from that obtained with the average shift $\gamma=2.85$. This indicates that a rescaling procedure with a constant Grüneisen parameter is adequate for this work.

The zero temperature solutions of the Eliashberg gap equations, $\Delta_1(\omega)$ and $\Delta_2(\omega)$, are shown in figures (3.16) and (3.17) for standard volume and a 5% volume decrease. As in the solutions for aluminum, the general overall heights of the gap functions are reduced with pressure and the shifts of the peaks to higher energies are reproduced. The gap at the gap edge was found to be $\Delta_0=1.346$ meV with $N(0)U_c=0.13$ for the standard volume spectrum and $\Delta_0=1.04$ meV for the spectrum shifted for a 5% volume decrease.

The finite temperature Eliashberg gap equations must be solved to obtain the critical temperature T_c since lead is a strong-coupling superconductor and the experimental evidence is that the gap at the gap edge and the transition temperature do not scale in the same way under pressure. This is in contrast to the case in aluminum where the weak-coupling B.C.S. ratio 3.52 was used to obtain a relationship between the transition temperature and the gap.

The frequency and temperature dependent gap $\Delta(\omega,T)$ is obtained by iteration of the equations (2.117) and (2.118),

$$\Delta(\omega,T) = [Z(\omega,T)]^{-1} \int_0^{\omega_c} d\omega' \; \mathrm{Re}\left[\frac{\Delta(\omega',T)}{[\omega'^2-\Delta^2(\omega',T)]^{\frac{1}{2}}}\right]$$

Figure 3.16 The gap functions $\Delta_1(\omega)$ (solid line) and $\Delta_2(\omega)$ (dashed line) for the McMillan-Rowell spectrum in lead at standard volume versus the energy ω.

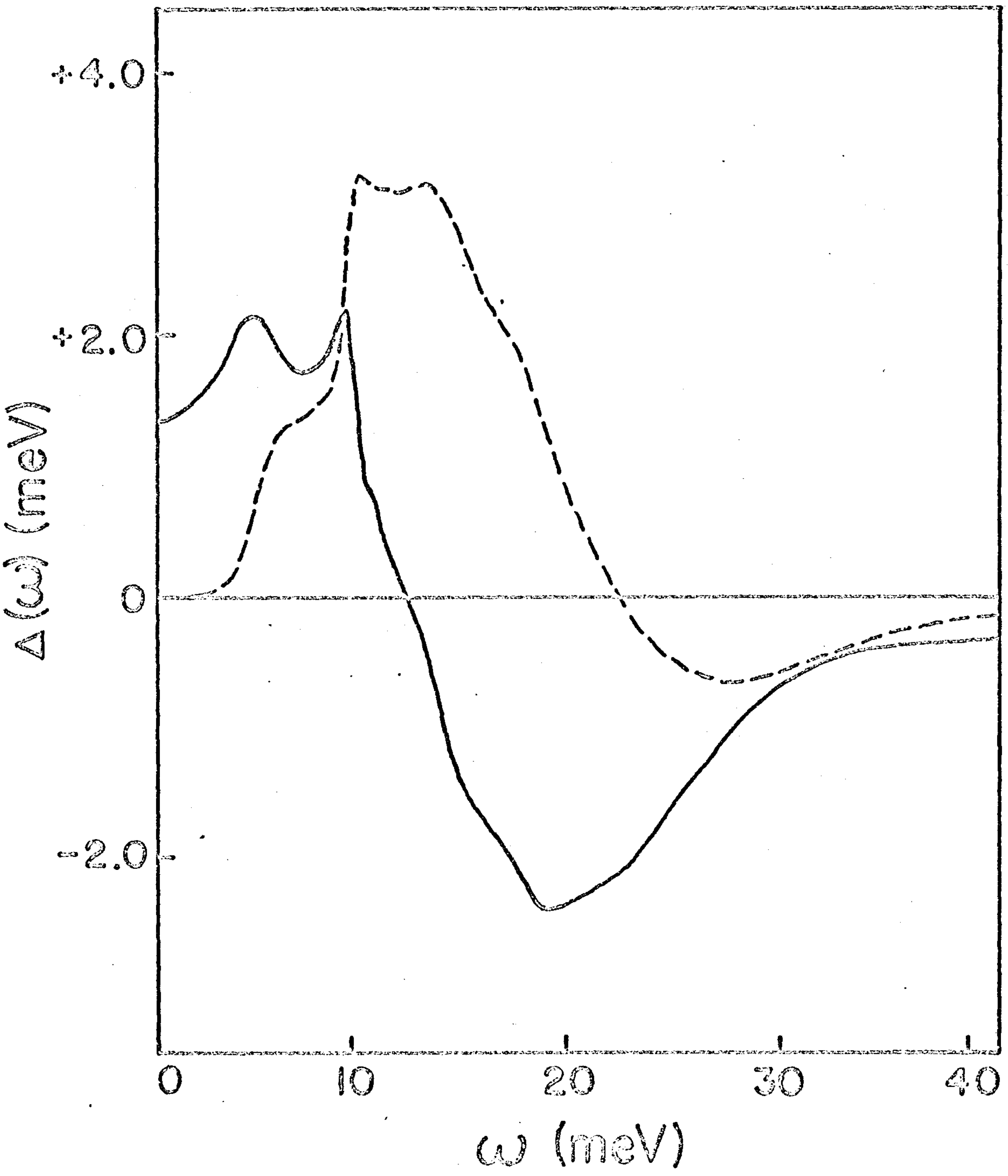

Figure 3.16

Figure 3.17 The gap functions $\Delta_1(\omega)$ (solid line) and $\Delta_2(\omega)$ (dashed line) for the rescaled McMillan-Rowell spectrum of figure 3.15 for a 5% volume decrease versus the energy ω.

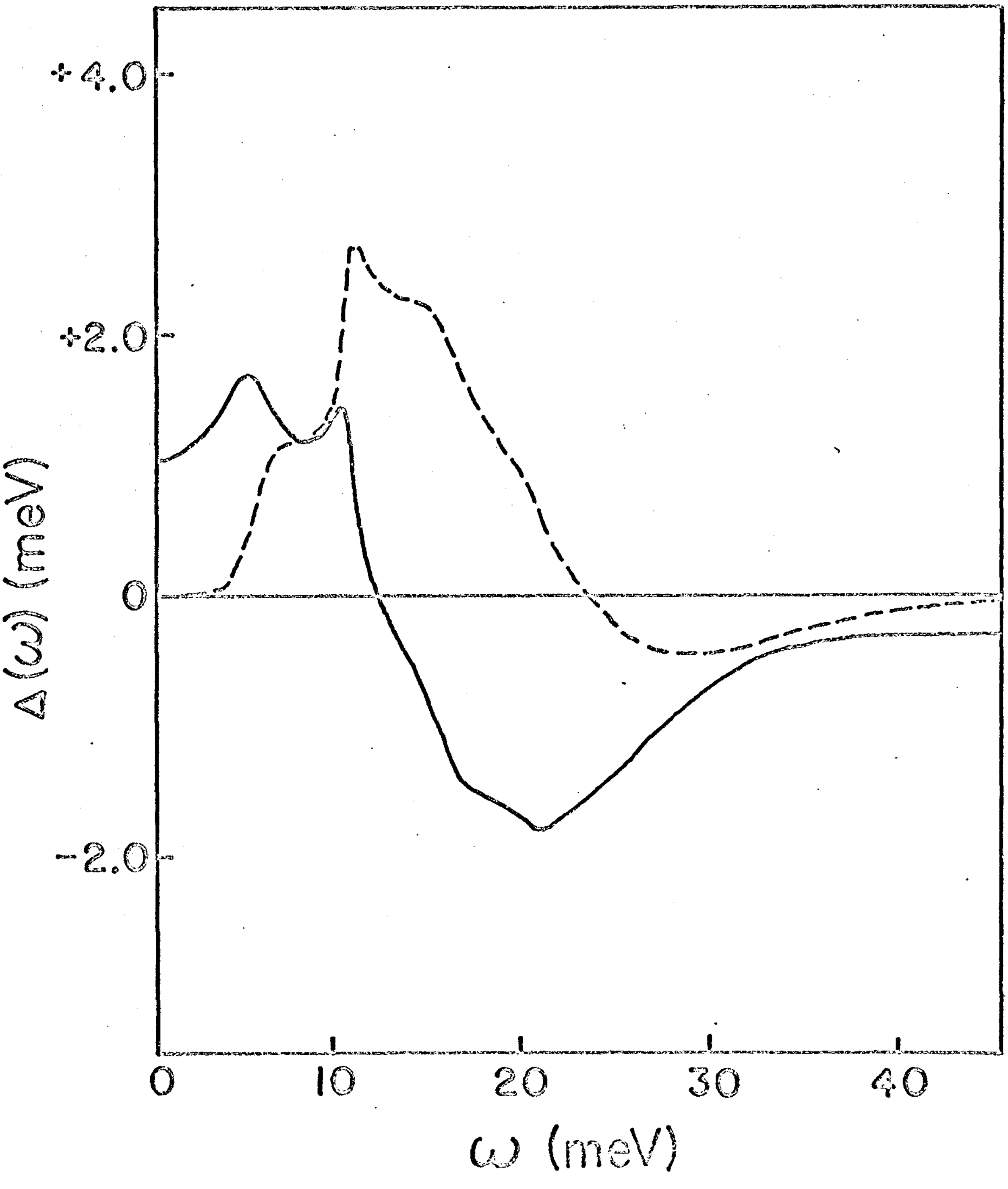

Figure 3.17

$$\times \{D_+(\omega,\omega') - D_+(\omega,-\omega') - N(0)U_c \tanh (\frac{\beta\omega'}{2})\} \qquad (3.45)$$

and

$$[1-Z(\omega,T)]\omega = \int_0^\infty d\omega' \; \mathrm{Re}[\frac{\omega'}{[\omega'^2-\Delta^2(\omega',T)]^{\frac{1}{2}}}]$$

$$\times \{D_-(\omega,\omega') + D_-(\omega,-\omega')\} \qquad (3.46)$$

where

$$D_\pm(\omega,\omega') = \int_0^\infty d\nu \; \alpha^2(\nu) \; F(\nu)$$

$$\times \; [\{N(\nu) + f(\omega')\} \{\frac{1}{\omega'+\omega+\nu+io^+} \pm \frac{1}{\omega'-\omega+\nu-io^+}\}] \qquad (3.47)$$

and $N(\nu)$ and $f(\omega')$ are the Bose and Fermi functions. At finite temperature the gap edge is given by

$$\Delta_0(T) = \mathrm{Real} \; \{\Delta(\Delta_0(T),T)\} \qquad .(3.48)$$

The equations were solved for the zero pressure McMillan-Rowell spectrum $\alpha^2(\omega)$ $F(\omega)$ of figure (3.15) for two temperatures below T_c but sufficiently close to T_c so that $\Delta_0(T)$ is a rapidly decreasing function of temperature in this region. From these two values of the gap the value of the critical temperature was obtained by extrapolation(25,26). A solution for the real and imaginary parts of the gap function $\Delta_1(\omega,T)$ and $\Delta_2(\omega,T)$ with

$$\Delta(\omega,T) = \Delta_1(\omega,T) + i \; \Delta_2(\omega,T) \qquad (3.49)$$

is shown as a function of frequency for a temperature near T_c and for P=0 in figure (3.18a). This solution compares well with the figure given by Scalapino, Wada and Swihart(25). For the McMillan-Rowell spectrum it was found that k_BT_c=0.63 meV for a ratio

$$\left(\frac{2\Delta_0}{k_BT_c}\right)_{0\%} = 4.27 \qquad .(3.50)$$

This agrees well with previous calculations(26) and the experimental value of 4.3.

Figure (3.18b) is a plot of $\Delta_1(\omega,T)$ and $\Delta_2(\omega,T)$ as a function of frequency for a volume change of 5% and a temperature near T_c as obtained by iteration of the gap equations, equations (3.45) and (3.46), with the rescaled $\alpha^2(\omega)\,F(\omega)$ spectrum of figure (3.15). The shifts of the peaks in $\alpha^2(\omega)\,F(\omega)$ are also evident in the solutions of the finite temperature gap equations.

The temperature variation of $\Delta_0(T)$ derived from these solutions is given in figure (3.19). The B.C.S. temperature variation fits the limited calculated data well. At 5% volume decrease it was found that k_BT_c=0.555 meV for a ratio

$$\left(\frac{2\Delta_0}{k_BT_c}\right)_{5\%} = 3.75 \qquad .(3.51)$$

This is closer to the weak coupling limit 3.52 than the

Figure 3.18 (a) The gap functions $\Delta_1(\omega,T)$ (solid line) and $\Delta_2(\omega,T)$ (dashed line) for the McMillan-Rowell spectrum at standard volume and T near T_c cersus the energy ω.

(b) The gap functions $\Delta_1(\omega,T)$ (solid line) and $\Delta_2(\omega,T)$ (dashed line) for the spectrum rescaled for a volume decrease of 5% and for T near T_c versus the energy ω.

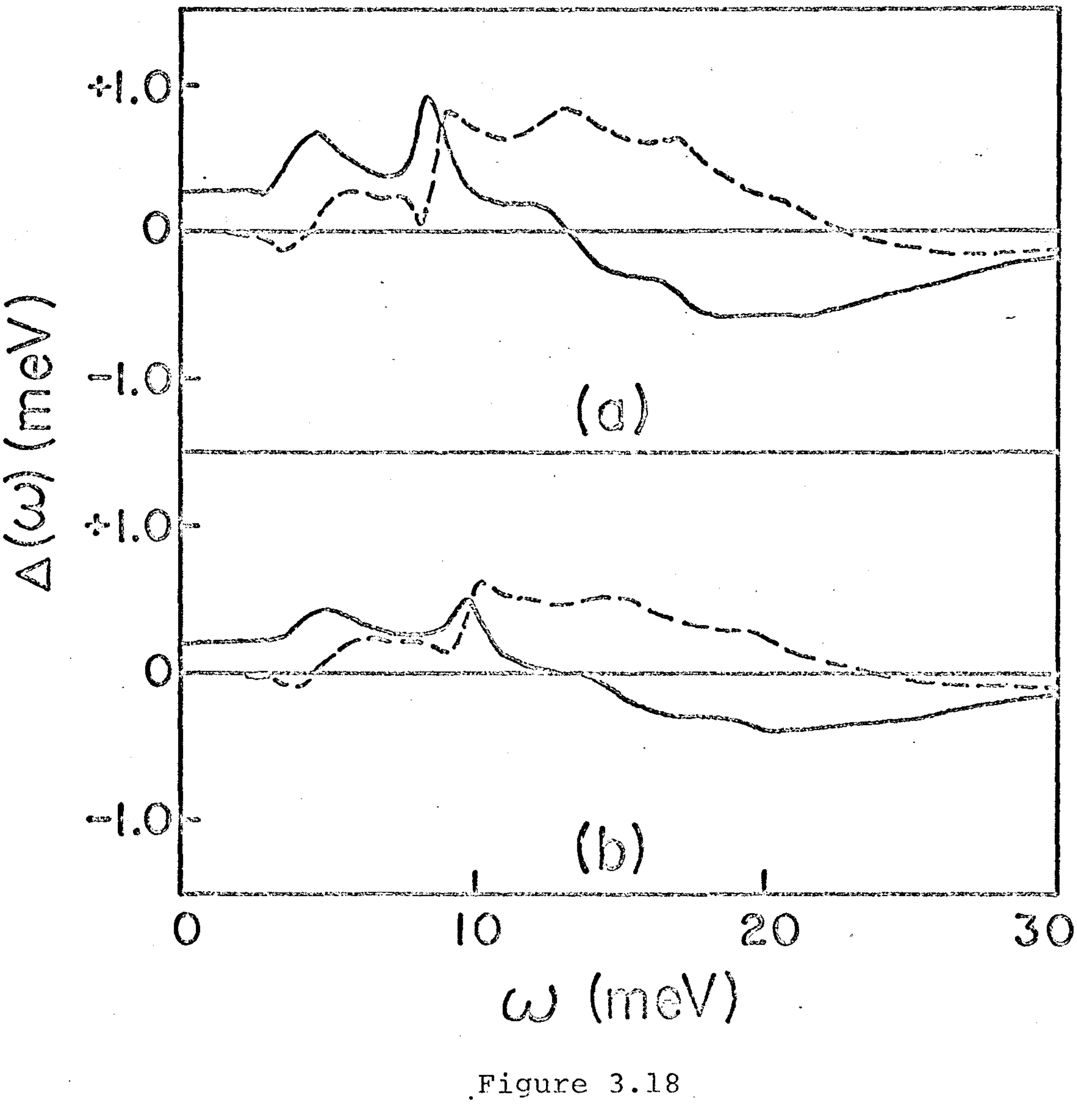

Figure 3.18

Figure 3.19 The variation of the gap Δ with temperature T in lead. The curves are the B.C.S. variation. The circled points are from the calculations at standard volume and the boxed points are the calculations for a 5% volume decrease.

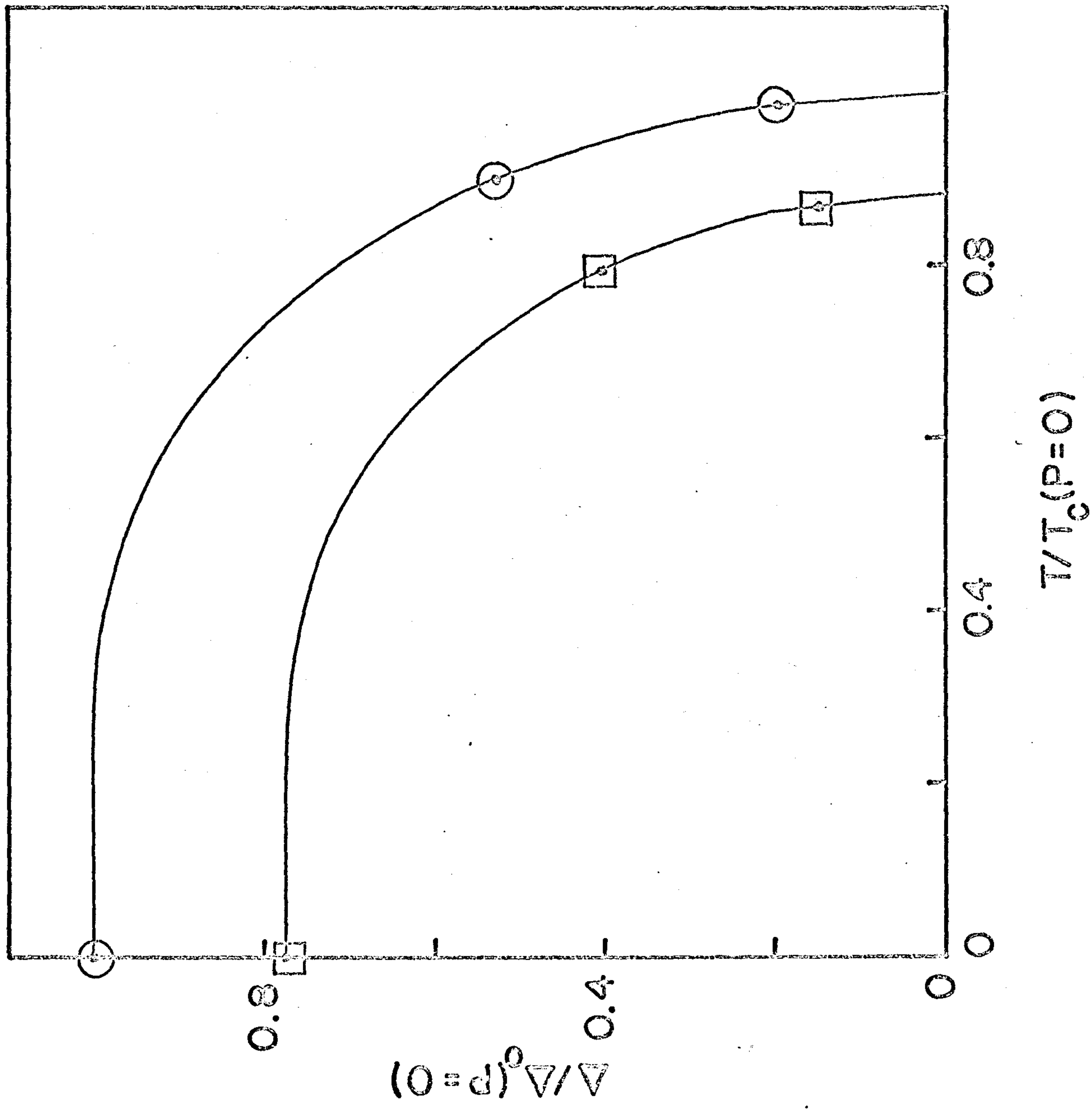

Figure 3.19

zero pressure ratio of 4.27. The gap Δ_0 and T_c scale differently under pressure so that the B.C.S. ratio decreases towards the weak coupling value. A comparison with the experimental results of Franck and Keeler$^{(41)}$ can be made with a calculation of $d\ \ell n\ \Delta_0/d\ \ell n\ T_c$. With a straight line variation of the critical temperature and gap with volume change as shown in figure (3.20), the value of $d\ \ell n\ \Delta_0/d\ \ell n\ T_c$ varies with volume change. At zero pressure

$$\left(\frac{d\ \ell n\ \Delta_0}{d\ \ell n\ T_c}\right)_{0\%} = 1.92 \tag{3.52}$$

and at 5% volume decrease

$$\left(\frac{d\ \ell n\ \Delta_0}{d\ \ell n\ T_c}\right)_{5\%} = 2.18 \quad . \tag{3.53}$$

Both these values are in close agreement with the experimental result

$$\frac{d\ \ell n\ \Delta_0}{d\ \ell n\ T_c} = 2.06 \quad . \tag{3.54}$$

The variation of the transition temperature with volume is plotted in figure (3.20) and compared with the experimental results quoted by Smith and Chu$^{(39)}$. The agreement at 5% volume decrease is good, so the calculation also account for the observed value of $d\ \ell n\ T_c/d\ \ell n\ V$.

Figure 3.20 The calculated variation of the transition temperature T_c (circled points) and the gap at the gap edge Δ_0 (boxed points) with volume decrease in lead. The solid line is the experimental variation of the transition temperature. The dashed line is a straight line interpolation between the calculated points for the variation of the gap.

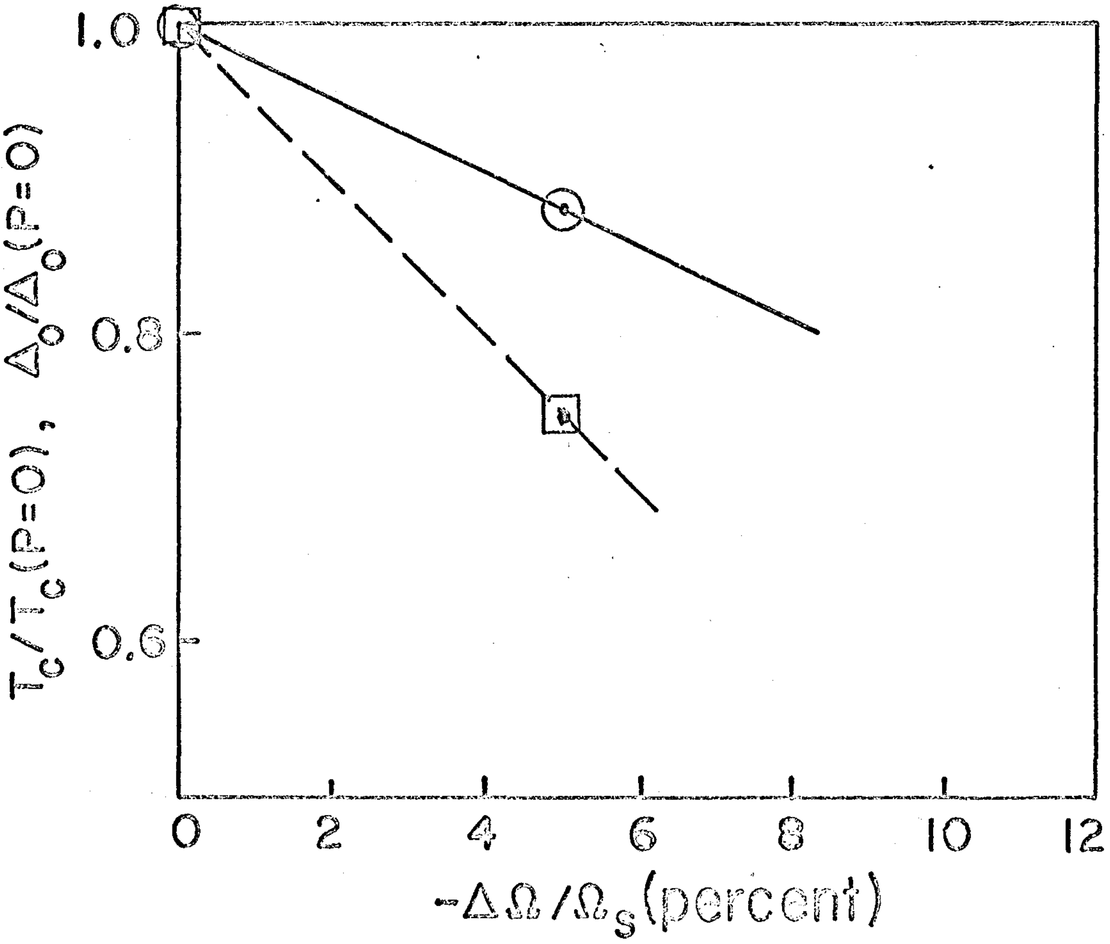
$T_c/T_c(P=0)$, $\Delta_o/\Delta_o(P=0)$
1.0
0.8
0.6
0
2
4
6
8
10
12
$-\Delta\Omega/\Omega_S$(percent)

Figure 3.20

3.6 Calculations in Mercury

First principle calculations of $\alpha^2(\omega)\ F(\omega)$ are as yet not available for the structure of mercury. As a consequence the same scaling procedure as was used for the face-centered cubic materials aluminum and lead was used for mercury. It must be stressed that the scaling law has not been established in detail for mercury or for tin or indium which will be discussed in the next section. The scaling procedure assumes there is no change in the crystal structure under stress since the shape of the spectrum is affected by such a structure change.

The Heine-Abarenkov pseudopotential at 5% volume decrease is compared to the standard volume pseudopotential in figure (3.21). For a 5% volume decrease the value of B to be used in the scaling of equation (3.39) was calculated to be 1.0428. In figure (3.22) the McMillan-Rowell spectrum(71) as obtained by inversion of tunneling results is compared with the rescaled spectrum for a 5% volume decrease with B=1.0428 and γ=3.0 (84). The $\alpha^2(\omega)\ F(\omega)$ spectrum for mercury of figure (3.22) should be compared to the lead spectrum of figure (3.15). The lead spectrum has two peaks-longitudinal and transverse- that are characteristic of the face centered cubic structure. The spectrum for mercury has a peak at low energy, that is at 1.0 to 2.0 meV. This appears to be the dominant structure in mercury.

Figure 3.21 The Heine-Abarenkov pseudopotential form factor in mercury at standard volume (solid line) and the rescreened form factor (dashed line) for a 5% volume decrease versus the momentum transfer $q/2k_F$.

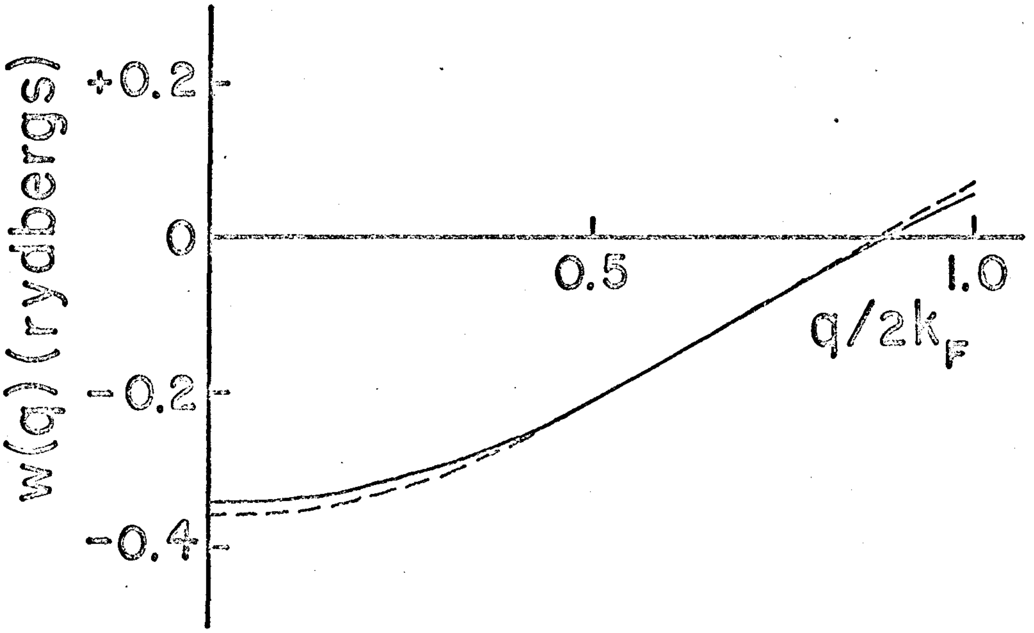

Figure 3.21

Figure 3.22 The McMillan-Rowell $\alpha^2(\omega)\ F(\omega)$ function in mercury (solid line) and the McMillan-Rowell spectrum rescaled for a 5% volume decrease (dashed line) versus the phonon energy ω. The Grüneisen parameter is $\gamma=3.0$.

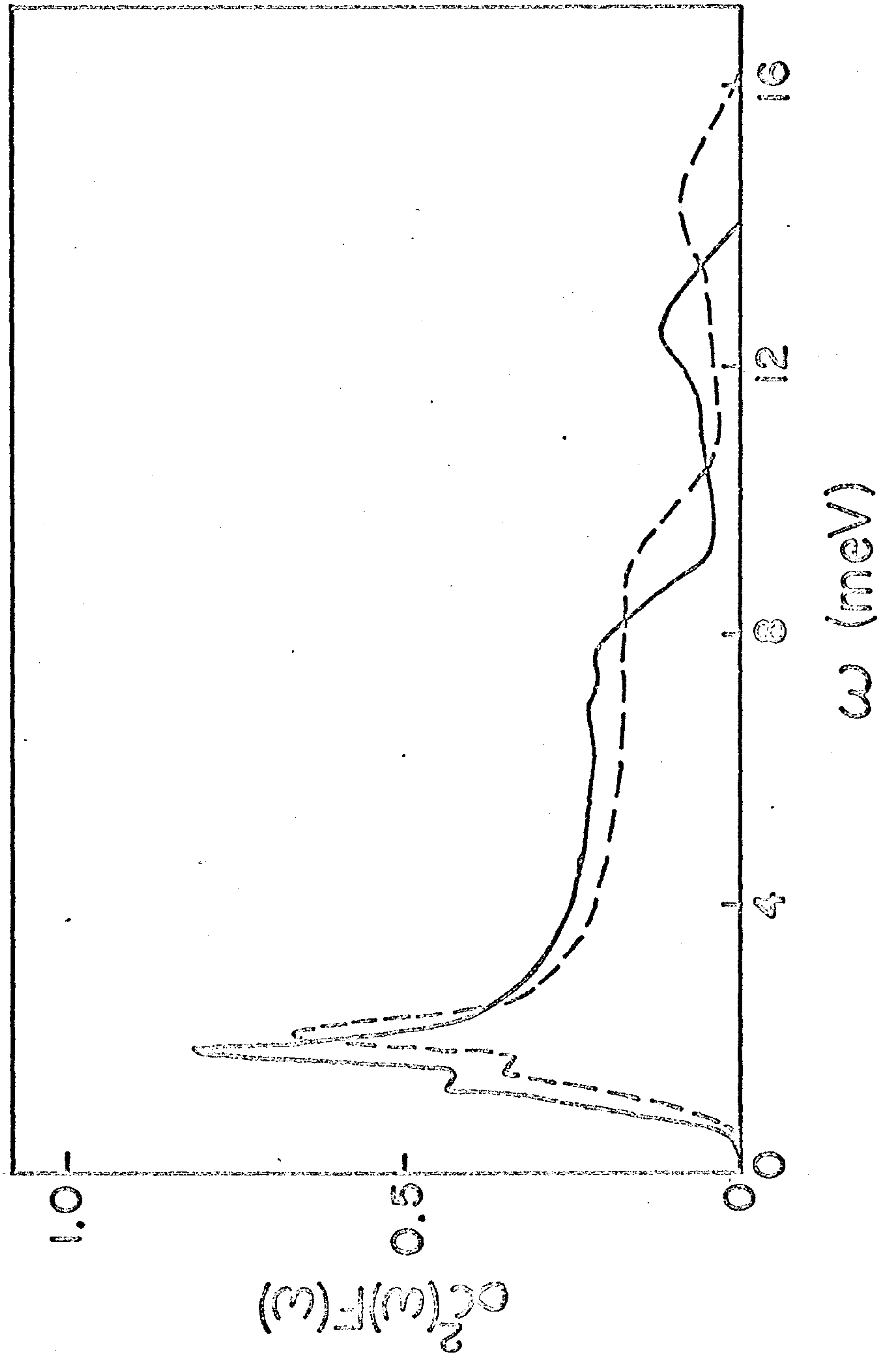

Figure 3.22

The zero temperature gap equations were solved at zero pressure for a gap Δ_0=0.825 meV to obtain $N(0)U_c$=0.09. The finite temperature equations were solved to obtain the transition temperature k_BT_c=0.358 meV for a B.C.S. ratio

$$\frac{2\Delta_0}{k_BT_c} = 4.61 \qquad .(3.55)$$

This value compares well with the experimental results and previous calculations$^{(26)}$. For the $\alpha^2(\omega)\ F(\omega)$ spectrum rescaled for a 5% volume decrease the zero temperature gap was found to be $(\Delta_0)_{5\%}$ = 0.675 meV and the transition temperature was calculated with the finite temperature equations with $(k_BT_c)_{5\%}$ = 0.318 meV for a B.C.S. ratio

$$\left(\frac{2\Delta_0}{k_BT_c}\right)_{5\%} = 4.25 \qquad .(3.56)$$

The gap and transition temperature variations with volume change are plotted in figure (3.23). As in the case of lead, the gap and the transition temperature were found to scale differently with volume change. With a straight line variation of the gap and the transition temperature, the derivative $d\ \ell n\ \Delta_0/d\ \ell n\ T_c$ was found to be

$$\left(\frac{d\ \ell n\ \Delta_0}{d\ \ell n\ T_c}\right)_{0\%} = 1.63 \qquad (3.57)$$

and

$$\left(\frac{d\ \ell n\ \Delta_0}{d\ \ell n\ T_c}\right)_{5\%} = 1.76 \qquad .(3.58)$$

Figure 3.23 The calculated variation of the gap at the gap edge Δ_0 (boxed points) and the transition temperature T_c (circled points) with volume change in mercury. The lines are straight line interpolations between the calculated points.

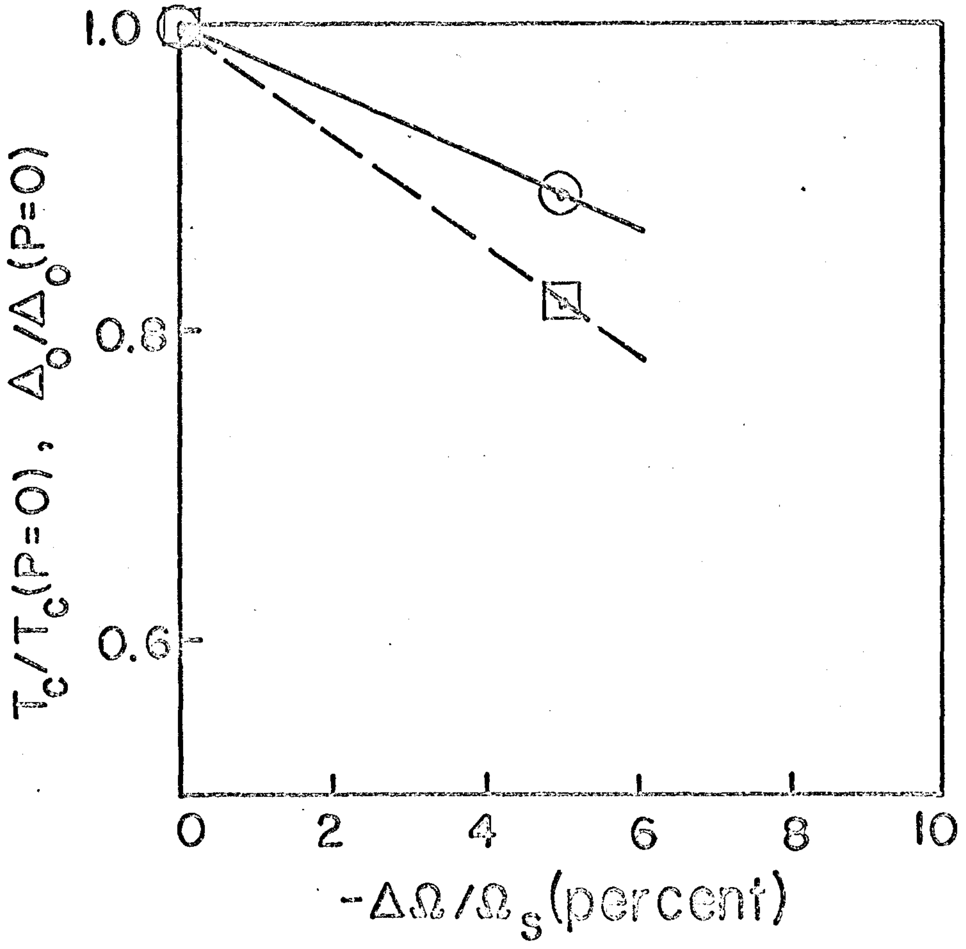
$T_c/T_c(P=0)$, $\Delta_o/\Delta_o(P=0)$
1.0
0.8
0.6
0
2
4
6
8
10
$-\Delta\Omega/\Omega_S$(percent)

Figure 3.23

As in the case for lead, the B.C.S. ratio tends toward the B.C.S. value of 3.52 for a volume decrease. It is seen that the derivative $d\ \ell n\ \Delta_0/d\ \ell n\ T_c$ for mercury is approximately 1.7 and is somewhat smaller than 2.0 as calculated in lead.

Although no experimental results for $\frac{d\ \ell n\ \Delta_0}{d\ \ell n\ T_c}$ in mercury are available as yet, Jennings and Swenson(38) quote the experimental value of $\frac{d\ \ell n\ T_c}{d\ \ell n\ V}$ in mercury for small pressures to be 3.0 and a Grüneisen parameter $\gamma=2.2$. The results of this work with $\gamma=3.0$ is that the derivative $\frac{d\ \ell n\ T_c}{d\ \ell n\ V}$ is approximately 2.0. The difference between these results is not totally understood, but it may be due to a failure of the scaling law in mercury.

3.7 Calculations in Tin and Indium

As in mercury, the structures of tin and indium are not of the face centered cubic type. However, the scaling procedure of equation (3.29) was applied to the McMillan-Rowell spectra(71) for these materials.

The pseudopotentials for 0% and 5% volume changes in tin are shown in figure (3.24a). The scaling parameter B obtained from these two pseudopotentials was 1.0445. The rescaled spectrum with $\gamma=2.25$ (84) and B=1.0445 is compared with the zero pressure tunneling spectrum of McMillan and Rowell in figure (3.25). At zero pressure the gap at the gap edge was set at $(\Delta_0)_{0\%} = 0.575$ meV with

McMASTER UNIVERSITY LIBRARY

Figure 3.24 (a) The Heine-Abarenkov pseudopotential form factor in tin at standard volume (solid line) and the form factor rescreened for a 5% volume decrease (dashed line) versus the momentum transfer $q/2k_F$.

(b) The Heine-Abarenkov pseudopotential form factor in indium at standard volume (solid line) and the form factor rescreened for a 5% volume decrease (dashed line) versus the momentum transfer $q/2k_F$.

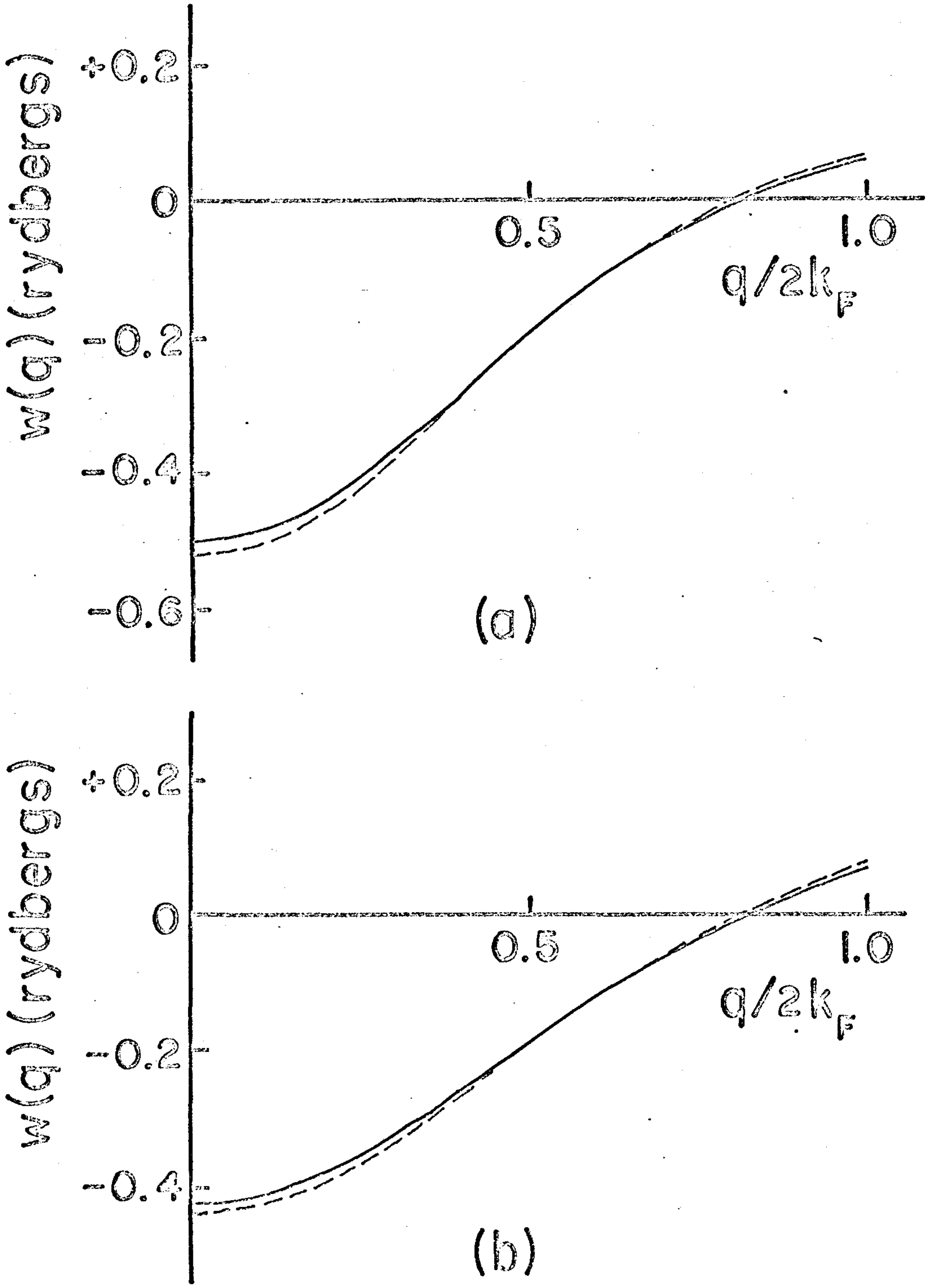
w(q) (rydbergs)
+0.2
0
-0.2
-0.4
-0.6
0.5
1.0
q/2k_F
(a)
w(q) (rydbergs)
+0.2
0
-0.2
-0.4
0.5
1.0
q/2k_F
(b)

Figure 3.24

Figure 3.25 The McMillan-Rowell $\alpha^2(\omega)$ $F(\omega)$ function in tin (solid line) and the rescaled $\alpha^2(\omega)$ $F(\omega)$ function for a 5% volume decrease (dashed line) versus the phonon energy ω. The Grüneisen parameter is $\gamma=2.25$.

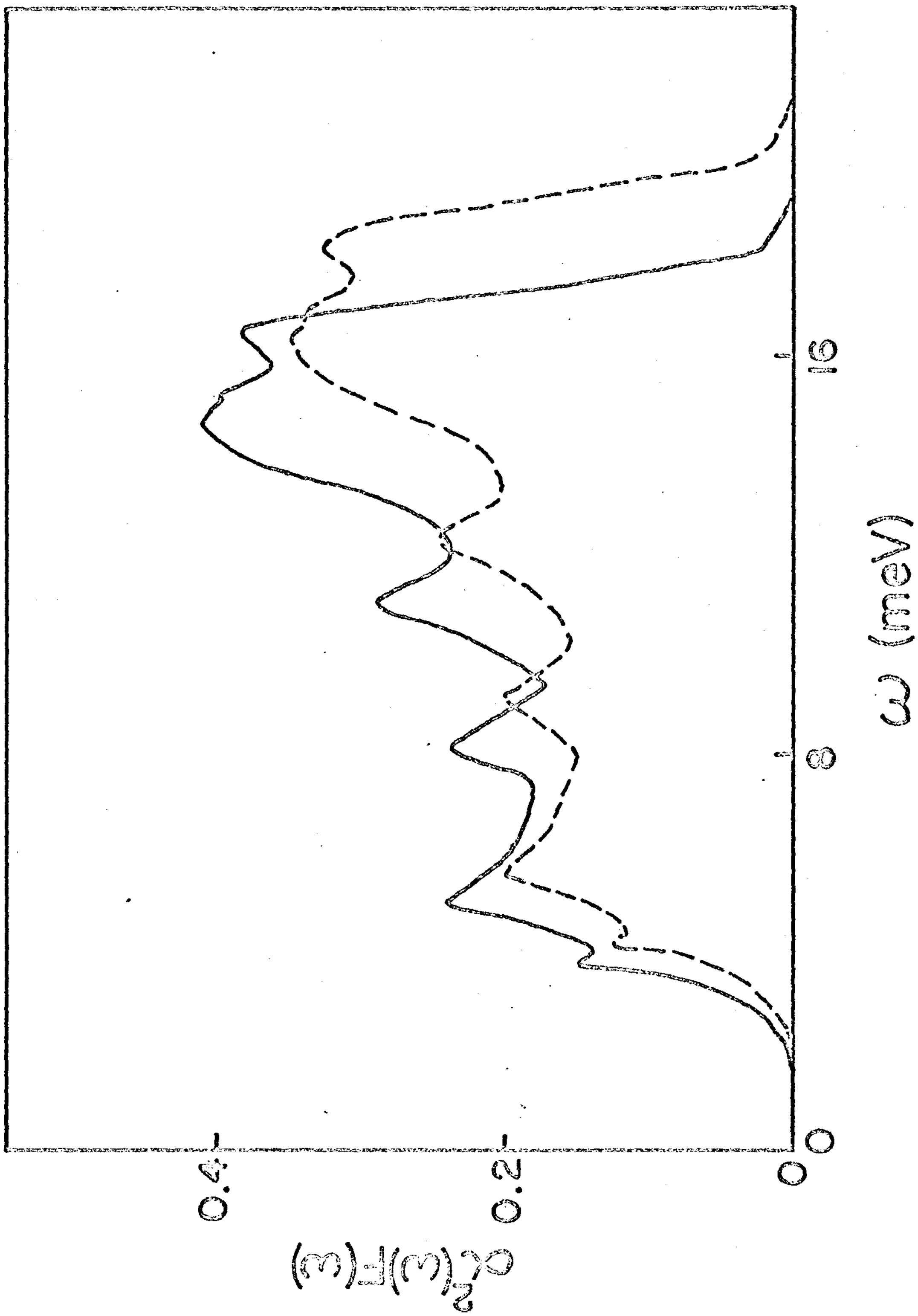

Figure 3.25

Figure 3.26 The McMillan-Rowell $\alpha^2(\omega)$ $F(\omega)$ function in indium (solid line) and the rescaled $\alpha^2(\omega)$ $F(\omega)$ function for a 5% volume decrease (dashed line) versus the phonon energy ω. The Grüneisen parameter is $\gamma=2.50$.

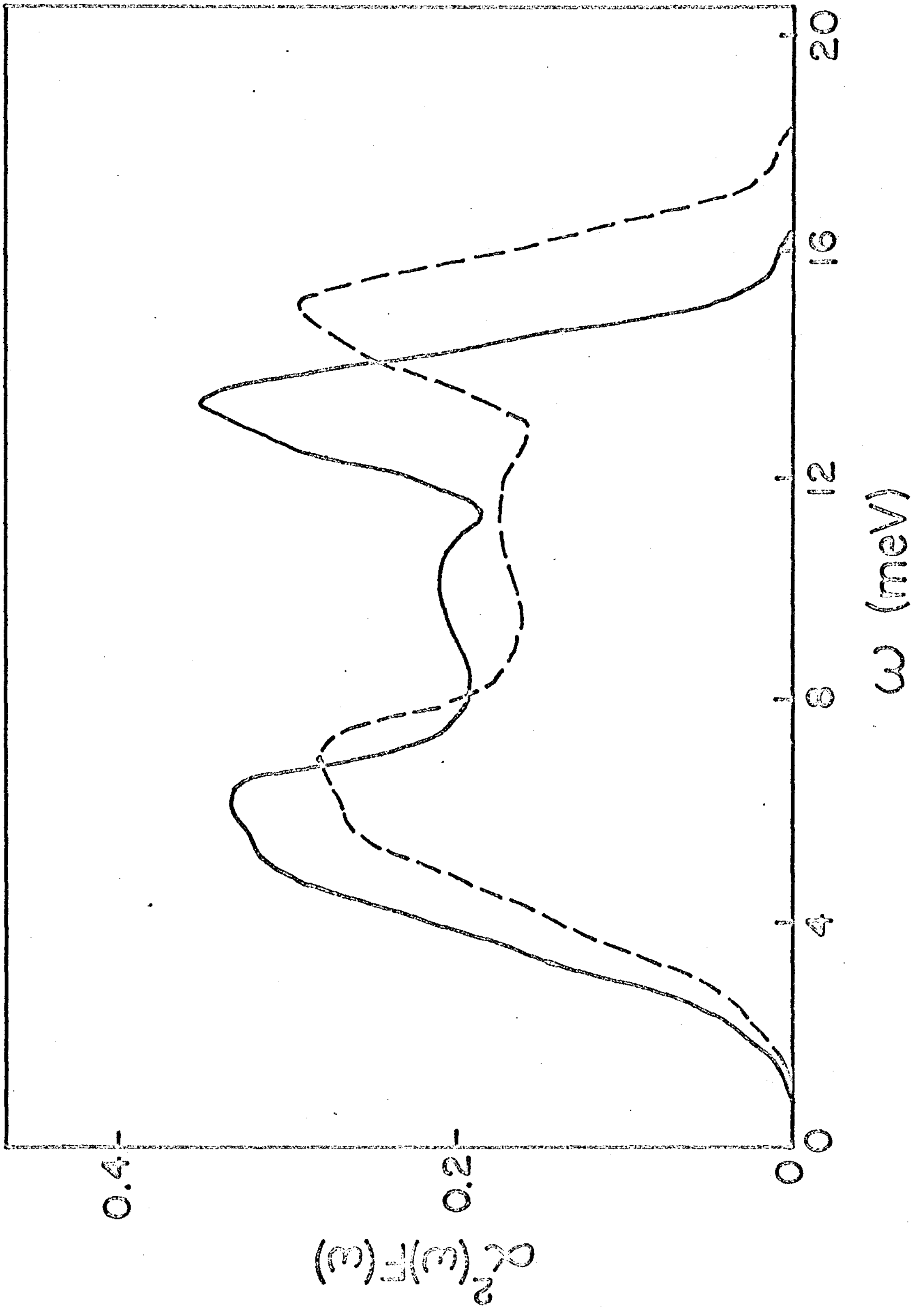

Figure 3.26

Figure 3.27 A comparison of the calculated critical temperature variation with volume change with the experimental variation (solid lines). The circled points are for tin. The lower and upper boxed points are for indium with Grüneisen parameters $\gamma=2.50$ and $\gamma=1.80$ respectively.

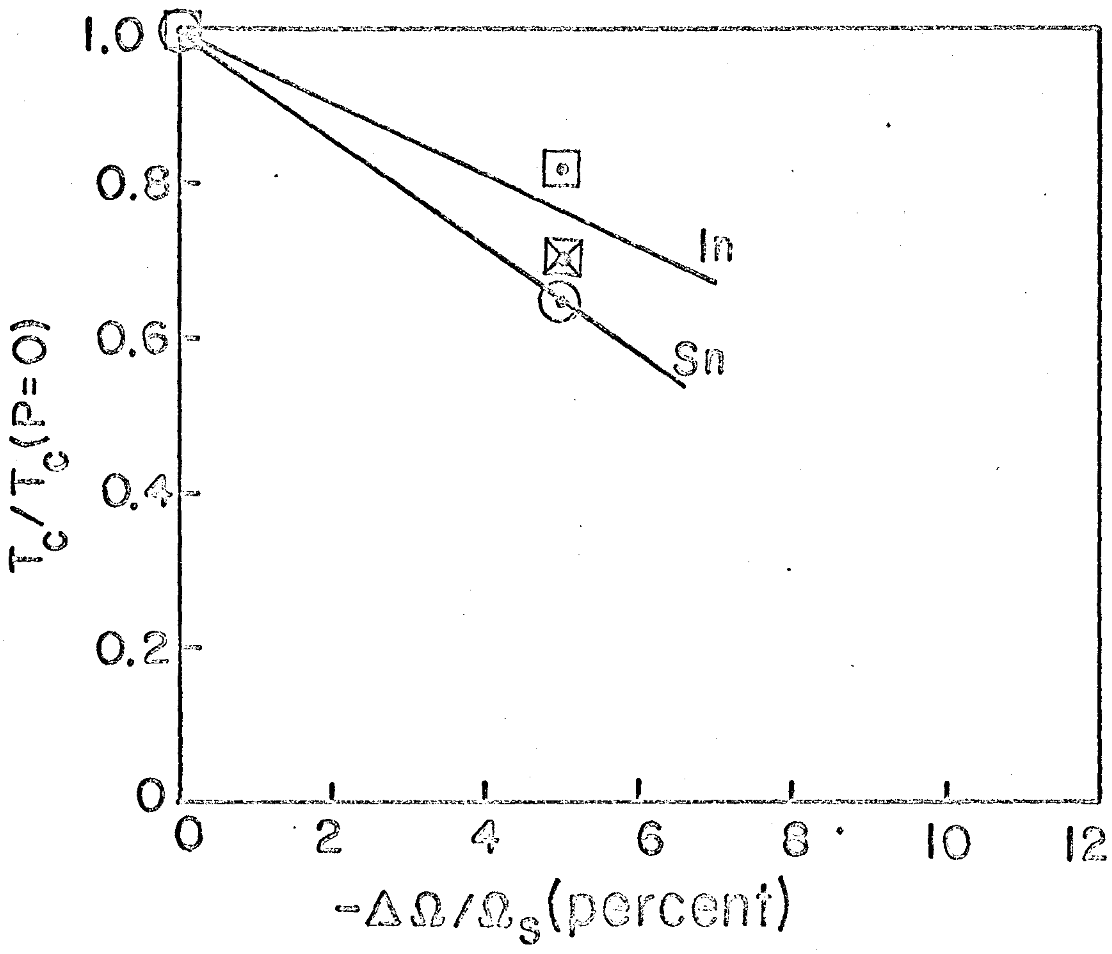
1.0
0.8
0.6
0.4
0.2
0
$T_c/T_c(P=0)$
0
2
4
6
8
10
12
$-\Delta\Omega/\Omega_s$(percent)
In
Sn

Figure 3.27

$N(0)U_c = 0.15$. At 5% volume change the gap was found to be 0.370 meV. A comparison with the experimental results as quoted by Smith and Chu(39) is made in figure (3.27) with a B.C.S. ratio 3.52. Reasonable agreement is evident.

In indium the pseudopotentials for 0% and 5% volume changes are shown in figure (3.24b). The parameter B was calculated to be 1.0604. In figure (3.26) the rescaled indium spectrum with $\gamma=2.5$ (84) and B=1.0604 is compared to the McMillan-Rowell spectrum as obtained from inversion of the tunneling results. The zero temperature gap equations were solved for the zero pressure spectrum of figure (3.26) for a gap $(\Delta_0)_{0\%} = 0.525$ meV with $N(0)U_c = 0.14$. For the 5% volume decrease spectrum of figure (3.26) the gap was calculated to be 0.368 meV, a value that is considerably low compared to the experimental results of figure (3.27) when plotted with the B.C.S. ratio 3.52. An average Grüneisen parameter from phenomenologically fitted dispersion curves calculated by the pseudopotential method as was done in aluminum is $\gamma=0.18$ (82). With $\gamma=0.18$, the gap for a 5% volume change is 0.430 meV. From figure (3.27) it is evident that a Grüneisen parameter $\gamma=0.18$ is too small to account for the experimental behaviour of the transition temperature. It appears that a γ of about 0.20 would provide sufficient frequency shifts.

3.8 Summary and Comparison with Other Work

In order to summarize the work of the previous sections the values of the rescreening parameter B are given in Table (3.1) for 2½% and 5% volume decreases. In Table (3.2) the ratios of the transition temperatures at finite pressure to the zero pressure transition temperatures are summarized. A comparison of the results of this work is made with the results calculated from McMillan's equation, equation (3.9),

$$k_B T_c = \frac{\hbar\, \omega_u}{1.45}\, e^{-\left[\frac{1.04(1+\lambda)}{\lambda-\mu^*(1+0.62\lambda)}\right]} \qquad .(3.59)$$

A comparison is also made with the results calculated from the Morel-Anderson$^{(20)}$ form of the B.C.S. relationship

$$k_B T_c = 1.41\, \hbar\, \omega\, e^{-\frac{1}{\lambda-\mu^*}} \qquad .(3.60)$$

The parameter λ is given by equation (3.6),

$$\lambda = 2 \int_0^\infty \frac{\alpha^2(\omega)\ F(\omega)}{\omega}\, d\omega \qquad .(3.61)$$

The scaling procedure of equation (3.39) can be combined with equation (3.61) to obtain a relationship between $\lambda_{\frac{\Delta\Omega}{\Omega_s}}$ at finite pressure at the zero pressure parameter λ_0. It is

$$\lambda_{\frac{\Delta\Omega}{\Omega_s}} = \frac{B}{\beta^2}\, \lambda_0 \qquad (3.62)$$

where β is the parameter relating the phonon frequency

TABLE 3.1

SCREENING RENORMALIZATION PARAMETER B

	$-\frac{\Delta\Omega}{\Omega_s} = 2.5\%$	$-\frac{\Delta\Omega}{\Omega_s} = 5\%$
Pb	1.0151	1.0348
Hg	1.0187	1.0428
In	1.0273	1.0604
Sn	1.0200	1.0445
Al	1.0263	1.0563

TABLE 3.2

COMPARISON OF THE EFFECT OF VOLUME CHANGE ON THE TRANSITION TEMPERATURE RATIO $T_c/T_c(P=0)$

				THIS WORK		McMILLAN'S FORMULA		MOREL-ANDERSON B.C.S. FORMULA	
	γ	λ_0%	μ*	$-\frac{\Delta\Omega}{\Omega_s}$ = 2½%	5%	2½%	5%	2½%	5%
Pb	2.85	1.53	0.13	--	0.881	0.936	0.868	0.966	0.927
Hg	3.00	1.66	0.09	--	0.888	0.962	0.920	0.981	0.957
In	2.50	0.83	0.14	--	0.701	0.835	0.695	0.891	0.792
	1.80	0.83	0.14	--	0.819	0.898	0.812	0.935	0.879
Sn	2.25	0.79	0.15	--	0.643	0.814	0.657	0.878	0.766
Al	2.60	0.46	0.16	0.439	0.178	0.440	0.171	0.603	0.340
	2.22	0.46	0.16	0.528	0.267	0.520	0.253	0.668	0.431

shifts and the Gruneisen parameter γ,

$$\beta = (1 - \gamma \frac{\Delta\Omega}{\Omega_s}) \quad .(3.63)$$

It is interesting that this model gives a very simple relationship for the dependence of the renormalization parameter λ on volume change.

The screening parameter B is plotted as a function of volume change in figure (3.28) for volume changes of 0%, 2½% and 5%. The variation is not strictly linear but may be approximately linear for very small volume changes. The results of Table (3.2) are compared with the straight line variations of the transition temperature decreases with volume change quoted by Smith and Chu(39) in figures (3.29), (3.30) and (3.31). In figure (3.29) the results calculated directly from the gap equations are given. A comparison of these results with those calculated from McMillan's formula shows that the agreement is good for all the materials with the exception of mercury. In mercury, the McMillan formula gives transition temperature ratios that are larger than those calculated directly from the gap equations. This is probably attributable to the different shape of the $\alpha^2(\omega)$ $F(\omega)$ spectrum for mercury since the McMillan formula is fitted to a niobium-type spectrum. The Morel-Anderson form of the B.C.S. relationship gives variations of the transition temperatures with

Figure 3.28 The renormalization factor B due to rescreening the pseudopotential as a function of volume change.

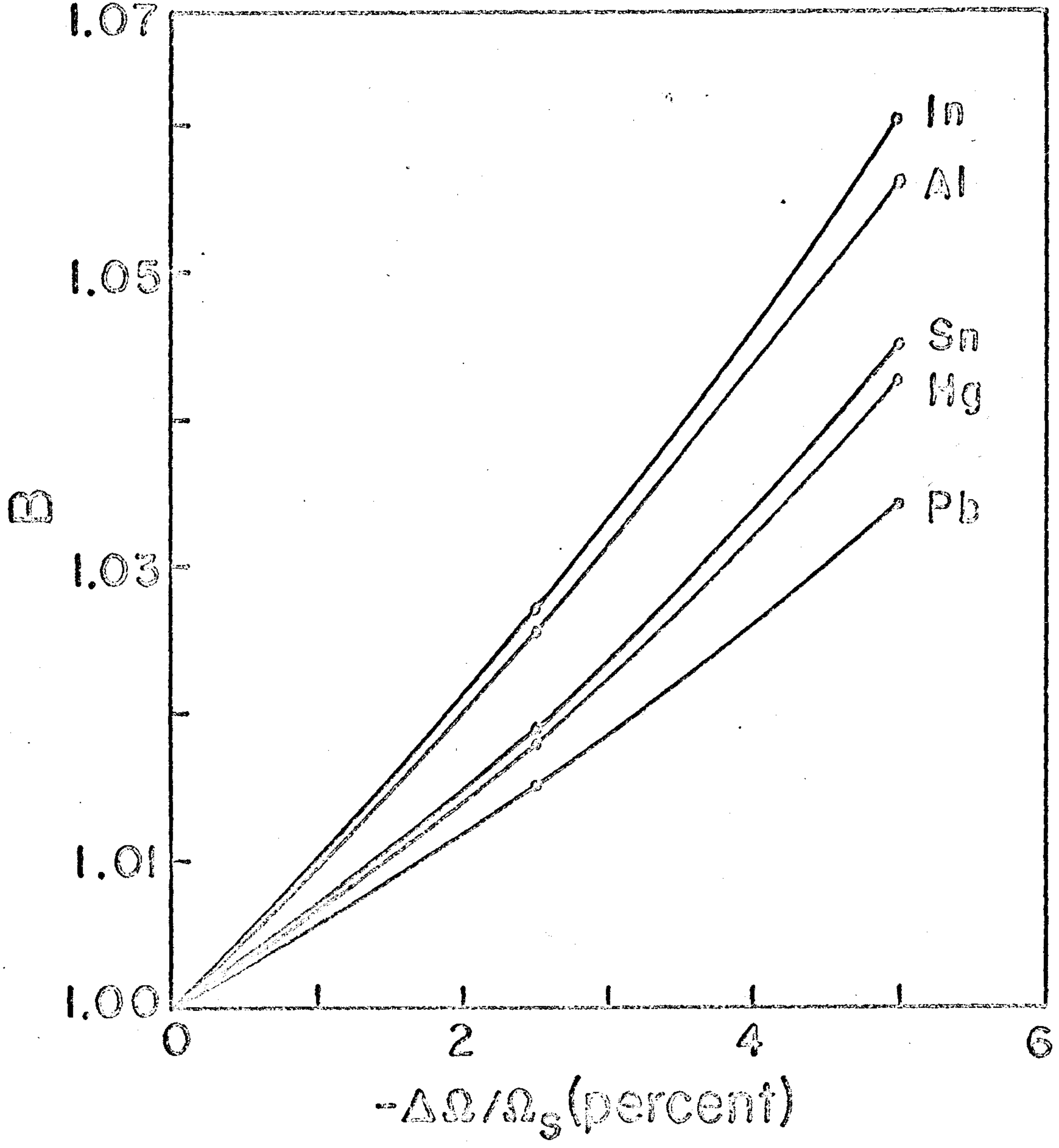
1.07
1.05
1.03
1.01
1.00
m
0
2
4
6
$-\Delta\Omega/\Omega_s$(percent)
In
Al
Sn
Hg
Pb

Figure 3.28

Figure 3.29 A summary of the variation of the transition temperature with volume change as calculated by the solution of the gap equations.

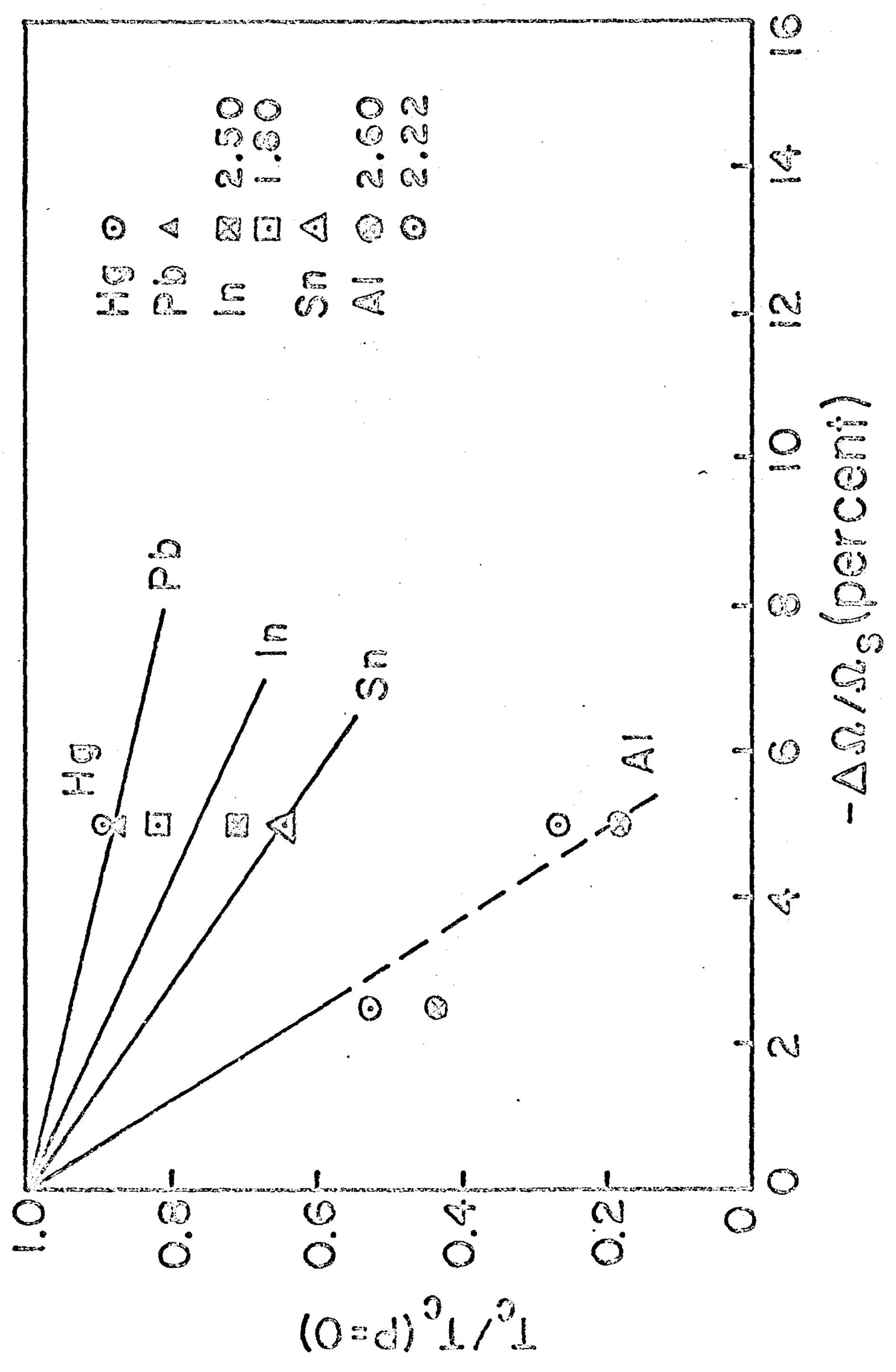
$T_c/T_c(P=0)$
1.0
0.8
0.6
0.4
0.2
0
$-\Delta\Omega/\Omega_S$ (percent)
0
2
4
6
8
10
12
14
16
Hg
Pb
In
Sn
Al
Hg ⊙
Pb △
In ⊠ 2.50
⊡ 1.80
Sn △
Al ⊗ 2.60
⊙ 2.22

Figure 3.29

Figure 3.30 The variation of the transition temperature with volume change as calculated with McMillan's formula. The legend for the points is the same as in figure 3.29.

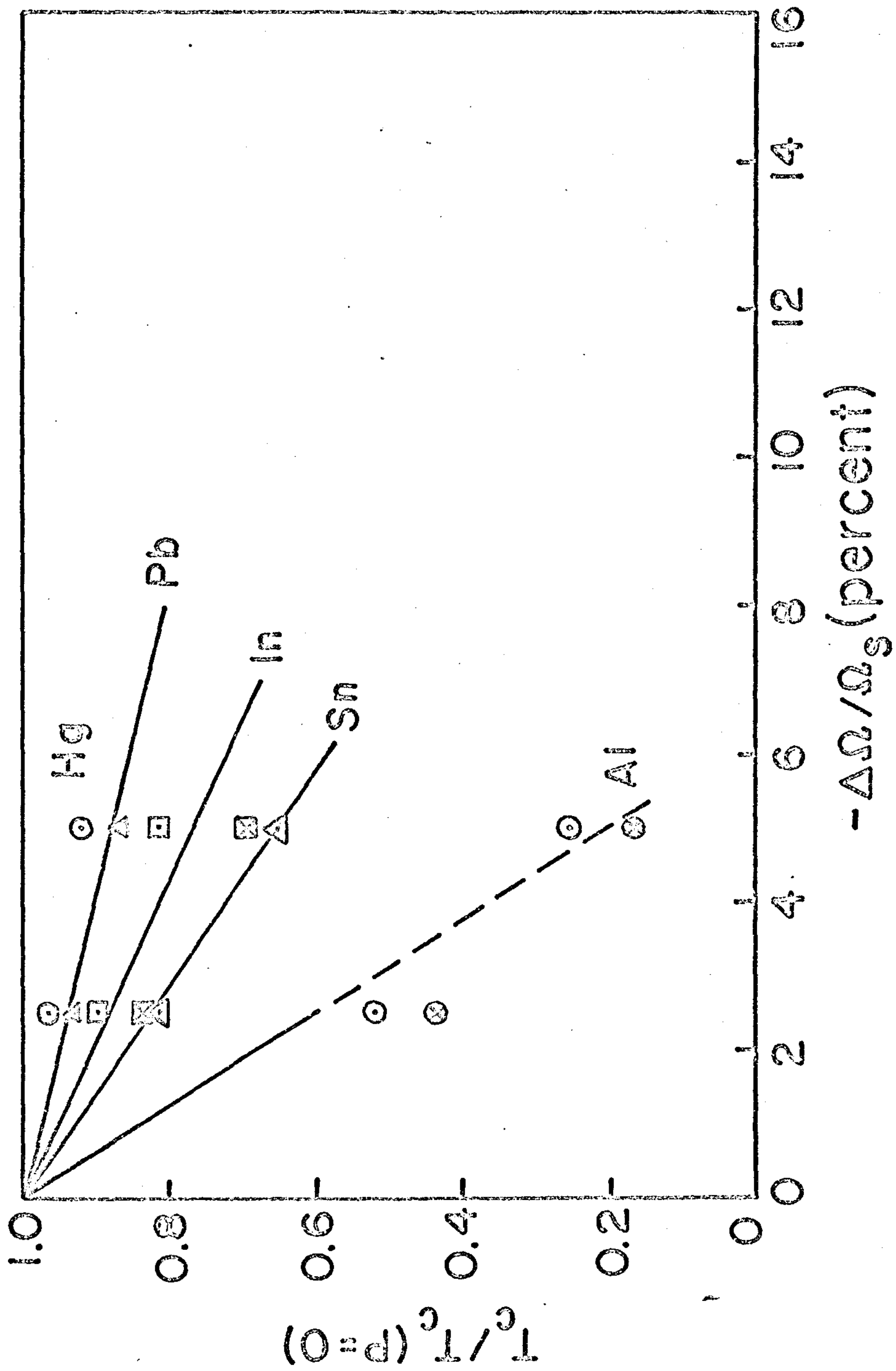
$T_c/T_c(P=0)$
1.0
0.8
0.6
0.4
0.2
0
0
2
4
6
8
10
12
14
16
$-\Delta\Omega/\Omega_s$ (percent)
Hg
Pb
In
Sn
Al

Figure 3.30

Figure 3.31 The variation of the transition temperature with volume change as calculated with the Morel-Anderson form of the B.C.S. formula. The legend for the points is the same as in figure 3.29.

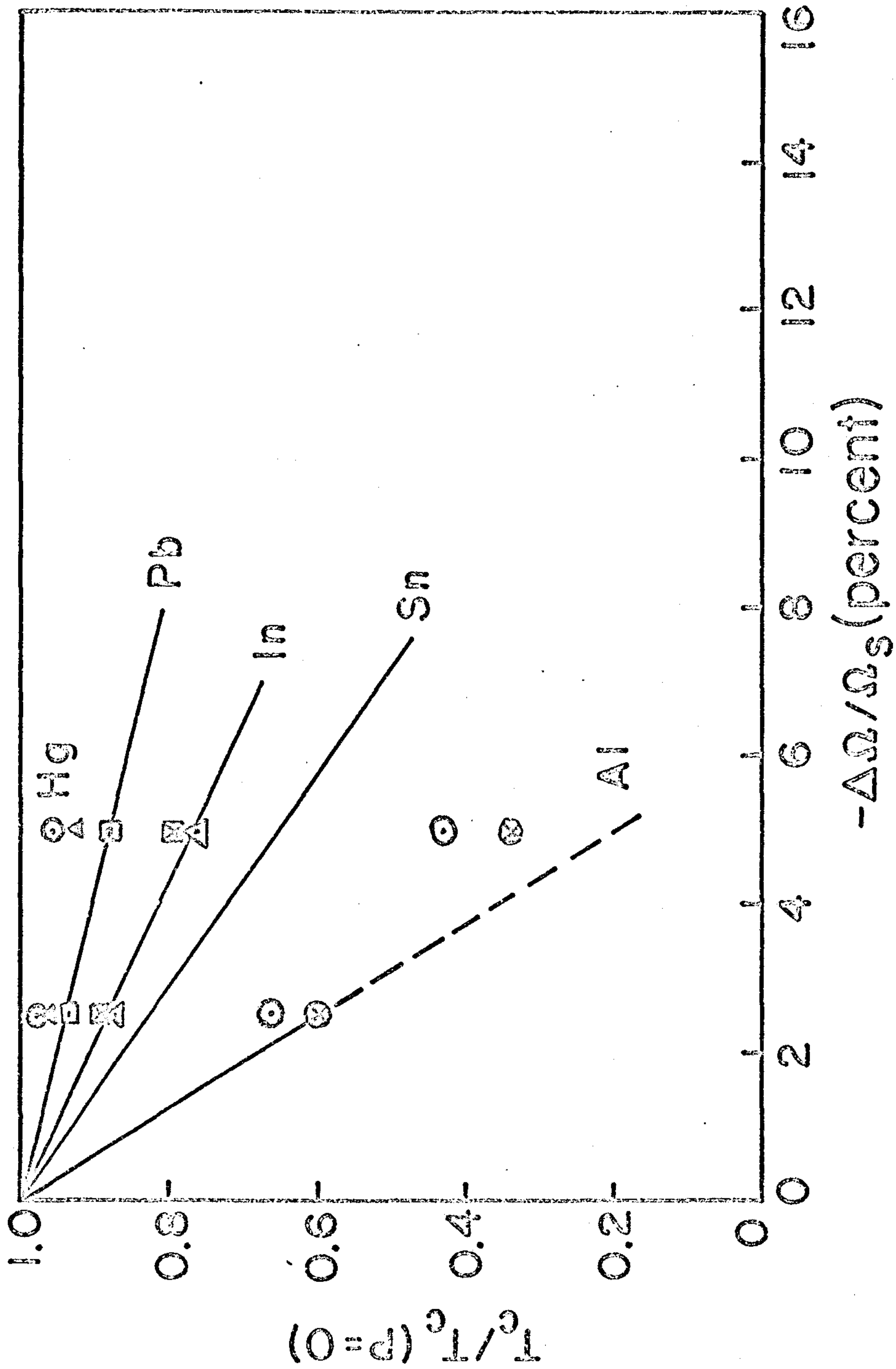
Hg
Pb
In
Sn
Al
0
2
4
6
8
10
12
14
16
$-\Delta\Omega/\Omega_s$ (percent)
1.0
0.8
0.6
0.4
0.2
0
$T_c/T_c\,(P=0)$

Figure 3.31

volume decrease that are not in good agreement with the results obtained by the solution of the gap equations or the use of McMillan's formula.

In Table (3.3) values of λ for 0%, 2½% and 5% volume decreases calculated by equation (3.62) are given. These are the values of the parameters to be used in calculating the temperature ratios for finite volume changes. In the model used here the parameters decrease with decreasing volume for all five metals under consideration.

It is useful to compare the results obtained here with the recent work of Seiden$^{(74)}$. He calculated the effect of pressure on superconductivity in simple metals with McMillan's formula, equation (3.59). The values of λ_0 used by Seiden are not in good agreement with the ones used in this work which are derived from the tunneling inversion spectra and which are expected to be more reliable. For the volume effect corresponding to the factor B, Seiden used the long-wavelength limit of the screened Coulomb interaction. By equation (2.55) this limit is $-\frac{2}{3}E_F$ so the variation with volume is $(\frac{1}{\Omega})^{4/3}$. For small volume changes in this approximation the parameter B is

$$B = (1 - (\frac{4}{3})\frac{\Delta\Omega}{\Omega_s}) \qquad .(3.64)$$

For 2½% and 5% volume changes equation (3.62) gives the parameters B=1.0333 and B=1.0667 for all the metals. Rescreening the bare pseudopotential gives different values

TABLE 3.3

VARIATION OF λ WITH VOLUME CHANGE

	γ	$\lambda_{0\%}$	$\lambda_{2\frac{1}{2}\%}$	$\lambda_{5\%}$
Pb	2.85	1.53	1.35	1.21
Hg	3.00	1.66	1.46	1.31
In	1.80	0.83	0.78	0.74
Sn	2.25	0.79	0.72	0.66
Al	2.22	0.46	0.42	0.39

as is evident in Table (3.1) and these are expected to be more accurate; the difference in the Grüneisen parameter necessary to obtain agreement with the experimental pressure dependence of the transition temperature is not negligible as will be shown later. The work in this thesis also serves to justify to some extent the use of McMillan's formula for a wide variety of $\alpha^2(\omega)\,F(\omega)$ spectra.

For small volume changes the renormalization parameter for finite pressure can be written

$$\lambda_{\frac{\Delta\Omega}{\Omega_s}} = \frac{(1 - \textcircled{a}\,\frac{\Delta\Omega}{\Omega_s})}{(1 - \gamma\,\frac{\Delta\Omega}{\Omega_s})^2}\,\lambda_0 \qquad (3.65)$$

where equations (3.62) and (3.64) have been combined and the factor 4/3 of equation (3.64) has been replaced by the parameter a to be determined by rescreening the pseudopotential. The ratio of the transition temperatures as obtained by McMillan's formula for small volume changes can be written as

$$\frac{T_c}{T_c(P=0)} = (1 - c\,\frac{\Delta\Omega}{\Omega_s}) \qquad ,(3.66)$$

where c is the slope of the critical temperature versus volume change curve. To first order in the volume change, the ratio can be inverted to obtain an expression for the Grüneisen parameter γ in terms of μ^*, λ_0, a and the slope c. This expression is

$$\gamma = (c + a\ f_1 f_2)/(1 + 2f_1 f_2) \qquad ,(3.67)$$

where

$$f_1 = \frac{1.04\,\lambda_0}{\lambda_0 - \mu^*(1+0.62\lambda_0)} \quad ,(3.68)$$

and

$$f_2 = 1 + \frac{(1+\lambda_0)\ (1-0.62\mu^*)}{\lambda_0 - \mu^*(1+0.62\lambda_0)} \quad .(3.69)$$

Equation (3.67) has been used to obtain the Grüneisen parameter γ from the slope c as taken from the quoted results of Smith and Chu and the parameters λ_0 and μ^* used in the work of this thesis as given in Table (3.2). The value for a was calculated from the parameter B for a 2½% volume change. In Table (3.4) the calculated Grüneisen parameters are compared with the parameters calculated with a=4/3. It is evident that the factor a is important for a good estimate of a Grüneisen parameter. If a is well known equation (3.67) can be used to determine Grüneisen parameters from the dependence of the critical temperature on volume change. It is again noted that the McMillan formula gives a Grüneisen parameter for mercury that appears to be too large.

TABLE 3.4

GRUNEISEN PARAMETERS FROM SLOPE OF $T_c/T_c(P=0)$ VERSUS $-\frac{\Delta\Omega}{\Omega_s}$ LINES

	a	γ	γ for a=4/3
Pb	0.604	2.88	3.59
Hg	0.748	4.42	5.17
In	1.092	1.91	2.06
Sn	0.796	2.07	2.40
Al	1.050	1.65	1.80

CHAPTER IV

A CONTRIBUTION TO THE THEORY OF SUPERCONDUCTIVITY IN BINARY ALLOYS OF SIMPLE METALS

4.1 Introduction

In this chapter the theory of strong-coupling superconductivity in a binary alloy of simple metals will be discussed. It has been seen in the previous two chapters that knowledge of the atomic force constants that determine the lattice dynamics and information on the electron-ion scattering cross section serve to totally specify the product function $\alpha^2(\omega) F(\omega)$ as calculated by Carbotte and Dynes(29,30) for a pure metal. In an alloy, on first inspection, there would seem to be two modifications necessary to obtain $\alpha^2(\omega) F(\omega)$. Firstly, since an alloy, unlike a pure metal, does not have translational symmetry the normal modes of the lattice vibrations are no longer strictly the independent phonon modes specified by a wave vector. Secondly, a modification of the Hamiltonian coupling the conduction electron and ion motion would seem necessary due to the presence of more than one type of ion.

Ng(44) has studied alloys of the thallium-lead-bismuth series by the method of neutron spectroscopy. This alloy series is particularly suitable for study because the conduction electron concentration can be varied over a wide range without a change in the crystal structure and the effects of mass disorder can be neglected(48). The work of Ng indicates that well defined phonon modes exist in these alloys although the neutron groups are broader than those observed in pure lead. Ng has analyzed the measured dispersion curves for these alloys in terms of atomic force constants and has derived an expression for the phonon widths due to force constant disorder in first order time-dependent perturbation theory. His analysis indicates that the force constant disorder is not large.

Dynes, Carbotte, Taylor and Campbell(31) have studied superconductivity in the thallium-lead-bismuth series. They have used the atomic force constants determined by Ng and a pseudopotential fitted to reproduce the measured phonon dispersion curves to calculate $\alpha^2(\omega)\ F(\omega)$ for a number of alloys. The calculated gaps are in good agreement with those from tunneling experiments performed with these alloys.

More recently, Dynes and Rowell(43) have inverted the gap equations for a number of alloys to obtain the function $\alpha^2(\omega)\ F(\omega)$ from tunneling experiments. Their results show that the peaks of the $\alpha^2(\omega)\ F(\omega)$ spectra are generally broadened as compared to lead. They attribute this broadening to disorder effects and have made calculations of $\alpha^2(\omega)\ F(\omega)$ which phenomenologically include effects of phonon broadening.

In this chapter the possibility of obtaining estimates of phonon broadening due to disorder effects in alloys with the use of pseudopotentials is investigated. In addition the effects of disorder on the electron-phonon interaction are studied.

4.2 The Structure-Dependent Energy of a Binary Alloy

In Chapter II the dynamical matrix for a pure metal of equation (2.85) was written in terms of an effective interatomic interaction potential. The total interaction energy was a sum of the energy due to direct Coulomb interactions among the bare ions and the structure-dependent conduction electron energy which was cast in the form of an indirect ion-ion interaction energy. In this section the structure-dependent energy of a binary alloy as derived by Hayes, Brooks and Bienenstock$^{(47)}$ will be discussed.

The model for the disordered binary alloy $A_x B_{1-x}$ consists of a fraction x of A ions and a fraction (1-x) of B ions of a total of N ions randomly arranged in a Bravais lattice. A bare pseudopotential form factor is attributed to each type of ion and the ions are screened with an electron gas of the density appropriate for the alloy. The notation of Hayes, Brooks and Bienenstock is to define $\sigma(\underset{\sim}{R}_\ell)$ such that

$\sigma(\underset{\sim}{R}_\ell) = +1$ if the site $\underset{\sim}{R}_\ell$ contains an A atom,

$$\sigma(\underset{\sim}{R}_\ell) = -1 \quad \text{if the site } \underset{\sim}{R}_\ell \text{ contains a B atom,} \tag{4.1}$$

so that

$$\frac{1}{N}\sum_\ell \left(\frac{1+\sigma(\underset{\sim}{R}_\ell)}{2}\right) e^{-i\underset{\sim}{q}\cdot\underset{\sim}{R}_\ell} = \frac{1}{N}\sum_\ell{}^{A} e^{-i\underset{\sim}{q}\cdot\underset{\sim}{R}_\ell} \tag{4.2}$$

where the sum on the right hand side is restricted to atoms of type A. An analogous equation holds for B with $(1+\sigma(\underset{\sim}{R}_\ell))$ replaced by $(1-\sigma(\underset{\sim}{R}_\ell))$. This notation is particularly convenient for an alloy of arbitrary concentrations of A and B ions.

In the above notation a matrix element of the lattice potential W as seen by a conduction electron is

$$<\underset{\sim}{k}+\underset{\sim}{q}|W|\underset{\sim}{k}> = \frac{1}{2N}\sum_\ell e^{-i\underset{\sim}{q}\cdot\underset{\sim}{R}_\ell}\{(1+\sigma(\underset{\sim}{R}_\ell))\ <\underset{\sim}{k}+\underset{\sim}{q}|w^A|\underset{\sim}{k}>$$

$$+\ (1-\sigma(\underset{\sim}{R}_\ell))\ <\underset{\sim}{k}+\underset{\sim}{q}|w^B|\underset{\sim}{k}> \tag{4.3}$$

The matrix elements are evaluated for electron states of wave vector $\underset{\sim}{k}$. The potentials w^A and w^B refer to ions A and B respectively. Equation (4.3) is the generalization of the diffraction model for an alloy.

The element $<\underset{\sim}{k}+\underset{\sim}{q}|W|\underset{\sim}{k}>$ can be expressed in a more convenient form(47) with the definition of an average pseudopotential $\bar{w}$ by

$$<\underset{\sim}{k}+\underset{\sim}{q}|\bar{w}|\underset{\sim}{k}> \equiv x<\underset{\sim}{k}+\underset{\sim}{q}|w^A|\underset{\sim}{k}> + (1-x)\ <\underset{\sim}{k}+\underset{\sim}{q}|w^B|\underset{\sim}{k}> \tag{4.4}$$

and a difference pseudopotential $\Delta\, w$ by

$$<\underset{\sim}{k}+\underset{\sim}{q}|\Delta w|\underset{\sim}{k}> \equiv \frac{1}{2}\ [<\underset{\sim}{k}+\underset{\sim}{q}|w^A|\underset{\sim}{k}> - <\underset{\sim}{k}+\underset{\sim}{q}|w^B|\underset{\sim}{k}>] \tag{4.5}$$

Then

$$<\underset{\sim}{k}+\underset{\sim}{q}|W|\underset{\sim}{k}> \;=\; S(\underset{\sim}{q})\;<\underset{\sim}{k}+\underset{\sim}{q}|\bar{w}|\underset{\sim}{k}> + F(\underset{\sim}{q})\;<\underset{\sim}{k}+\underset{\sim}{q}|\Delta w|\underset{\sim}{k}> \qquad (4.6)$$

where

$$F(\underset{\sim}{q}) \equiv \frac{1}{N}\sum_{\ell} e^{-i\underset{\sim}{q}\cdot\underset{\sim}{R}_{\ell}}\,[\sigma(\underset{\sim}{R}_{\ell}) - <\sigma>_{R}] \qquad (4.7)$$

with

$$<\sigma>_{R} \equiv \frac{1}{N}\sum_{\ell}\sigma(\underset{\sim}{R}_{\ell}) \qquad .(4.8)$$

$S(\underset{\sim}{q})$ is the usual structure factor of equation (2.63)

$$S(\underset{\sim}{q}) = \frac{1}{N}\sum_{\ell} e^{-i\underset{\sim}{q}\cdot\underset{\sim}{R}_{\ell}} \qquad .(4.9)$$

The quantity $<\sigma>_{R}$ has the value 2x-1.

Each of the two terms on the right hand side of equation (4.5) consists of a factor that depends on the arrangement of the ions and a factor that is structure-independent. A useful property of $F(\underset{\sim}{q})$ is that for all ions in their equilibrium positions, $\underset{\sim}{R}_{\ell}=\underset{\sim}{R}_{\ell}^{0}$,

$$F(\underset{\sim}{\kappa}_{n}) = 0 \qquad (4.10)$$

where $\underset{\sim}{\kappa}_{n}$ is a reciprocal lattice vector. Since $S(\underset{\sim}{q})$ is unity if $\underset{\sim}{q}$ is an inverse lattice vector and zero otherwise for all ions in their equilibrium positions it follows that for all ions in their equilibrium positions only the first term or the second term on the right hand side of equation (4.6) is non-zero for an arbitrary $\underset{\sim}{q}$.

Hayes, Brooks and Bienenstock$^{(47)}$ have written the structure-dependent energy E_{sd} for a binary alloy in analogy to the corresponding energy in the pure metal as in equation (2.74). The expression for E_{sd} is (per ion)

$$E_{sd} = \frac{1}{2N} \sum_{\substack{\ell,\ell' \\ \ell\neq\ell'}} \frac{2}{N} \sum_{\underset{\sim}{q}}{}' e^{i\underset{\sim}{q}\cdot(\underset{\sim}{R}_\ell - \underset{\sim}{R}_{\ell'})}$$

$$\times \{E_{11}(\underset{\sim}{q}) + [\sigma(\underset{\sim}{R}_{\ell'}) - \langle\sigma\rangle_R]E_{12}(\underset{\sim}{q}) + [\sigma(\underset{\sim}{R}_\ell) - \langle\sigma\rangle_R]E_{21}(\underset{\sim}{q})$$

$$+ [\sigma(\underset{\sim}{R}_\ell) - \langle\sigma\rangle_R]\ [\sigma(\underset{\sim}{R}_{\ell'}) - \langle\sigma\rangle_R]E_{22}(\underset{\sim}{q})\} \qquad .(4.11)$$

In the local approximation the E_{ij} for i, j = 1, 2 are defined by

$$E_{ij}(\underset{\sim}{q}) \equiv \frac{-\ \Omega_0\ q^2}{8\pi\ e^2} w_i^{*o}(\underset{\sim}{q})\ w_j^o(\underset{\sim}{q})\ \left(\frac{\varepsilon(\underset{\sim}{q})-1}{\varepsilon(\underset{\sim}{q})}\right) \qquad (4.12)$$

where

$$\begin{aligned} w_1^o(\underset{\sim}{q}) &= \bar{w}^o(\underset{\sim}{q}) \quad , \\ w_2^o(\underset{\sim}{q}) &= \Delta\ w^o(\underset{\sim}{q}) \quad . \end{aligned} \qquad (4.13)$$

The equation for E_{ij} is directly comparable to $E(\underset{\sim}{q})$ of equation (2.73). Ω_0 is the volume per ion and $\varepsilon(\underset{\sim}{q})$ is the dielectric function. In the case of an alloy the structure-dependent electronic energy contains contributions from the bare average pseudopotential $\bar{w}^o$ and the difference bare pseudopotential $\Delta\ w^o$. For a pure metal only the first term on the right hand side of equation (4.11) is present with $w_1^o(q)$ replaced by $w^o(q)$.

Apart from the local approximation, the expressions E_{ij} as written in equation (4.12) differ from those of Hayes, Brooks and Bienenstock$^{(47)}$ in that the leading coefficient in the expression for the valence pseudowavefunction in terms of plane waves is taken to be unity and the conduction electron charge that arises from the sum over core states is taken to be part of an effective valence$^{(46)}$.

In addition to the conduction electron contribution to the structure-dependent energy, the inter-ionic Coulomb energy E_c must be included. This energy is$^{(47)}$ (per ion)

$$E_c = \frac{1}{2N} \sum_{\substack{\ell,\ell' \\ \ell\neq\ell'}} \frac{e^2}{4|\underset{\sim}{R}_\ell - \underset{\sim}{R}_{\ell'}|}\{[(1+\sigma(\underset{\sim}{R}_\ell))Z_A$$

$$+ (1-\sigma(\underset{\sim}{R}_{\ell'}))Z_B]\ [(1+\sigma(\underset{\sim}{R}_{\ell'}))Z_A + (1-\sigma(\underset{\sim}{R}_{\ell'}))Z_B]\} \qquad .(4.14)$$

A_A and Z_B are the valence numbers of the A and B ions. The expression for E_c can be rewritten in a form similar to equation (4.11) with the application of the Ewald-Fuchs method$^{(46)}$ and a rearrangement of the projection operators. In the new form E_c is

$$E_c = \frac{1}{2N} \sum_{\ell,\ell'} \sum_{\underset{\sim}{q}}{}' \frac{1}{N} v(\underset{\sim}{q})\ e^{i\underset{\sim}{q}\cdot(\underset{\sim}{R}_\ell - \underset{\sim}{R}_{\ell'})}$$

$$\times \; \{\bar{Z}^2 + [\sigma(\underset{\sim}{R}_{\ell'}) - \langle\sigma\rangle_R]_{\Delta Z \;\; Z} \; \bar{Z} \; \Delta Z$$

$$+ \; [\sigma(\underset{\sim}{R}_{\ell}) - \langle\sigma\rangle_R] \; \Delta Z \; \bar{Z}$$

$$+ \; [\sigma(\underset{\sim}{R}_{\ell}) - \langle\sigma\rangle_R] \; [\sigma(\underset{\sim}{R}_{\ell'}) - \langle\sigma\rangle_R] \; (\Delta Z)^2\}$$

$$- \text{ (self-energy term)} \qquad ,(4.15)$$

where $\bar{Z}$ is the average charge and ΔZ the difference,

$$\bar{Z} = x \, Z_A + (1-x) Z_B \qquad ,$$

$$\Delta Z = \frac{1}{2} \, (Z_A - Z_B) \qquad , \qquad (4.16)$$

and

$$v(\underset{\sim}{q}) = \frac{4\pi \, e^2}{\Omega_0 \, q^2} \qquad .(4.17)$$

It should be noted that for Z_A equal to Z_B only the first term in equation (4.15) is non-zero and E_c is then the inter-ionic Coulomb energy equivalent to that of a pure metal, as expected.

Equations (4.11) and (4.15) can be combined to give the total structure-dependent energy. The total energy is to be used to describe the lattice dynamics of the alloy and in this context the self-energy terms are unimportant and are dropped. The sum over ℓ and ℓ' can thus be restricted to $\ell \neq \ell'$. With the definitions

$$E'_{11}(\underset{\sim}{q}) \equiv 2E_{11}(\underset{\sim}{q}) + \bar{Z}^2 \, v(\underset{\sim}{q}) \qquad ,$$

$$E'_{12}(\underset{\sim}{q}) \equiv 2E_{12}(\underset{\sim}{q}) + \bar{Z}\,\Delta Z\; v(\underset{\sim}{q}) \qquad ,$$

$$E'_{21}(\underset{\sim}{q}) \equiv 2E_{21}(\underset{\sim}{q}) + \Delta Z\,\bar{Z}\; v(\underset{\sim}{q}) \qquad ,$$

$$E_{22}(\underset{\sim}{q}) \equiv 2E_{22}(\underset{\sim}{q}) + (\Delta Z)^{2}\; v(\underset{\sim}{q}) \qquad ,(4.18)$$

the potential energy $W(\underset{\sim}{R}_1,\underset{\sim}{R}_2\ldots\underset{\sim}{R}_N)$ is

$$W(\underset{\sim}{R}_1,\underset{\sim}{R}_2\ldots\underset{\sim}{R}_N) = \frac{1}{2N}\sum_{\substack{\ell,\ell' \\ \ell\neq\ell'}}\;\sum_{\underset{\sim}{q}}{}'\; e^{i\underset{\sim}{q}\cdot(\underset{\sim}{R}_{\ell}-\underset{\sim}{R}_{\ell'})}$$

$$\times\{E'_{11}(\underset{\sim}{q}) + [\sigma(\underset{\sim}{R}_{\ell'}) - \langle\sigma\rangle_R]E'_{12}(\underset{\sim}{q})$$

$$+ [\sigma(\underset{\sim}{R}_{\ell}) - \langle\sigma\rangle_R]E'_{21}(\underset{\sim}{q}) + [\sigma(\underset{\sim}{R}_{\ell}) - \langle\sigma\rangle_R]\,[\sigma(\underset{\sim}{R}_{\ell'}) - \langle\sigma\rangle_R]$$

$$\times\, E'_{22}(\underset{\sim}{q})\} \qquad .(4.19)$$

This is an expression for the potential energy of the lattice written in terms of two-body potentials $V(\underset{\sim}{R}_{\ell},\underset{\sim}{R}_{\ell'})$. The two-body potentials are functions of ion separation distance and also contain information on the arrangement of the A and B ions in the lattice through $\sigma(\underset{\sim}{R}_{\ell})$ and $\sigma(\underset{\sim}{R}_{\ell'})$.

4.3 Theory of Calculation of Phonon Widths

In Chapter II the Born-von Kármán force constant model was discussed for an arbitrary potential $W(\underset{\sim}{R}_1,\underset{\sim}{R}_2\ldots\underset{\sim}{R}_N)$. Equation (4.19) is an expression for this potential in terms of two-body potentials $V(\underset{\sim}{R}_\ell,\underset{\sim}{R}_{\ell'})$ with

$$W(\underset{\sim}{R}_1,\underset{\sim}{R}_2\ldots\underset{\sim}{R}_N) = \frac{1}{2}\sum_{\substack{\ell,\ell'\\ \ell\neq\ell'}} V(\underset{\sim}{R}_\ell,\underset{\sim}{R}_{\ell'}) \qquad .(4.20)$$

The atomic force constants $\Phi_{\alpha\beta}(\ell,\ell')$ are obtained from equation (2.4),

$$\Phi_{\alpha\beta}(\ell,\ell') = \left[\frac{\partial^2 W}{\partial R_\alpha(\ell)\ \partial R_\beta(\ell')}\right]_0 \qquad .(4.21)$$

The force constants derived from equation (4.19) are for $\ell\neq\ell'$

$$\Phi_{\alpha\beta}(\ell,\ell') = \frac{1}{N}\sum_{\underset{\sim}{q}}{}' \ 2\cos\left[\underset{\sim}{q}\cdot(\underset{\sim}{R}^0_\ell-\underset{\sim}{R}^0_{\ell'})\right]$$

$$\times\ \{E'_{11}(\underset{\sim}{q}) + [\sigma(\underset{\sim}{R}_{\ell'}) - \langle\sigma\rangle_R]E'_{12}(\underset{\sim}{q})$$

$$+\ [\sigma(\underset{\sim}{R}_\ell) - \langle\sigma\rangle_R]E'_{21}(\underset{\sim}{q})$$

$$+\ [\sigma(\underset{\sim}{R}_\ell) - \langle\sigma\rangle_R]\ [\sigma(\underset{\sim}{R}_{\ell'}) - \langle\sigma\rangle_R]$$

$$\times\ E'_{22}(\underset{\sim}{q})\}\ q_\alpha q_\beta \qquad .(4.22)$$

For $\ell=\ell'$ equation (2.18) can be used to obtain

$$\Phi_{\alpha\beta}(\ell,\ell) = -\sum_{\substack{\ell''\\ \ell''\neq\ell}} \Phi_{\alpha\beta}(\ell,\ell'') \qquad .(4.23)$$

In order to obtain equation (4.22) the fact that the $w_i{}^o(\underset{\sim}{q})$ are real has been used to equate $E'_{21}(\underset{\sim}{q})$ and $E'_{12}(\underset{\sim}{q})$. The exponentials have been combined to give the cosine factor.

The force constants $\Phi_{\alpha\beta}(\ell,\ell')$ are in principle completely specified by the pseudopotentials and a knowledge of the ion arrangement. It is now necessary to establish the Hamiltonian to be used to describe the lattice dynamics of the alloy. The procedure will be to make a configuration average (C.A.) of the force constants for a disordered alloy. The difference between the actual and average force constants will be treated as a perturbation.

The configuration averaged force constants are $\overline{\Phi}_{\alpha\beta}(\ell,\ell')$ defined by

$$\overline{\Phi}_{\alpha\beta}(\ell,\ell') = \langle\Phi_{\alpha\beta}(\ell,\ell')\rangle_{\text{C.A.}} \tag{4.24}$$

and the differences are $\Delta\Phi_{\alpha\beta}(\ell,\ell')$ where

$$\Delta\Phi_{\alpha\beta}(\ell,\ell') = \Phi_{\alpha\beta}(\ell,\ell') - \overline{\Phi}_{\alpha\beta}(\ell,\ell') \quad . \tag{4.25}$$

Equation (4.28) gives directly that

$$\langle\Delta\Phi_{\alpha\beta}(\ell,\ell')\rangle_{\text{C.A.}} = 0 \quad . \tag{4.26}$$

The Hamiltonian that describes the lattice dynamics is

$$H = \sum_{\alpha,\ell} \frac{p_\alpha^{\,2}(\ell,t)}{2\,M} + \frac{1}{2} \sum_{\substack{\alpha,\beta\\ \ell,\ell'}} \overline{\Phi}_{\alpha\beta}(\ell,\ell')\; u_\alpha(\ell,t)\; u_\beta(\ell',t)$$

$$+ \frac{1}{2} \sum_{\substack{\alpha,\beta\\ \ell,\ell'}} \Delta\Phi_{\alpha\beta}(\ell,\ell')\; u_\alpha(\ell,t)\; u_\beta(\ell',t) \quad . \tag{4.27}$$

The first two terms of the Hamiltonian are those of a lattice with force constants $\bar{\Phi}_{\alpha\beta}(\ell,\ell')$; the third term is the perturbation term.

In order to obtain the configuration average of the force constants, a configuration average of the right-hand side of equation (4.22) must be made. The configuration average $<\sigma(R_\ell)>_{C.A.}$ is $<\sigma>_R$. The average $<[\sigma(R_\ell) - <\sigma>_R] [\sigma(R_{\ell'}) - <\sigma>_R]>_{C.A.}$ has been made in Appendix A. The result is

$$<[\sigma(R_\ell) - <\sigma>_R][\sigma(R_{\ell'}) - <\sigma>_R]>_{C.A.} = (f_2 - <\sigma>_R^2) + (1-f_2)\delta_{\ell\ell'} \tag{4.28}$$

where

$$f_2 = \frac{<\sigma>_R^2 N - 1}{N - 1} \quad . \tag{4.29}$$

The configuration averaged force constants for $\ell \neq \ell'$ are

$$\bar{\Phi}_{\alpha\beta}(\ell,\ell') = \frac{1}{N} \sum_{\underset{\sim}{q}}{}' \, 2 \cos [\underset{\sim}{q} \cdot (\underset{\sim}{R}_\ell^o - \underset{\sim}{R}_{\ell'}^o)] \{E_{11}'(\underset{\sim}{q}) + [(f_2 - <\sigma>_R^2) + (1 - f_2)\delta_{\ell\ell'}] \, E_{22}'(\underset{\sim}{q})\} q_\alpha q_\beta \ . \tag{4.30}$$

The term with the Kronecker delta $\delta_{\ell\ell'}$ does not contribute for $\ell \neq \ell'$. For large N, f_2 is approximately $<\sigma>_R^2$ so all the coefficients of $E_{22}'(\underset{\sim}{q})$ vanish. The result is that the average force constants are those for a pure lattice described by an average ion valence $\bar{Z}$ and a bare pseudopotential form factor $\bar{w}^o(\underset{\sim}{q})$.

Calculations of phonon dispersion curves in the average lattice approximation have not been made to complement this study. It may be that the average lattice approximation will not give reasonable phonon frequencies. There is some evidence that the phonon frequencies are controlled by the average conduction electron concentration Dynes, Carbotte, Taylor and Campbell$^{(31)}$ have calculated the product function $\alpha^2(\omega)\,F(\omega)$ in the alloys $Pb_{0.4}Tl_{0.6}$ and $Tl_{0.8}\,Bi_{0.2}$ both of which have an average of 3.4 electrons per atom. They find the spectra to be almost identical for the two alloys. Tunneling results agree well with these calculations. This might indicate that the conduction electron density may be the important factor rather than the details of the ion cores. With this in mind the Hamiltonian of equation (4.27) with the $\bar{\Phi}_{\alpha\beta}(\ell,\ell')$ defined by equation (4.30),

$$\bar{\Phi}_{\alpha\beta}(\ell,\ell') = \frac{1}{N}\sum_{\underset{\sim}{q}}{}' \; 2\cos\,[\underset{\sim}{q}\cdot(\underset{\sim}{R}^{o}_{\ell} - \underset{\sim}{R}^{o}_{\ell'})]\; E'_{11}(\underset{\sim}{q})q_\alpha q_\beta \;, \tag{4.31}$$

for $\ell \neq \ell'$ will be used to obtain expressions for phonon broadening due to force constant disorder.

The difference between equations (4.22) and (4.31) are the $\Delta\Phi_{\alpha\beta}(\ell,\ell')$ for $\ell \neq \ell'$,

$$\Delta\Phi_{\alpha\beta}(\ell,\ell') = \frac{1}{N}\sum_{\underset{\sim}{q}}{}' \; 2\cos\,[\underset{\sim}{q}\cdot(\underset{\sim}{R}^{o}_{\ell} - \underset{\sim}{R}^{o}_{\ell'})]$$
$$\{[\sigma(\underset{\sim}{R}_{\ell'}) - \langle\sigma\rangle_R]\; E'_{12}(\underset{\sim}{q}) + [\sigma(\underset{\sim}{R}_{\ell}) - \langle\sigma\rangle_R]\; E'_{21}(\underset{\sim}{q})$$
$$+ [\sigma(\underset{\sim}{R}_{\ell}) - \langle\sigma\rangle_R][\sigma(\underset{\sim}{R}_{\ell'}) - \langle\sigma\rangle_R]\; E'_{22}(\underset{\sim}{q})\}q_\alpha q_\beta \;. \tag{4.32}$$

For $\ell = \ell'$ the $\Delta\Phi_{\alpha\beta}(\ell,\ell')$ are

$$\Delta\Phi_{\alpha\beta}(\ell,\ell) = -\sum_{\substack{\ell' \\ \ell'\neq\ell}} \Delta\Phi_{\alpha\beta}(\ell,\ell') \ . \qquad (4.33)$$

The force constants $\bar{\Phi}_{\alpha\beta}(\ell,\ell')$ and the difference $\Delta\Phi_{\alpha\beta}(\ell,\ell')$ are completely specified with a knowledge of the pseudopotential form factors by equations (4.31) and (4.32). In the part that follows the physical properties of the lattice will be discussed in terms of Green's functions. The techniques are standard(85,86). The Hamiltonian of equation (4.27) will be used to obtain a self-energy for the Green's function from which the phonon widths can be calculated.

The $\Delta\Phi_{\alpha\beta}(\ell,\ell')$ will be used to obtain a perturbation expansion for the Green's function $D_{\alpha\beta}(\ell t,\ell' t')$ defined(85) ($\hbar = 1$)

$$D_{\alpha\beta}(\ell t,\ell' t') \equiv 2\pi\langle\langle u_\alpha(\ell,t);u_\beta(\ell',t')\rangle\rangle \ . \qquad (4.34)$$

The frequency transform of $D_{\alpha\beta}(\ell t,\ell' t')$ is

$$D_{\alpha\beta}(\ell,\ell';\omega) = \frac{1}{2\pi}\int_{-\infty}^{\infty} D_{\alpha\beta}(\ell t,\ell' t')e^{i\omega(t-t')}dt \ . \qquad (4.35)$$

$D_{\alpha\beta}(\ell,\ell';\omega)$ is the transform of the retarded Green's function(85)

$$\langle\langle u_\alpha(\ell,t);u_\beta(\ell',t')\rangle\rangle_r = -i\Theta(t-t')\langle[u_\alpha(\ell,t),\ u_\beta(\ell',t')]\rangle \qquad (4.36)$$

in the upper half frequency plane. < > denotes a thermal average. In the lower half plane $D_{\alpha\beta}(\ell,\ell';\omega)$ is the transform of the advanced Green's function

$$<<u_\alpha(\ell,t);u_\beta(\ell',t')>>_a = i\Theta(t'-t)<[u_\alpha(\ell,t),u_\beta(\ell',t')]> \ . \tag{4.37}$$

The $u_\alpha(\ell,t)$ and $p_\alpha(\ell,t)$ of the Hamiltonian of equation (4.27) are the Heisenberg position and momentum operators and satisfy the equal-time commutation relations of equations (2.23). The Green's function $D_{\alpha\beta}(\ell t,\ell' t')$ satisfies the equation of motion

$$i\frac{d}{dt}D_{\alpha\beta}(\ell t,\ell' t') = 2\pi\delta(t-t')<[u_\alpha(\ell,t),\ u_\beta(\ell',t')]> + 2\pi<<[u_\alpha(\ell,t),H];u_\beta(\ell',t')>> \tag{4.38}$$

where H is the Hamiltonian of equation (4.27). For the Hamiltonian with the configuration averaged force constants $\bar{\Phi}_{\alpha\beta}(\ell,\ell')$, the Green's function will be denoted by $P_{\alpha\beta}(\ell t,\ell' t')$.

In a manner analogous to the work of Elliott and Taylor$^{(85)}$ a Dyson equation can be obtained that expresses the Green's function D in terms of the Green's function P and the difference force constants $\Delta\Phi_{\alpha\beta}(\ell,\ell')$. The Dyson equation is

$$D_{\alpha\beta}(\ell,\ell';\omega) = P_{\alpha\beta}(\ell,\ell';\omega) + \sum_{\substack{\gamma,\delta\\ \ell'',\ell'''}} P_{\alpha\gamma}(\ell,\ell'';\omega)\Delta\Phi_{\gamma\delta}(\ell'',\ell''') \times D_{\alpha\beta}(\ell''',\ell';\omega)\ . \tag{4.39}$$

In matrix notation equation (4.39) is

$$D = P + P\Delta\Phi D \ , \tag{4.40}$$

and an iteration of equation (4.40) leads to

$$D = P + P\Delta\Phi P + P\Delta\Phi P\Delta\Phi P + \ldots \ . \tag{4.41}$$

The Green's sunction $D_{\alpha\beta}(\ell,\ell';\omega)$ does not have translational symmetry. The translational symmetry can be restored by a configuration average. The averaged Green's function is denoted by $\bar{D}$,

$$\bar{D} \equiv \langle P + P\Delta\Phi P + P\Delta\Phi P\Delta\Phi P + \ldots\rangle_{C.A.} \ . \tag{4.42}$$

The configuration average in the approximation to be used here is obtained in the following way. Terms of the type $\langle\Delta\Phi P\Delta\Phi P\Delta\Phi\rangle_{C.A.}$ are to be considered of higher order than the term $\langle\Delta\Phi P\Delta\Phi\rangle_{C.A.}$ which will be kept. The average $\langle\Delta\Phi\rangle_{C.A.}$ vanishes so only the terms with an even number of factors $\Delta\Phi$ will contribute. These terms are factored into averages containing only two factors $\Delta\Phi$. In this approximation $\bar{D}$ is

$$\begin{aligned} \bar{D} = P &+ P\langle\Delta\Phi P\Delta\Phi\rangle_{C.A.}P \\ &+ P\langle\Delta\Phi P\Delta\Phi\rangle_{C.A.}\ P\langle\Delta\Phi P\Delta\Phi\rangle_{C.A.}P + \ldots \ . \end{aligned} \tag{4.43}$$

Equation (4.43) can be formally summed to obtain

$$\bar{D} = P + P\langle\Delta\Phi P\Delta\Phi\rangle_{C.A.}\bar{D} \ . \tag{4.44}$$

Since the configuration average restores translational symmetry equation (4.44) can be transformed to momentum space by the normal coordinate transformation of equation (2.9) and D will be diagonal in the momentum,

$$\overline{D}_{\lambda\lambda'}(\underset{\sim}{q};\omega) = P_{\lambda\lambda'}(\underset{\sim}{q};\omega) + \sum_{\lambda'',\lambda'''} P_{\lambda\lambda''}(\underset{\sim}{q};\omega)\; X'_{\lambda''\lambda'''}(\underset{\sim}{q};\omega)$$

$$\times\; \overline{D}_{\lambda'''\lambda'}(\underset{\sim}{q};\omega) \tag{4.45}$$

where

$$X' = \langle \Delta\Phi\ P\ \Delta\Phi \rangle_{C.A.} \quad .(4.46)$$

In the momentum representation $P_{\lambda\lambda'}(\underset{\sim}{q};\omega)$ is diagonal,

$$P_{\lambda\lambda'}(\underset{\sim}{q};\omega) = \frac{\delta_{\lambda\lambda'}}{\omega^2-\omega^2(\underset{\sim}{q};\lambda)} \quad ,(4.47)$$

and $X'_{\lambda\lambda'}(\underset{\sim}{q};\omega)$ is given by

$$X'_{\lambda\lambda'}(\underset{\sim}{q};\omega) = \sum_{\substack{\alpha,\beta\\ \ell,\ell'}} \frac{\xi_\alpha(\underset{\sim}{q};\lambda)\xi_\beta{}^*(\underset{\sim}{q};\lambda')\ e^{iq.(R^0_\ell-R^0_{\ell'})}}{NM}\; X'_{\alpha\beta}(\ell,\ell';\omega) \quad .(4.48)$$

The function $X'_{\alpha\beta}(\ell,\ell';\omega)$ is given in equation (4.46).

A full solution for $D_{\lambda\lambda'}(\underset{\sim}{q};\omega)$ would require an inversion of a three-by-three matrix Y'. From equation (4.49) Y' is

$$Y'_{\lambda\lambda'}(\underset{\sim}{q};\omega) = \delta_{\lambda\lambda'} - \sum_{\lambda''} P_{\lambda\lambda''}(\underset{\sim}{q};\omega)\; X'_{\lambda''\lambda'}(\underset{\sim}{q};\omega) \tag{4.50}$$

so in matrix notation

$$\overline{D} = (1-PX')^{-1}P \qquad .(4.51)$$

The solution of equation (4.51) would provide an expression for $D_{\lambda\lambda'}(\underset{\sim}{q};\omega)$ with a typical self-energy term in contrast to $P_{\lambda\lambda'}(\underset{\sim}{q};\omega)$. If $X'_{\lambda\lambda'}(\underset{\sim}{q};\omega)$ were diagonal in λ, Elliott and Taylor$^{(85)}$ give that

$$\mathrm{Im}\,\{\underset{\phi\to 0}{\mathrm{limit}}\; X'_{\lambda}(\underset{\sim}{q};\omega+i\phi)\} = -\,\omega^2\,\Gamma(\omega) \qquad (4.52)$$

where $\omega\,\Gamma(\omega)$ is related to the width of the spectral function and is the broadening discussed by Ng$^{(44)}$. With the assumption that $\overline{D}_{\lambda\lambda'}(\underset{\sim}{q};\omega)$ can be taken to be diagonal to a good approximation, a form for $\omega\,\Gamma(\omega)$ can be derived from equation (4.48). The function P on the right hand side of equation (4.46) can be written as

$$P_{\alpha\beta}(\ell,\ell';\omega) = \sum_{\underset{\sim}{q},\lambda} \frac{\xi^*_\alpha(\underset{\sim}{q};\lambda)\;\xi_\beta(\underset{\sim}{q};\lambda)\;e^{-i\underset{\sim}{q}\cdot(\underset{\sim}{R}^0_\ell-\underset{\sim}{R}^0_{\ell'})}}{NM[\omega^2-\omega^2(\underset{\sim}{q};\lambda)]} \qquad .(4.53)$$

Then X' of equation (4.46) is substituted into equation (4.48) and an expression for $\Delta(\omega) = \omega\,\Gamma(\omega)$ is reducible to

$$\Delta(\omega(\underset{\sim}{q};\lambda) = \frac{\pi}{2N^2M^2\omega^2} \sum_{\underset{\sim}{q}',\lambda'} \delta(\omega(\underset{\sim}{q};\lambda) - \omega(\underset{\sim}{q}';\lambda'))$$

$$\times \left< \left| \sum_{\substack{\alpha,\beta\\ \ell,\ell'}} \Delta\Phi_{\alpha\beta}(\ell,\ell')\;\xi^*_\alpha(\underset{\sim}{q};\lambda)\;\xi_\beta(\underset{\sim}{q}';\lambda')\;e^{-i\underset{\sim}{q}\cdot\underset{\sim}{R}^0_\ell}\right.\right.$$

$$\left.\left.\times\, e^{i\underset{\sim}{q}'\cdot\underset{\sim}{R}^0_{\ell'}}\right|^2\right>_{C.A.} \qquad .(4.54)$$

Ng$^{(44)}$ has written a similar result for the phonon width due to force constant disorder. His result does not contain a configuration average. Otherwise the two results are very similar.

An expression for the width $\Delta(\omega)$ is obtained in terms of the $\Delta\Phi_{\alpha\beta}(\ell,\ell')$ expressed in terms of the pseudopotentials by a substitution of equations (4.32) and (4.33) into equation (4.54). Since the $\Delta\Phi_{\alpha\beta}(\ell,\ell')$ contain terms with factors $[\sigma(\underset{\sim}{R}_\ell)-\langle\sigma\rangle_R]$ and $[\sigma(\underset{\sim}{R}_{\ell'})-\langle\sigma\rangle_R] \times [\sigma(\underset{\sim}{R}_\ell)-\langle\sigma\rangle_R]$, the configuration average in equation (4.54) will have to be performed over two, three and four factor terms. The two factor term has already been discussed and the average is given in equation (4.28). In Appendix A the averages over the two, three and four factor terms are discussed in more detail.

As an example of the evaluations to be made, consider the contribution of the first term of $\Delta\Phi_{\alpha\beta}(\ell,\ell')$ of equation (4.32) to the width. The configuration average to be performed is

$$
\begin{aligned}
T = \Big\langle & \sum_{\substack{\ell,\ell',\ell'',\ell''' \\ \alpha,\beta,\gamma,\delta}} \frac{1}{N^2} \sum_{\underset{\sim}{k},\underset{\sim}{k}'}{}' \; e^{i(\underset{\sim}{k}-\underset{\sim}{q})\cdot\underset{\sim}{R}^0_\ell} \; e^{-i(\underset{\sim}{k}-\underset{\sim}{q}')\cdot\underset{\sim}{R}^0_{\ell'}} \\
& \times [\sigma(\underset{\sim}{R}_{\ell'}) - \langle\sigma\rangle_R] E'_{12}(\underset{\sim}{k}) \; e^{-i(\underset{\sim}{k}'-\underset{\sim}{q})\cdot\underset{\sim}{R}^0_{\ell''}} \; e^{i(\underset{\sim}{k}'-\underset{\sim}{q}')\cdot\underset{\sim}{R}^0_{\ell'''}} \\
& \times [\sigma(\underset{\sim}{R}_{\ell'''}) - \langle\sigma\rangle_R] E'^{*}_{12}(\underset{\sim}{k}') k_\alpha \; \xi^*_\alpha(\underset{\sim}{q};\lambda) k_\beta \; \xi_\beta(\underset{\sim}{q}';\lambda') \\
& \times k'_\gamma \; \xi_\gamma(\underset{\sim}{q};\lambda) k'_\delta \; \xi^*_\delta(\underset{\sim}{q}';\lambda') \Big\rangle_{C.A.} \qquad .(4.55)
\end{aligned}
$$

The configuration average required is

$$<[\sigma(\underset{\sim}{R}_{\ell'}) - <\sigma>_R]\ [\sigma(\underset{\sim}{R}_{\ell'''}) - <\sigma>_R]>_{C.A.}$$

$$= (f_2 - <\sigma>_R{}^2) + (1-f_2)\delta_{\ell'\ell'''} \tag{4.56}$$

where f_2 is given in equation (4.29). The contribution to T from the term with no Kronecker delta is

$$T_1 = \sum_{\alpha,\beta,\delta,\gamma} N^2 \sum_{\underset{\sim}{k},\underset{\sim}{k}'}{}' \{(f_2 - <\sigma>_R{}^2)\ S^*(\underset{\sim}{k}'-\underset{\sim}{q}')\ S(\underset{\sim}{k}-\underset{\sim}{q}')\}\ S^*(\underset{\sim}{k}-\underset{\sim}{q})$$

$$\times\ S(\underset{\sim}{k}'-\underset{\sim}{q})k_\alpha\ \xi^*_\alpha(\underset{\sim}{q};\lambda)k_\beta\ \xi_\beta(\underset{\sim}{q}';\lambda')k'_\gamma\ \xi_\gamma(\underset{\sim}{q};\lambda)k'_\delta\ \xi^*_\delta(\underset{\sim}{q}';\lambda')$$

$$\times\ E'_{12}(\underset{\sim}{k})\ E'_{12}{}^*(\underset{\sim}{k}') \qquad ,(4.57)$$

The contribution to T from the term with the Kronecker delta differs from T_1 only by the replacement of the term in {} by $\frac{1}{N}(1-f_2)\ S(\underset{\sim}{k}-\underset{\sim}{q}'-\underset{\sim}{k}'+\underset{\sim}{q}')$. The sums over $\underset{\sim}{k}$ and $\underset{\sim}{k}'$ can be performed since the structure factor $S(\underset{\sim}{q})$ is known for the ions in their equilibrium positions. The contribution of the term T to the width of the phonon mode $(\underset{\sim}{q};\lambda)$ is, for large N,

$$\Delta(\omega(\underset{\sim}{q};\lambda))_T = \frac{[1-<\sigma>_R{}^2]\pi}{2N\ M^2\omega^2(\underset{\sim}{q};\lambda)} \sum_{\underset{\sim}{\kappa}_m,\underset{\sim}{\kappa}_n} \sum_{\alpha,\beta,\delta,\gamma} \sum_{\lambda',\underset{\sim}{q}'\neq\underset{\sim}{q}}$$

$$\times\ \delta(\omega(\underset{\sim}{q};\lambda) - \omega(\underset{\sim}{q}';\lambda'))\ (\underset{\sim}{\kappa}_n+\underset{\sim}{q})_\alpha\ \xi^*_\alpha(\underset{\sim}{q};\lambda)$$

$$\times\ (\underset{\sim}{\kappa}_n+\underset{\sim}{q})_\beta\ \xi_\beta(\underset{\sim}{q}';\lambda')\ (\underset{\sim}{\kappa}_m+\underset{\sim}{q})_\gamma\ \xi_\gamma(\underset{\sim}{q};\lambda)$$

$$\times\ (\underset{\sim}{\kappa}_m+\underset{\sim}{q})_\delta\ \xi^*_\delta(\underset{\sim}{q}';\lambda')\ E'_{12}(\underset{\sim}{\kappa}_n+\underset{\sim}{q})\ E'^{\,*}_{12}(\underset{\sim}{\kappa}_m+\underset{\sim}{q}) \qquad .(4.58)$$

The sum over $\underset{\sim}{q}'$ is restricted by the energy conserving delta-function. There is a double sum over reciprocal lattice vectors $\underset{\sim}{\kappa}_n$ and $\underset{\sim}{\kappa}_m$.

The evaluation of all the contributions to the width $\Delta(\omega)$ of equation (4.54) follows the same general pattern used in the evaluation of the first term to obtain equation (4.58). There are no formal difficulties, although there are a large number of terms.

The contribution to the width given in equation (4.58) can be reduced to a simple analytical formula in a spherical Debye model with three phonon branches with a dispersion relation

$$\omega = s\ q \qquad (4.59)$$

for each branch λ. The sound velocity is denoted by s. The contribution should be identical for each branch λ so a sum over λ can be taken with a multiplicative factor of $\frac{1}{3}$. The sum of λ and λ' can be performed with the aid of the completeness relations for the polarization vectors to obtain factors of $\delta_{\gamma\alpha}$ and $\delta_{\delta\beta}$. The sum over the reciprocal lattice vectors is restricted to $\underset{\sim}{\kappa}_n = 0$ and $\underset{\sim}{\kappa}_m = 0$. Equation (4.58) then reduces to

$$[\Delta(\omega(\underset{\sim}{q}))]_T = \frac{[1-\langle\sigma\rangle_R^{\,2}]\pi}{6N\ M^2\omega^2(\underset{\sim}{q})} \sum_{\substack{\underset{\sim}{q}' \\ \underset{\sim}{q}'\neq\underset{\sim}{q}}} \delta(sq - sq')q^4\ E'_{12}(\underset{\sim}{q})\ E'^{\,*}_{12}(\underset{\sim}{q}) \qquad .(4.60)$$

The sum over $\underset{\sim}{q}'$ can be converted to an integral and the integration can be easily performed to obtain

$$[\Delta(\omega(\underset{\sim}{q}))]_T = \frac{[1-\langle\sigma\rangle_R{}^2]\ \Omega_0\ q^6 \left|E'_{12}(\underset{\sim}{q})\right|^2}{12\pi\ M^2\omega^2(\underset{\sim}{q})s} \quad .(4.61)$$

Equation (4.61) is an analytic form for the contribution of the first term to the broadening in the Debye model.

4.4 Theory of Strong-Coupling Superconductivity in Binary Alloys of Simple Metals

In this section the electron-phonon interaction that enters the strong-coupling theory of superconductivity is approximately modified to account for force constant disorder in a binary alloy. The view is taken that the conduction electron states can be represented by plane waves as is usual in pseudopotential theory.

The problem that is initially considered is one in which the lattice vibrations are treated as in a pure crystal but the lattice potential that determines the electron-phonon interaction term is that of the alloy and given by equation (4.6),

$$\langle\underset{\sim}{k}+\underset{\sim}{q}|W|\underset{\sim}{q}\rangle = S(\underset{\sim}{q})\ \langle\underset{\sim}{k}+\underset{\sim}{q}|\overline{w}|\underset{\sim}{k}\rangle + F(\underset{\sim}{q})\ \langle\underset{\sim}{k}+\underset{\sim}{q}|\Delta w|\underset{\sim}{k}\rangle \quad .(4.62)$$

The notation is the same as that of section 4.2. The Hamiltonian that describes the lattice vibrations contains the average force constants $\overline{\Phi}_{\alpha\beta}(\ell,\ell')$. The Hamiltonian that describes the ion and electron motion and contains the modified electron-phonon interaction is

$$H = \frac{1}{2} \sum_{\alpha,\ell} \frac{p_\alpha^{\,2}(\ell,t)}{M} + \frac{1}{2} \sum_{\substack{\alpha,\beta \\ \ell,\ell'}} \overline{\Phi}_{\alpha\beta}(\ell,\ell')\ u_\alpha(\ell,t)\ u_\beta(\ell',t)$$

$$+ \sum_{\underset{\sim}{k},\underset{\sim}{q},\sigma} \frac{1}{N} \sum_{\ell} -i\underset{\sim}{q}.\underset{\sim}{u}(\ell,t)\ [<\underset{\sim}{k}+\underset{\sim}{q}|\overline{w}|\underset{\sim}{k}>$$

$$+ [\sigma(\underset{\sim}{R}_\ell) - <\sigma>_R]\ <\underset{\sim}{k}+\underset{\sim}{q}|\Delta w|\underset{\sim}{k}>]\ e^{-i\underset{\sim}{q}.\underset{\sim}{R}_\ell^0}\ c^\dagger_{\underset{\sim}{k}+\underset{\sim}{q},\sigma}\ c_{\underset{\sim}{k},\sigma}$$

$$+ \sum \varepsilon_{\underset{\sim}{k}}\ c^\dagger_{\underset{\sim}{k},\sigma}\ c_{\underset{\sim}{k},\sigma} \qquad ,(4.63)$$

where the electron operators are in second-quantized form. The third term is the modified interaction between the electrons and ions and is directly comparable to the equivalent term for a pure metal of equation (2.92),

$$H_{e-p} = \sum_{\underset{\sim}{k},\underset{\sim}{q},\sigma} \frac{1}{N} \sum_{\ell} -i\underset{\sim}{q}.\underset{\sim}{u}(\ell)\ <\underset{\sim}{k}+\underset{\sim}{q}|w|\underset{\sim}{k}>\ e^{-i\underset{\sim}{q}.\underset{\sim}{R}_\ell^0}\ c^\dagger_{\underset{\sim}{k}+\underset{\sim}{q},\sigma}\ c_{\underset{\sim}{k},\sigma} \qquad .(4.64)$$

The difference between the two is the term characterized by the factor $[\sigma(\underset{\sim}{R}_\ell) - <\sigma>_R]\ <k+q|\Delta w|k>$.

In Appendix B the equations of motion for the one-electron Green's function $G(x;x')$ defined by

$$G(x;x') = -\, i<T\ \psi(x)\ \psi^\dagger(x')> \qquad (4.65)$$

where $\psi(x)$ is the electron field operator are outlined and a perturbation series for G in terms of G_0, the free electron propagator and the Green's function $D_{\alpha\beta}(\ell t,\ell' t')$ with

$$D_{\alpha\beta}(\ell t,\ell' t') = - i\langle T\, u_\alpha(\ell,t)\; u_\beta(\ell' t')\rangle \tag{4.66}$$

is developed. For the average lattice $D_{\alpha\beta}(\ell t,\ell' t')$ is denoted by $P_{\alpha\beta}(\ell t,\ell' t')$ where

$$P_{\alpha\beta}(\ell,\ell';\omega) = \sum_{\substack{q \\ \lambda,\lambda'}} \frac{\xi_\alpha(\underset{\sim}{q};\lambda)\; \xi^*_\beta(\underset{\sim}{q};\lambda')\; e^{i\underset{\sim}{q}\cdot(\underset{\sim}{R}^0_\ell-\underset{\sim}{R}^0_{\ell'})}}{NM}\, P_{\lambda\lambda'}(\underset{\sim}{q};\omega) \quad .(4.67)$$

The Green's function $P_{\lambda\lambda'}(\underset{\sim}{q};\omega)$ can be written in the spectral representation,

$$P_{\lambda\lambda'}(\underset{\sim}{q};\omega) = \int_0^\infty B_{\lambda\lambda'}(\underset{\sim}{q};\nu)\; \left[\frac{1}{\omega-\nu+i\delta} - \frac{1}{\omega+\nu-i\delta}\right] \tag{4.68}$$

where for zero temperature

$$B_{\lambda\lambda'}(\underset{\sim}{q};\nu) = \frac{1}{2\nu}\,\delta(\nu-\omega(\underset{\sim}{q};\lambda))\,\delta_{\lambda\lambda'} \quad .(4.69)$$

In Appendix B it is shown that the configuration averaged self-energy in the Nambu scheme leads to a function $\alpha^2(\omega)\;F(\omega)$ that consists of a sum of two terms. The first term is equivalent to $\alpha^2(\omega)\;F(\omega)$ calculated for a pure metal with a pseudopotential form factor $\overline{w}(\underset{\sim}{q})$ and is given by$^{(23)}$

$$\overline{\alpha^2(\omega)\;F(\omega)} = \sum_{\lambda,\lambda'} \frac{N(0)}{8\pi\; k_F^2} \int d\Omega_{\underset{\sim}{q}} \int_0^{2k_F} q\,dq \left|\overline{g}_{\underset{\sim}{q};\lambda}\right|^2 B_{\lambda\lambda'}(\underset{\sim}{q},\omega) \quad .(4.70)$$

The coupling constant $\bar{g}_{\underset{\sim}{q};\lambda}$ differs from the coupling constant $g_{\underset{\sim}{q};\lambda}$ of equation (2.97) in that the factor $\frac{1}{\sqrt{2\omega(\underset{\sim}{q};\lambda)}}$ is contained in $B_{\lambda\lambda'}(\underset{\sim}{q},\omega)$. The second term consists of the additional contribution to $\alpha^2(\omega)\ F(\omega)$

$$\Delta[\alpha^2(\omega)\ F(\omega)] = [1-\langle\sigma\rangle_R^{\,2}] \sum_{\lambda,\lambda'} \frac{1}{N} \sum_{\underset{\sim}{q}'} \frac{N(0)}{8\pi\ k_F^{\,2}} \int d\Omega_{\underset{\sim}{q}}$$

$$\times \int_0^{2k_F} q\,dq\ \left(\frac{i\underset{\sim}{q}\cdot\underset{\sim}{\xi}(\underset{\sim}{q}';\lambda)}{\sqrt{MN}}\right) \left(\frac{-i\underset{\sim}{q}\cdot\underset{\sim}{\xi}^{*}(\underset{\sim}{q}';\lambda')}{\sqrt{MN}}\right) \Delta w^{*}(\underset{\sim}{q})\ \Delta w(\underset{\sim}{q})$$

$$\times\ B_{\lambda\lambda'}(\underset{\sim}{q}',\omega) \qquad ,(4.71)$$

so that for the alloy

$$\alpha^2(\omega)\ F(\omega) = \overline{\alpha^2(\omega)\ F(\omega)} + \Delta[\alpha^2(\omega)\ F(\omega)] \qquad .(4.72)$$

The second term can be considered to be a fluctuation term.

The effects of force constant disorder on the phonon modes, that is, the phonon broadening can be included in a claculation of $\alpha^2(\omega)\ F(\omega)$ by a suitable modification of the spectral function $B_{\lambda\lambda'}(\underset{\sim}{q}',\omega)$. It should be noted that this replacement represents a factorization, since the configuration average should be performed over a product of the coupling constant and the spectral function. In the procedure outlined above, the configuration averages are performed separately.

CHAPTER V

CONCLUSIONS

5.1 Effect of Pressure on Superconductivity

The effects of hydrostatic pressure on the superconducting transition temperatures and gaps have been studied within the strong-coupling theory of superconductivity in the metals aluminum, lead, mercury, tin and indium. A scaling model that includes the shifts of phonon frequencies in terms of a constant Grüneisen parameter for all modes and that takes into account the change in the electron-phonon coupling constant by means of a rescreened pseudopotential has been studied. The scaling model has been established in some detail in aluminum and lead and has been applied to the other three metals under study. The model provides a simple method for obtaining the phonon kernel of the Eliashberg gap equations at finite pressure from the zero pressure kernel.

The zero temperature Eliashberg gap equations were solved for the five metals at zero and finite volume changes. The solutions of the gap equations were seen to be affected in a pronounced manner; they are generally decreased and the shifts of the van Hove peaks of the phonon density of states spectra at finite pressure are reproduced in the gap functions.

For the weak-coupling materials aluminum, tin and indium the assumption that the gap at the gap edge and the transition temperature scale in the same way with volume decrease lead to results in good agreement with results obtained with the use of McMillan's phenomenological formula. For the strong-coupling materials lead and mercury the finite temperature gap equations were solved to obtain the variation of the transition temperature with pressure. In both mercury and lead the gap and transition temperature were found to scale differently. The transition temperature in lead was found to scale with volume decrease in a manner consistent with McMillan's formula. In mercury the comparison was not good, and this may be due to the distinctive phonon density of states in mercury as compared to the other four metals. In both lead and mercury reasonable results for the relationship of the different scaling of the gap at the gap edge and the transition temperature were obtained. In lead the result obtained is in good agreement with the experimental results as obtained by tunneling studies under pressure. In mercury no experimental results are available for a comparison.

This work to some extent verifies the usefulness of McMillan's formula for a wide variety of spectra. For small volume changes, McMillan's formula has been inverted to obtain a relationship to determine a Grüneisen parameter from the dependence of the transition temperature on volume decrease.

A product of this work is that the variation of the phonon-renormalized electronic effective mass under pressure is obtained in a simple manner. The scaling procedures for the phonon density of states and the electron-phonon coupling constant determined the variation of the mass renormalization. Apart from the inter-relationship between the effective mass and the superconducting properties of the material, there are probably other properties in which the variation of the effective mass with pressure may be observed. Such observations would serve to complement the superconductivity studies.

Although more thorough observations show and will show a more complicated behaviour of the phonon frequency shifts under pressure it is believed that the simple model used here incorporates many of the essential features necessary to understand many of the effects of hydrostatic pressure on the superconducting properties of simple metals. It is hoped that these calculations will serve to stimulate others to further investigate pressure-dependent effects in superconductors.

5.2 Superconductivity in Binary Alloys

The structure-dependent energy of a binary alloy of simple metals as formulated by Hayes, Brooks and Bienenstock has been used to obtain a formalism for the calculation of phonon widths due to force constant disorder with pseudopotentials. Calculations of the widths have not as yet been made within this formalism but the investigations are being continued by the author.

The electron-phonon interaction Hamiltonian has been modified in an approximation that decouples the phonon propagator and the electron-phonon coupling constant. This formulation, in conjunction with the phonon propagator modified to include effects of broadening due to force constant disorder, is to be applied to the study of superconductivity calculations in alloys of simple metals.

While this study is at a preliminary stage it is hoped that this presentation will stimulate the continuation of investigations on this topic.

APPENDIX A

CONFIGURATION AVERAGES

The configuration averages to be made are of the form $<[\sigma(\underset{\sim}{R}_{\ell}) - <\sigma>_R]\ [\sigma(\underset{\sim}{R}_{\ell'}) - <\sigma>_R]>_{C.A.}$ with up to four factors $[\sigma(\underset{\sim}{R}_{\ell}) - <\sigma>_R]$ included. To begin, the average $<\sigma(\underset{\sim}{R}_{\ell})\ \sigma(\underset{\sim}{R}_{\ell'})>_{C.A.}$ is found. If $\ell=\ell'$, this is unity since $\sigma^2(\underset{\sim}{R}_{\ell})$ is unity. If $\ell\neq\ell'$, the average is the sum of the conditional probabilities (with appropriate signs) for finding an A or B atom at $R_{\ell'}$ for an A or B atom at R_{ℓ}. The probability of finding an A atom at R_{ℓ} is x. With an A atom at R_{ℓ} the probability of finding an A atom at $R_{\ell'}$ is $\frac{x\ N-1}{N-1}$. This term contributes with a positive sign. The form possible combinations are taken into account so

$$<\sigma(\underset{\sim}{R}_{\ell})\ \sigma(\underset{\sim}{R}_{\ell'})>_{C.A.} = [x\ \frac{x\ N-1}{N-1} + (1-x)\ \frac{(1-x)N-1}{N-1}$$

$$- x\ \frac{(1-x)N-1}{N-1} - (1-x)\ \frac{x\ N-1}{N-1}]\ (1-\delta_{\ell\ell'})$$

$$+ \delta_{\ell\ell'} \qquad .(A.1)$$

Collection of terms on the right hand side of equation (A.1) provides

$$<\sigma(\underset{\sim}{R}_{\ell})\ \sigma(\underset{\sim}{R}_{\ell'})>_{C.A.} = \frac{N}{N-1}\ 4x(1-x)\,\delta_{\ell\ell'} - \frac{1}{N-1}\ 4x(1-x) \qquad (A.2)$$

With

$$\langle\sigma\rangle_R = 2x-1 \tag{A.3}$$

equation (A.2) can be written

$$\langle\sigma(\underset{\sim}{R}_{\ell})\ \sigma(\underset{\sim}{R}_{\ell'})\rangle_{\text{C.A.}} = f_2 + (1-f_2)\delta_{\ell\ell'} \tag{A.4}$$

where

$$f_2 = \frac{\langle\sigma\rangle_R^{\,2} N-1}{N-1} \ . \tag{A.5}$$

Since

$$\langle\sigma(\underset{\sim}{R}_{\ell})\rangle_{\text{C.A.}} = \langle\sigma\rangle_R \tag{A.6}$$

the average with two factors is

$$\langle[\sigma(\underset{\sim}{R}_{\ell}) - \langle\sigma\rangle_R]\ [\sigma(\underset{\sim}{R}_{\ell'}) - \langle\sigma\rangle_R]\rangle_{\text{C.A.}} = (f_2 - \langle\sigma\rangle_R^{\,2}) + (1-f_2)\delta_{\ell\ell'} \ . \tag{A.7}$$

The three factor term is averaged in a manner exactly analogous to the two factor term. The three factor term is expanded so that only the average $\langle\sigma(\underset{\sim}{R}_{\ell})\ \sigma(\underset{\sim}{R}_{\ell'})\ \sigma(\underset{\sim}{R}_{\ell''})\rangle_{\text{C.A.}}$ must be found in addition to equation (A.7). For all three sites different, $\ell\neq\ell'\neq\ell''$, there are eight possible combinations of A and B placements. These are added together and multiplied by a factor $(1-\delta_{\ell\ell'})\ (1-\delta_{\ell\ell''})\ (1-\delta_{\ell'\ell''})$. There are also contributions from the cases with two sites equal and all three sites the same. The result is

$$<\sigma(\underset{\sim}{R}_\ell)\ \sigma(\underset{\sim}{R}_{\ell'})\ \sigma(\underset{\sim}{R}_{\ell''})>_{C.A.} = f_3(1-\delta_{\ell\ell'})\ (1-\delta_{\ell\ell''})\ (1-\delta_{\ell'\ell''})$$

$$+ <\sigma>_R \{\delta_{\ell\ell'}(1-\delta_{\ell\ell''})\ (1-\delta_{\ell'\ell''}) + \delta_{\ell\ell''}(1-\delta_{\ell\ell'})\ (1-\delta_{\ell'\ell''})$$

$$+ \delta_{\ell\ell'}(1-\delta_{\ell\ell'})\ (1-\delta_{\ell\ell''})$$

$$+ <\sigma>_R\ \delta_{\ell\ell'}\ \delta_{\ell\ell''}\ \delta_{\ell'\ell''} \qquad ,(A.8)$$

where

$$f_3 = (<\sigma>_R{}^3\ N^2 - 3<\sigma>_R N + 2<\sigma>_R)/(N-1)\ (N-2) \qquad .(A.9)$$

Equation (A.8) is combined with equations (A.7) and (A.6) to provide

$$<[\sigma(\underset{\sim}{R}_\ell) - <\sigma>_R]\ [\sigma(\underset{\sim}{R}_{\ell'}) - <\sigma>_R]\ [\sigma(\underset{\sim}{R}_{\ell''}) - <\sigma>_R]>_{C.A.}$$

$$= (f_3 - 3f_2<\sigma>_R + 2<\sigma>_R{}^3)$$

$$+ (f_2<\sigma>_R - f_3)\ \{\delta_{\ell\ell'} + \delta_{\ell\ell''} + \delta_{\ell'\ell''}\}$$

$$+ (2f_3 - 2<\sigma>_R)\ \delta_{\ell\ell'}\ \delta_{\ell\ell''} \qquad .(A.10)$$

In the final form triple Kronecker delta terms have been reduced to double Kronecker delta terms where appropriate, for example,

$$\delta_{\ell\ell'}\ \delta_{\ell\ell''}\ \delta_{\ell'\ell''} \rightarrow \delta_{\ell\ell'}\ \delta_{\ell\ell''} \qquad .(A.11)$$

The four factor average is found with the additional average $<\sigma(R_\ell)\ \sigma(R_{\ell'})\ \sigma(R_{\ell''})\ \sigma(R_{\ell'''})>_{C.A.}$ for all combinations of ion sites. With this average and the averages of equations (A.8), (A.7) and (A.6), the result is

$$<[\sigma(\underset{\sim}{R}_\ell) - <\sigma>_R]\ [\sigma(\underset{\sim}{R}_{\ell'}) - <\sigma>_R]\ [\sigma(\underset{\sim}{R}_{\ell''}) - <\sigma>_R]\ [\sigma(\underset{\sim}{R}_{\ell''})$$

$$- <\sigma>_R]>_{C.A.}$$

$$= (f_4 - 4<\sigma>_R f_3 + 6<\sigma>_R^2 f_2 - 3<\sigma>_R^4)$$

$$+ (f_2 - f_4 - 2<\sigma>_R^2 + 2<\sigma>_R f_3 + <\sigma>_R^2 - <\sigma>_R^2 f_2)$$

$$x\ \{\delta_{\ell\ell'} + \delta_{\ell\ell''} + \delta_{\ell\ell'''} + \delta_{\ell'\ell''} + \delta_{\ell'\ell'''} + \delta_{\ell''\ell'''}\}$$

$$+ (2f_4 - 2f_2 - 2<\sigma>_R f_3 + 2<\sigma>_R^2)\ \{\delta_{\ell\ell'}\ \delta_{\ell'\ell''} + \delta_{\ell\ell''}\ \delta_{\ell''\ell'''}$$

$$+ \delta_{\ell\ell'''}\ \delta_{\ell'''\ell'} + \delta_{\ell'\ell''}\ \delta_{\ell''\ell'''}\} \qquad ,(A.12)$$

where

$$f_4 = [<\sigma>_R^4 N^3 - 6<\sigma>_R^2 N^2 + (8<\sigma>_R^2 + 3)N-6]/(N-1)(N-2)(N-3)$$

$$.(A.13)$$

These are all the averages necessary in the work of Chapter IV.

APPENDIX B

EQUATIONS OF MOTION

A perturbation expansion for the one-electron Green's function $G(x;x')$ defined by

$$G(x;x') \equiv - i\langle T\ \psi(x)\ \psi^{\dagger}(x')\rangle \tag{B.1}$$

is to be found. T is Wick's time ordering operator and <> denotes a thermal average. The electron field operator is

$$\psi(x) = \frac{1}{\sqrt{\Omega}} \sum_{\underset{\sim}{k}} e^{i\underset{\sim}{k}\cdot\underset{\sim}{x}}\ c_{\underset{\sim}{k}}(t) \tag{B.2}$$

where Ω is the volume and the operator $c_{\underset{\sim}{k}}(t)$ destroys an electron with crystal momentum $\underset{\sim}{k}$ and energy $\varepsilon_{\underset{\sim}{k}}$ measured relative to the Fermi level μ.

The Hamiltonian to be used is

$$H = \frac{1}{2}\sum_{\alpha,\ell} \frac{p_{\alpha}^{2}(\ell,t)}{M} + \frac{1}{2}\sum_{\substack{\alpha,\beta\\ \ell,\ell'}} u_{\alpha}(\ell,t)\ \Phi_{\alpha\beta}(\ell,\ell')\ u_{\beta}(\ell',t)$$

$$+ \sum_{\underset{\sim}{k},\underset{\sim}{q}} \frac{1}{N} \sum_{\ell} - i\underset{\sim}{q}\cdot\underset{\sim}{u}(\ell,t)\ [\overline{w}(\underset{\sim}{q}) + (\sigma(\underset{\sim}{R}_{\ell}) - \langle\sigma\rangle_{R})\ \Delta\ w(\underset{\sim}{q})]$$

$$\times\ e^{-i\underset{\sim}{q}\cdot\underset{\sim}{R}_{\ell}^{0}}\ c^{\dagger}_{\underset{\sim}{k}+\underset{\sim}{q}}\ c_{\underset{\sim}{k}} + \sum_{\underset{\sim}{k}} \varepsilon_{\underset{\sim}{k}}\ c^{\dagger}_{\underset{\sim}{k}}\ c_{\underset{\sim}{k}}\ . \tag{B.3}$$

This is the Hamiltonian of equation (4.63) and is discussed in the text. The $u_\alpha(\ell,t)$ and $p_\alpha(\ell,t)$ are Heisenberg operators.

The electron field operators satisfy the equations of motion ($\hbar=m=1$; m is the electron mass)

$$i \frac{\partial}{\partial t} \psi(x) = -(\underset{\sim}{\nabla}_{\underset{\sim}{x}}{}^{2}-\mu)\ \psi(x) + (\sum_{\alpha,\beta} \zeta_\alpha(\ell,\underset{\sim}{x})\ u_\alpha(\ell,t))\ \psi(x)$$

$$\text{(B.4)}$$

$$i \frac{\partial}{\partial t} \psi^\dagger(x) = (\nabla_x{}^{2} + \mu)\ \psi^\dagger(x) - (\sum_{\alpha,\beta} \zeta_\alpha(\ell,\underset{\sim}{x})\ u_\alpha(\ell,t))\psi^\dagger(x)$$

where the function ζ is

$$\zeta_\alpha(\ell,\underset{\sim}{x}) \equiv \sum_{\underset{\sim}{q}} \frac{-iq_\alpha}{N}\ [\bar{w}(\underset{\sim}{q}) + (\sigma(\underset{\sim}{R}_\ell) - \langle\sigma\rangle_R)\ \Delta\ w(\underset{\sim}{q})]$$

$$\times\ e^{-i\underset{\sim}{q}\cdot\underset{\sim}{R}_\ell{}^{0}}\ e^{i\underset{\sim}{q}\cdot\underset{\sim}{x}} \qquad .\text{(B.5)}$$

The equation of motion for $G(x;x')$ is constructed with the aid of equations (B.4). It is

$$(i \frac{\partial}{\partial t} + \underset{\sim}{\nabla}_{\underset{\sim}{x}}{}^{2} + \mu)\ G(x;x') = \delta^4(x-x')$$

$$+ \sum_{\alpha,\ell} \zeta_\alpha(\ell,\underset{\sim}{x})\ G_\alpha(x;x':\ell t) \qquad \text{(B.6)}$$

where the Green's function $G_\alpha(x;x':\ell t)$ is

$$G_\alpha(x;x':\ell t) \equiv -\ i\langle T\ \psi(x)\ \psi(x')\ u_\alpha(\ell,t)\rangle \qquad .\text{(B.7)}$$

The equation conjugate to equation (B.6) is

$$(i \frac{\partial}{\partial t} - \underset{\sim}{\nabla}_{\underset{\sim}{x}}{}^{2} - \mu)\ G(x';x) = -\ \delta^4(x-x') - \sum_{\alpha,\beta} \zeta_\alpha(\ell,\underset{\sim}{x})\ G_\alpha(x',x:\ell t)$$

$$.\text{(B.8)}$$

The Green's functions D, H and F are defined by

$$D_{\alpha\beta}(\ell t,\ell' t') = -\, i\langle T\; u_{\alpha}(\ell,t)\; u_{\beta}(\ell',t')\rangle \qquad ,$$

$$\begin{aligned} H_{\alpha\beta}(\ell t,\ell' t') &= \langle T\; p_{\alpha}(\ell,t)\; u_{\beta}(\ell',t')\rangle \\ &= -\,\langle T\; u_{\alpha}(\ell,t)\; p_{\beta}(\ell',t')\rangle \qquad , \end{aligned} \tag{B.9}$$

$$F_{\alpha\beta}(\ell t,\ell' t') = -\, i\langle T\; p_{\alpha}(\ell,t)\; p_{\beta}(\ell',t')\rangle \qquad .$$

The equation of motion for D is

$$i\; M\, \frac{\partial}{\partial t}\, D_{\alpha\beta}(\ell t,\ell' t') = H_{\alpha\beta}(\ell t,\ell' t') \tag{B.10}$$

and furthermore

$$\begin{aligned} -\, M\, \frac{\partial^2}{\partial t^2}\, D_{\alpha\beta}(\ell t,\ell' t') &= \delta(t-t')\;\delta_{\alpha\beta}\;\delta_{\ell\ell'} \\ &+ \sum_{\gamma,\ell''} \phi_{\alpha\gamma}(\ell,\ell'')\; D_{\alpha\beta}(\ell'' t,\ell' t') \\ &- i \int d^3x'\; \zeta_{\alpha}(\ell,\underset{\sim}{x}')\; G_{\beta}(x't;x't^{+}:\ell' t') \end{aligned} \tag{B.11}$$

where $t^{+}>t$, $t^{+}\to t$.

The equation of motion for the Green's function $G_{\alpha}(x;x':\ell t'')$ is

$$\begin{aligned} \left(i\,\frac{\partial}{\partial t} + \underset{\sim}{\nabla}_{\underset{\sim}{x}}^{\,2} + \mu\right) G_{\alpha}(x;x':\ell t'') &= \delta^4(x-x')\; G_{\alpha}(\ell,t'') \\ + i \sum_{\beta,\ell'} \zeta_{\beta}(\ell',\underset{\sim}{x})\; G_{\beta\alpha}(x;x':\ell' t,\ell t'') \end{aligned} \tag{B.12}$$

where

$$G_{\alpha^{(1)}\ldots\alpha^{(m)}}(x_1x_2\ldots x_n;x_1'x_2'\ldots x_n':\ell^{(1)}t^{(1)},\ell^{(2)}t^{(2)}\ldots\ell^{(m)}t^{(m)})$$

$$= (-i)^n\ (-i)^{[m/2]}\ \langle T\ \psi(x_1)\ldots\psi(x_n)\ \psi^\dagger(x_n')\ldots\psi^\dagger(x_1')$$

$$\times\ u_{\alpha^{(1)}}(\ell^{(1)},t^{(1)})\ldots u_{\alpha^{(m)}}(\ell^{(m)},t^{(m)})\rangle \qquad .(B.13)$$

The equation of motion for the Green's function of equation (B.13) is

$$(i\,\frac{\partial}{\partial t_1} + \nabla^2_{\underset{\sim}{x}_1} + \mu)\ G_{\alpha^{(1)}\ldots\alpha^{(m)}}(x_1\ldots x_n;x_1'\ldots x_n':\ell^{(1)}t^{(1)}\ldots$$

$$\ell^{(m)}t^{(m)})$$

$$= \sum_{j=1}^{n}\ (-1)^{j+1}\ \delta^4(x_1-x_j')\ G_{\alpha^{(1)}\ldots\alpha^{(2)}}(x_2\ldots x_n;x_1'\ldots x_{j-1}'x_{j+1}'\ldots$$

$$x_n':\ell^{(1)}t^{(1)}\ldots\ell^{(m)}t^{(m)})$$

$$+\ (i)^c\sum_{\beta,\ell''}\ \zeta_\beta(\ell'',\underset{\sim}{x}_1)\ G_{\beta\alpha^{(1)}\alpha^{(2)}\ldots\alpha^{(m)}}(x_1\ldots x_n;x_1'\ldots x_n':$$

$$\ell''t_1,\ell^{(1)}t^{(1)}\ldots\ell^{(m)}t^{(m)}) \qquad (B.14)$$

where

$$\begin{aligned} c &= 4,\ \text{if } m \text{ is even} \\ &= 1,\ \text{if } m \text{ is odd} \end{aligned} \qquad .(B.15)$$

The equation conjugate to equation (B.15) is

$$(i\partial_t - \nabla_{\underset{\sim}{x}}^{\ 2} - \mu)\ G_0(x_1;x) = -\ \delta^4(x_1-x) \qquad .(B.16)$$

In the usual fashion equations (B.14) and (B.16) are used to provide the expansion

$$G_{\alpha^{(1)}\dots\alpha^{(m)}}(x_1\dots x_n;x'_1\dots x'_n:\ell^{(1)}t^{(1)},\ell^{(2)}t^{(2)}\dots\ell^{(m)}t^{(m)})$$

$$= \sum_{j=1}^{n} (-1)^{j+1}\, G_0(x_1;x'_j)\; G_{\alpha^{(1)}\dots\alpha^{(m)}}(x_2\dots x_n;$$

$$x'_1\dots x'_{j-1}\; x'_{j+1}\dots x'_n:\ell^{(1)}t^{(1)}\dots\ell^{(m)}t^{(m)})$$

$$+ (i)^c \int d^4x\; G_0(x_1;x) \sum_{\beta,\ell''} \zeta_\beta(\ell'',\underset{\sim}{x})\; G_{\beta\alpha^{(1)}\dots\alpha^{(m)}}(xx_2\dots x_n;$$

$$x'_1\dots x'_n:\ell''t,\ell^{(1)}t^{(1)}\dots\ell^{(m)}t^{(m)}) \qquad (B.17)$$

where c is given by equation (B.15).

A very similar analysis lends to

$$D_{\alpha^{(1)}\dots\alpha^{(m)}}(\ell^{(1)}t^{(1)},\ell^{(2)}t^{(2)}\dots\ell^{(m)}t^{(m)})$$

$$= \sum_{j=2}^{m} D^0_{\alpha^{(1)}\alpha^{(j)}}(\ell^{(1)}t^{(1)},\ell^{(j)}t^{(j)})$$

$$D_{\alpha^{(2)}\dots\alpha^{(j-1)}\alpha^{(j+1)}\dots\alpha^{(m)}}(\ell^{(2)}t^{(2)}\dots\ell^{(j-1)}t^{(j-1)}$$

$$\times\; \ell^{(j+1)}t^{(j+1)}\dots\ell^{(m)}t^{(m)})$$

$$- (i)^c \sum_{\alpha,\ell} \int dt\, d^3x'\; D^0_{\alpha^{(1)}\alpha}(\ell^{(1)}t^{(1)},\ell t)\; \zeta_\alpha(\ell,\underset{\sim}{x}')$$

$$\times\; G_{\alpha^{(2)}\dots\alpha^{(m)}}(x't;x't^+:\ell^{(2)}t^{(2)}\dots\ell^{(m)}t^{(m)}) \qquad .(B.18)$$

The Green's function for the electron, $G(x;x')$, can be expressed in terms of the bare Green's functions G_0 and D^0 with the use of equations (B.17) and (B.18).

In the theory of superconductivity as discussed in section 2.5 of Chapter II, the Hamiltonian is recast in the Nambu scheme with the introduction of the Gorkov anomolous Green's functions. The self-energy in the Nambu self-consistent scheme is written in terms of the renormalized electron Green's function G which is now a two-by-two matrix and the renormalized Green's function D. For the average lattice D is denoted by P.

In a straight-forward manner equations (B.17) and (B.18) can be used to obtain an expression for the phonon contribution to the self-energy, Σ_p. It is

$$\Sigma_p(\underset{\sim}{p},i\omega_n) = -\frac{1}{\beta}\sum_{\underset{\sim}{p}',n'} \tau_3\, G(\underset{\sim}{p}',i\omega_{n'})\tau_3$$

$$\times \Big\{ \sum_{\substack{\alpha,\beta\\ \ell,\ell'}} \frac{i(\underset{\sim}{p}-\underset{\sim}{p}')_\alpha}{N} \left(\bar{w}^*(\underset{\sim}{p}-\underset{\sim}{p}') + [\sigma(\underset{\sim}{R}_\ell) - \langle\sigma\rangle_R]\, \Delta w^*(\underset{\sim}{p}-\underset{\sim}{p}')\right)$$

$$\times \frac{-i(\underset{\sim}{p}-\underset{\sim}{p}')_\beta}{N} \left(\bar{w}(\underset{\sim}{p}-\underset{\sim}{p}') + [\sigma(\underset{\sim}{R}_{\ell'}) - \langle\sigma\rangle_R]\, \Delta w(\underset{\sim}{p}-\underset{\sim}{p}')\right)$$

$$\times e^{i(\underset{\sim}{p}-\underset{\sim}{p}')\cdot(\underset{\sim}{R}^0_\ell-\underset{\sim}{R}^0_{\ell'})}\, P_{\alpha\beta}(\ell,\ell';i\omega_n-i\omega_{n'})\Big\} \qquad .(B.19)$$

The notation in equation (B.19) is that of section 2.5 of Chapter II. The relationship of equation (4.67) between $P_{\alpha\beta}(\ell,\ell';\omega)$ and $P_{\lambda\lambda'}(\underset{\sim}{q};\omega)$ can be used along with the configuration average of equation (4.28) to obtain the configuration averaged self-energy

$$\langle \Sigma_p(\underset{\sim}{p}, i\omega_n)\rangle_{C.A.} = -\frac{1}{\beta}\sum_{\underset{\sim}{p}',n'} \tau_3\, G(\underset{\sim}{p}', i\omega_{n'})\,\tau_3$$

$$\times \sum_{\underset{\sim}{q}'} \sum_{\ell,\ell'} \frac{1}{NM}\sum_{\lambda\lambda'} \left(\frac{i(\underset{\sim}{p}-\underset{\sim}{p}')\cdot\underset{\sim}{\xi}(\underset{\sim}{q}';\lambda)}{N}\right)\left(\frac{-i(\underset{\sim}{p}-\underset{\sim}{p}')\cdot\underset{\sim}{\xi}^*(\underset{\sim}{q}';\lambda')}{N}\right)$$

$$\times \{\bar{w}(\underset{\sim}{p}-\underset{\sim}{p}')\,\bar{w}^*(\underset{\sim}{p}-\underset{\sim}{p}') + [f_2 - \langle\sigma\rangle_R^{\,2} + (1-f_2)\delta_{\ell\ell'}]\;\Delta\, w(\underset{\sim}{p}-\underset{\sim}{p}')$$

$$\times \Delta\, w^*(\underset{\sim}{p}-\underset{\sim}{p}')\}\; e^{i(\underset{\sim}{p}-\underset{\sim}{p}')\cdot(\underset{\sim}{R}^0_\ell-\underset{\sim}{R}^0_{\ell'})}\; e^{i\underset{\sim}{q}'\cdot(\underset{\sim}{R}^0_\ell-\underset{\sim}{R}^0_{\ell'})}$$

$$\times P_{\lambda\lambda'}(\underset{\sim}{q}', i\omega_n - i\omega_{n'}) \qquad .(B.20)$$

In the limit of large N, f_2 is $\langle\sigma\rangle_R^{\,2}$ so the corresponding part of equation (B.20) vanishes. Equation (B.20) can be divided into two parts, the first with the factor $\bar{w}\;\bar{w}^*$ and the second with $\Delta\, w\;\Delta\, w^*$. In the first term the sums over ℓ, ℓ' and $\underset{\sim}{q}'$ can be performed. In the second term only the ℓ and ℓ' sums can be performed analytically.

The self-energy Σ_p is

$$\langle \Sigma_p(\underset{\sim}{p}, i\omega_n)\rangle_{C.A.} = -\frac{1}{\beta}\sum_{\underset{\sim}{p}',n'} \tau_3\, G(\underset{\sim}{p}', i\omega_{n'})\,\tau_3$$

$$\times \{ \sum_{\lambda,\lambda'} \left|\bar{g}_{\underset{\sim}{p}-\underset{\sim}{p}';\lambda}\right|^2 P_{\lambda\lambda'}(\underset{\sim}{p}-\underset{\sim}{p}', i\omega_n - i\omega_{n'})$$

$$+ (1-\langle\sigma\rangle_R^{\,2})\; \frac{1}{N^2 M}\sum_{\underset{\sim}{q}'} \;(i(\underset{\sim}{p}-\underset{\sim}{p}')\cdot\underset{\sim}{\xi}(\underset{\sim}{q}';\lambda))\;\; (-i(\underset{\sim}{p}-\underset{\sim}{p}')$$

$$\times\; \xi^*(\underset{\sim}{q}';\lambda'))\;\; \Delta\, w(\underset{\sim}{p}-\underset{\sim}{p}')\;\; \Delta\, w^*(\underset{\sim}{p}-\underset{\sim}{p}')\;\; P_{\lambda\lambda'}(\underset{\sim}{q}', i\omega_n - i\omega_{n'})\} \qquad .(B.21)$$

The coupling constant $\bar{g}_{\underset{\sim}{p}-\underset{\sim}{p}',\lambda}$ corresponds to the average pseudopotential and differs from the coupling constant of equation (2.97) by a factor $\frac{1}{\sqrt{2\omega(\underset{\sim}{q};\lambda)}}$ which is contained in $P_{\lambda\lambda'}$. With the specification of the spectral function $B_{\lambda\lambda'}(\underset{\sim}{q};\omega)$ by

$$P_{\lambda\lambda'}(\underset{\sim}{q};\omega) = \int_0^\infty B_{\lambda\lambda'}(\underset{\sim}{q};\nu)\ \left[\frac{1}{\omega-\nu+i\delta} - \frac{1}{\omega+\nu-i\delta}\right] \qquad ,(B.22)$$

the function $\alpha^2(\omega)\ F(\omega)$ is specified by$^{(23)}$

$$\begin{aligned} \alpha^2(\omega)\ F(\omega) = {} & \sum_{\lambda\lambda'} \frac{N(0)}{8\pi\ k_F^{\ 2}} \int d\Omega_{\underset{\sim}{q}} \int_0^{2k_F} q\,dq \left|\bar{g}_{\underset{\sim}{q};\lambda}\right|^2 B_{\lambda\lambda'}(\underset{\sim}{q},\omega) \\ & + [1-\langle\sigma\rangle_R^{\ 2}] \sum_{\lambda,\lambda'} \frac{1}{N} \sum_{\underset{\sim}{q}'} \frac{N(0)}{8\pi\ k_F^{\ 2}} \int d\Omega_{\underset{\sim}{q}} \int_0^{2k_F} q\,dq \\ & \times \left(\frac{i\underset{\sim}{q}\cdot\underset{\sim}{\xi}(\underset{\sim}{q}';\lambda)}{\sqrt{MN}}\right) \left(\frac{-i\underset{\sim}{q}\cdot\underset{\sim}{\xi}^{*}(\underset{\sim}{q}';\lambda')}{\sqrt{MN}}\right) \Delta\ w^{*}(\underset{\sim}{q})\ \Delta\ w(\underset{\sim}{q}) \\ & \times B_{\lambda\lambda'}(\underset{\sim}{q}',\omega) \end{aligned} \qquad (B.23)$$

where k_F is the Fermi momentum and $N(0)$ is the electron density of states at the Fermi surface.

REFERENCES

(1) H. K. Onnes, Commun. Phys. Lab. Univ. Leiden, No. 119b (1911).

(2) W. Meissner and R. Ochsenfeld, Naturwissenschaften 21, 787 (1933).

(3) C. J. Gorter and H. Casimir, Physica 1, 306 (1934).

(4) F. London and H. London, Proc. Roy. Soc. (London) A149, 71 (1935).

(5) D. Shoenberg, Proc. Roy. Soc. (London) A175, 49 (1940).

(6) A. B. Pippard, Proc. Roy. Soc. (London) A216, 547 (1953).

(7) H. Fröhlich, Phys. Rev. 79, 845 (1950).

(8) E. Maxwell, Phys. Rev. 78, 477 (1950).

(9) B. Serin, C. A. Reynolds and L. B. Nesbitt, Phys. Rev. 80, 761 (1950).

(10) B. B. Goodman, Proc. Phys. Soc. (London) A66, 217 (1953).

(11) W. S. Corak, B. B. Goodman, C. B. Satterthwaite and A. Wexler, Phys. Rev. 102, 656 (1956).

(12) J. Bardeen, L. N. Cooper and J. R. Schrieffer, Phys. Rev. 106, 162 (1957).

(13) J. Bardeen, L. N. Cooper and J. R. Schrieffer, Phys. Rev. 108, 1175 (1957).

(14) I. Giaver, Phys. Rev. Letters 5, 147 (1960).

(15) I. Giaver, H. R. Hart and K. Mergle, Phys. Rev. 126, 941 (1962).

(16) J. M. Rowell, P. W. Anderson and D. E. Thomas, Phys. Rev. Letters <u>10</u>, 334 (1963).

(17) G. M. Eliashberg, Zh. Eksperim. i Teor. Fiz. <u>38</u>, 966 (1960) [English transl.: Soviet Phys. - JETP <u>11</u>, 696 (1960)].

(18) L. P. Gorkov, Zh. Eksperim. i Teor. Fiz. <u>34</u>, 735 (1958) [English transl.: Soviet Phys. - JETP <u>7</u>, 505 (1958)].

(19) Y. Nambu, Phys. Rev. <u>117</u>, 648 (1960).

(20) P. Morel and P. W. Anderson, Phys. Rev. <u>125</u>, 1263 (1962).

(21) G. J. Culler, B. C. Fried, R. W. Huff and J. R. Schrieffer, Phys. Rev. Letters <u>8</u>, 399 (1962).

(22) J. R. Schrieffer, D. J. Scalapino and J. W. Wilkins, Phys. Rev. Letters <u>10</u>, 336 (1963).

(23) D. J. Scalapino, J. R. Schrieffer and J. W. Wilkins, Phys. Rev. <u>148</u>, 263 (1966).

(24) A. B. Migdal, Zh. Eksperim. i Teor. Fiz. <u>34</u>, 1438 (1958) [English transl.: Soviet Phys. - JETP <u>7</u>, 996 (1958)].

(25) D. J. Scalapino, Y. Wada and J. C. Swihart, Phys. Rev. Letters <u>14</u>, 102 (1965).

(26) J. C. Swihart, D. J. Scalapino and Y. Wada, Phys. Rev. Letters <u>14</u>, 106 (1965).

(27) Vinay Ambegoakar and James Woo, Phys. Rev. <u>139</u>, A1818 (1965).

(28) T. M. Wu, Phys. Rev. Letters <u>19</u>, 508 (1967).

(29) J. P. Carbotte and R. C. Dynes, Phys. Letters 25A, 685 (1967).

(30) J. P. Carbotte and R. C. Dynes, Phys. Rev. 172, 476 (1968).

(31) R. C. Dynes, J. P. Carbotte, D. W. Taylor and C. K. Campbell, Phys. Rev. 178, 713 (1969).

(32) G. J. Sizoo and H. K. Onnes, Leiden Commun. 180b (1925).

(33) G. Lazarew and L. S. Kan, J. Phys. USSR 8, 193 (1944).

(34) N. B. Brandt and N. I. Ginzburg, Zh. Eksperim. i Teor. Fiz. 44, 1876 (1963) [English transl.: Soviet Physics - JETP 17, 1262 (1963)].

(35) M. Levy and J. L. Olsen, Rev. Sci. Instr. 36, 233 (1965).

(36) J. L. Olsen, E. Bucher, M. Levy, J. Muller, E. Corenzwit and T. Geballe, Rev. Mod. Phys. 36, 168 (1964).

(37) P. F. Chester and G. O. Jones, Phil Mag. 44, 1281 (1953).

(38) L. D. Jennings and C. A. Swenson, Phys. Rev. 112, 31 (1958).

(39) T. F. Smith and C. W. Chu, Phys. Rev. 159, 353 (1967).

(40) N. V. Zavaritskii, E. S. Itskevich and A. N. Voronovskii, Zh. Eksperim. i Teor. Fiz. Pis'ma 7, 271 (1968).

(41) J. P. Franck and W. J. Keeler, Phys. Rev. Letters 20, 379 (1968).

(42) J. P. Franck, W. J. Keeler and T. M. Wu, Solid State Commun. 7, 483 (1968).

(43) R. C. Dynes and J. M. Rowell, (to be published).

(44) S. C. Ng, Ph.D. Thesis, McMaster University, Hamilton, Canada (unpublished) (1967).

(45) D. C. Mattis, Phys. Rev. 106, 721 (1957).

(46) W. A. Harrison, Pseudopotentials in the Theory of Metals (W. A. Benjamin, Inc., New York, 1966).

(47) Timothy M. Hayes, Harvey Brooks and Arthur Bienenstock, Phys. Rev. 175, 699 (1968).

(48) B. N. Brockhouse, E. D. Hallman and S. C. Ng, in Magnetic and Inelastic Scattering of Neutrons by Metals, edited by T. J. Rowland and P. A. Beck (Gordon and Breach Science Publishers, Inc., New York, to be published).

(49) M. Born and T. von Karman, Phys. Zeit. 13, 297 (1912).

(50) R. C. Dynes, J. P. Carbotte and E. J. Woll, Jr., Solid State Commun. 6, 101 (1968).

(51) M. Born and K. Huang, Dynamical Theory of Crystal Lattices (Oxford University Press, 1954).

(52) J. R. Schrieffer, Theory of Superconductivity (W. A. Benjamin, Inc., New York, 1964).

(53) J. C. Phillips and L. Kleinman, Phys. Rev. 116, 287 (1959).

(54) L. Kleinman and J. C. Phillips, Phys. Rev. 118, 1153 (1960).

(55) E. Antončík, J. Phys. Chem. Solids **10**, 314 (1959).

(56) M. H. Cohen and V. Heine, Phys. Rev. **122**, 1821 (1961).

(57) F. Bassani and V. Celli, J. Phys. Chem. Solids **20**, 64 (1961).

(58) B. J. Austin, V. Heine and L. J. Sham, Phys. Rev. **127**, 276 (1962).

(59) J. M. Ziman, *Principles of the Theory of Solids* (Cambridge University Press, 1964).

(60) C. Herring, Phys. Rev. **57**, 1169 (1940).

(61) J. Hubbard, Proc. Roy. Soc. (London) **A244**, 199 (1958).

(62) Charles Kittel, *Introduction to Solid State Physics* (John Wiley and Sons, Inc., New York, 1966).

(63) N. W. Ashcroft and J. Lekner, Phys. Rev. **145**, 83 (1966).

(64) A. O. E. Animalu and V. Heine, Phil. Mag. **12**, 1249 (196$\overset{5}{4}$).

(65) V. Heine and I. Abarenkov, Phil. Mag. **9**, 451 (1964).

(66) P. P. Ewald, Ann. Physik **64**, 253 (1921).

(67) D. J. Scalapino, in *Superconductivity*, edited by R. D. Parks (Marcel Dekker, Inc., New York, 1969).

(68) V. Ambegoakar, in *Astrophysics and the Many-Body Problem* (Brandeis Summer Institute 1962) (W. A. Benjamin, Inc., New York, 1963).

(69) V. Ambegoakar, in *Many-Body Physics* (Les Houches 1967), edited by C. DeWitt and R. Balian (Gordon and Breach Science Publishers, Inc., New York, 1968).

(70) W. L. McMillan and J. M. Rowell, Phys. Rev. Letters 14, 108 (1965).

(71) W. L. McMillan and J. M. Rowell, in Superconductivity, edited by R. D. Parks (Marcel Dekker, Inc., New York, 1969).

(72) V. L. Ginzburg, Zh. Eksperim. i Teor. Fiz. 44, 2104 (1963) [English transl.: Soviet Phys. - JETP 17, 1415 (1963)].

(73) W. L. McMillan, Phys. Rev. 167, 331 (1968).

(74) P. E. Seiden, Phys. Rev. 179, 458 (1969).

(75) R. E. Hodder, Phys. Rev. 180, 530 (1969).

(76) G. Gilat and L. J. Raubenheimer, Phys. Rev. 144 390 (1966).

(77) L. van Hove, Phys. Rev. 89, 1189 (1953).

(78) R. C. Dynes, Ph.D. Thesis, McMaster University, Hamilton, Canada (unpublished) (1968).

(79) William B. Daniels, in Lattice Dynamics, edited by R. F. Wallis (Pergamon Press Inc., New York, 1965).

(80) Duane C. Wallace, Phys. Rev. 176, 832 (1968).

(81) G. Gilat and R. M. Nicklow, Phys. Rev. 143, 487 (1966).

(82) D. W. Taylor, private communication.

(83) John L. Yarnell, John L. Warren and Seymour H. Koenig, in Lattice Dynamics, edited by R. F. Wallis (Pergamon Press Inc., New York, 1965).

(84) J. L. Olsen, K. Andres and T. H. Geballe, Phys. Letters 26A, 239 (1968).

(85) R. J. Elliott and D. W. Taylor, Proc. Roy. Soc. A296, 161 (1967).

(86) D. N. Zubarev, Soviet Phys. Uspekhi 3, 320 (1960).